

Copyright is owned by the Author of the thesis. Permission is given for a copy to be downloaded by an individual for the purpose of research and private study only. The thesis may not be reproduced elsewhere without the permission of the Author.

Characterization of *Colocasia esculenta* L. Schott var. *esculenta* grown in Tonga for Food Applications

A thesis presented in partial fulfilment of the requirements for the degree of

Master

in

Food Technology

At Massey University, Palmerston North, New Zealand

Asena Toivaha Faanunu

2025



Abstract

This study characterized two *Colocasia esculenta* L. Schott var. *esculenta* cultivars, Holoitounga and Lau'ila, focusing on their corms and ungelatinized flours, and evaluated their potential to partially substitute wheat flour in crackers, shortbread biscuits and bread. Fresh corms were analyzed for physicochemical, microstructure, and cooking characteristics, while derived flours were assessed for nutritional composition, microstructure, water and oil absorption properties, pasting behaviour, thermal properties, foaming and emulsion properties and rheological behaviour, including protein fortification with egg white, casein and pea protein.

Holoitounga exhibited higher dry matter (38.43 %), amylose content (12.75%), dietary fiber (4.54 g/100g), crude fat (1.76 g/100g) and carbohydrates (89.29 g/100g), with loosely packed starch granules and shorter cooking time (12-14 minutes), whereas Lau'ila had higher starch (68.40 %) and protein contents (3.49 g/100g), higher amylopectin content (90.55 %), and denser microstructure, contributing to longer cooking time (14-16 minutes) and greater cohesiveness. Holoitounga flour showed finer particle size with an average diameter of 74.08 μm , higher bulk density (0.59 g/mL), water absorption index (4.70 g/g), water absorption capacity (94.61 g/100g), oil absorption capacities (92.51 g/100g) gelatinization temperature (78.92 $^{\circ}\text{C}$) and pasting viscosity (4952.33 cP). Lau'ila, in contrast, displayed higher swelling power (5.64 g/g), water solubility (0.30 g/g) and foaming capacity (7.69 %). Protein fortification significantly improved the rheological properties of both flours, particularly the egg white and casein protein, making them more comparable to wheat flour dough.

In bakery applications, low to moderate substitution levels ($\leq 50\%$) maintained acceptable physical, textural, and nutritional attributes with shortbreads and crackers tolerating higher levels (50% - 100%) better than bread. Holoitounga samples consistently outperformed those from Lau'ila in puffiness, colour, and texture, likely due to their higher amylose content. Nutritionally, substitution reduced energy and protein content but increased carbohydrates and sugars, indicating the need for protein enrichment at higher substitution levels. These findings highlight the potential of Tongan taro flours, particularly Holoitounga, in supporting import substitution strategies, while future research should explore storage stability, sensory acceptance, and further protein fortification to enhance their application in gluten-reduced and gluten-free bakery products.

Acknowledgement

My master's research journey has been both challenging and rewarding, and I give thanks to God for granting me the strength to persevere through personal loss and difficult times. I am reminded of the saying "NO MAN IS AN ISLAND", as this project would not have been completed without the support of many people. I am grateful to the New Zealand Government for awarding me the Manaaki New Zealand Scholarship (2024-25). This opportunity has allowed me to pursue a long-awaited project that will contribute to the development of my homeland, Tonga.

My sincere appreciation to my supervisor, Professor Jaspreet Singh, for his invaluable guidance, support and encouragement throughout my research. I also thank Professor Lovedeep Kaur for her support and constructive feedback, which greatly improved the quality of my work. My sincere thanks go out to Michelle Tamahana, Chris Hall, Warwick Johnson, Arthur Xu, Robert Wieliczko, and Garry Radford for their technical assistance and guidance during my experiments.

I am deeply grateful to the Pasifika Student Success team, Professor Palatasa Havea, Sunlou Liuvaie, and the rest of the staff for their mentorship and unwavering support of my well-being, especially during my most challenging times. I owe much to their kindness and care. To the Pasifika friends, Taa'imalie mei Langi Wesleyan Church, for making Palmerston feel like my home away from home.

Special thanks to my parents, Taniela and Lose Foliaki, and my siblings for their support through prayers and constant encouragement. Not forgetting my nephews and nieces, Taniela, Lose, Anapesi, Lepeka, Bowen, Jonathan, Hiva, Mele'ana, and Ilaisaane, whose joyful presence provided much-needed moments of relief from the demands and stresses of this journey.

Also, a sincere thanks to my mother-in-law, Siueti Faanunu and my husband's family for their steadfast support, particularly in assisting with cleaning, packing and ensuring the safe delivery of my samples from Tonga. Finally, to my husband, I am forever grateful for your love, care, prayers, and unwavering support. You selflessly carried out my responsibilities without complaint, allowing me to focus entirely on my studies. I am indebted to you for all you have done for our family during this journey.

Table of Contents

Abstract.....	ii
Acknowledgement.....	ii
Table of Contents	iii
List of Figures.....	vi
List of Table.....	viii
Chapter 1: Introduction.....	1
1.1 Taro production and its socioeconomic importance in Tonga.....	2
1.2 Taro Botany	2
1.3 Food Application of Taro Corm	4
1.4 Research aims and significance	5
1.5 Thesis outline	6
Chapter 2: Review of Literature.....	8
2.1 Introduction.....	8
2.2 Characterization of taro corms.....	9
2.2.1 <i>Nutritional composition of taro corm</i>	9
2.2.2 <i>Microstructure of taro corm and starch morphology</i>	10
2.2.3 <i>Taro starch Structure</i>	13
2.2.4 <i>Cooking characteristics of taro corms</i>	16
2.2.5 <i>Colour characteristics of taro parenchyma</i>	17
2.3 Characterization of ungelatinized taro flour	17
2.3.1 <i>Physicochemical properties</i>	17
2.3.2 <i>Functional properties of taro flour</i>	22
2.4 Applications and technological challenges of taro flour in bakery products.....	30
2.4.1 <i>Use of taro flour in bakery formulations</i>	30
2.4.2 <i>Physical and sensory characteristics</i>	33
2.4.3 <i>Nutritional impacts</i>	34
2.5 Research gaps and rationale.....	34
Chapter 3: Characterization of taro corms.....	36
3.1 Introduction.....	36
3.2 Method and Materials	37

3.2.1	<i>Materials</i>	37
3.2.2	<i>Methods</i>	38
3.3	Results and Discussion	43
3.3.1	<i>Dry matter content, total starch content, total amylose and amylopectin content of taro corms</i>	43
3.3.2	<i>Proximate Composition</i>	44
3.3.3	<i>Colour characteristics of raw taro corms</i>	46
3.3.4	<i>Microstructural properties of raw taro corms</i>	47
3.3.5	<i>Cooking characteristics</i>	49
3.3.6	<i>Texture profile analysis of the cooked taro corms</i>	52
3.4	Conclusion	53
Chapter 4: Characterization of ungelatinized taro flours		54
4.1	Introduction.....	54
4.2	Materials and Methods.....	55
4.2.1	<i>Preparation of ungelatinized taro flours</i>	55
4.2.2	<i>Physicochemical Characterizations</i>	55
4.2.3	<i>Methods for Functional Characterization</i>	58
4.2.4	<i>Rheological analysis of taro flour and its protein fortified blends in a powder-and-water system</i>	60
4.2.5	<i>Statistical Analysis</i>	61
4.3	Results and Discussions.....	61
4.3.1	<i>Physicochemical Characteristics</i>	61
4.3.1.2.	<i>Bulk density (BD), Water absorption index (WAI), water solubility index (WSI), swelling power (SP), and pH</i>	62
4.3.1.3.	<i>Colour characteristics</i>	64
4.3.1.4.	<i>Particle size distribution</i>	65
4.3.1.5.	<i>Microstructural properties</i>	66
4.3.2	<i>Functional Characteristics</i>	68
4.3.3	<i>Rheological properties of taro flour-protein systems</i>	75
4.4	Conclusion	83
Chapter 5: Application of ungelatinized taro flour in bakery products		84
5.1	Introduction.....	84
5.2	Materials and Methods.....	86

5.2.1	<i>Materials</i>	86
5.2.1.1.	<i>Ingredients and formulation of crackers</i>	86
5.2.1.2.	<i>Preparations of crackers</i>	86
5.2.1.3.	<i>Ingredients and formulations of shortbread cookies</i>	87
5.2.1.4.	<i>Preparation of shortbread cookies</i>	87
5.2.1.5.	<i>Ingredients and formulations of bread</i>	88
5.2.1.6.	<i>Preparation of composite bread</i>	88
5.2.2	<i>Methods</i>	88
5.2.1.1.	<i>Nutrition Composition of the bakery products</i>	88
5.2.1.2.	<i>Measuring the puffiness (%) of crackers</i>	89
5.2.1.3.	<i>Measuring the volume of shortbread cookies</i>	89
5.2.1.4.	<i>Measuring the loaf weight, height and width</i>	89
5.2.1.5.	<i>Colour analysis of crackers and breadcrumbs</i>	89
5.2.1.6.	<i>Texture analysis of bakery products</i>	90
5.2.1.7.	<i>Statistical Analysis</i>	90
5.3.	<i>Results and Discussions</i>	91
5.3.1.	<i>Crackers</i>	91
5.3.2.	<i>Shortbread Cookies</i>	97
5.3.3.	<i>Breads</i>	101
5.4.	<i>Conclusion</i>	110
Chapter 6: General Discussions and Conclusions		111
6.1	<i>Introduction</i>	111
6.2	<i>Main findings and discussions</i>	111
6.3	<i>Concluding remarks</i>	114
6.4	<i>Future recommendations and Way forward</i>	115
References		116

List of Figures

Figure 1 <i>Colocasia esculenta</i> var. <i>esculenta</i> (dasheen) has a large central corm (A), and <i>C. esculenta</i> var. <i>antiquorum</i> (eddoe) has a small central corm with multiple relatively large cormels (Deo et al., 2009)	3
Figure 2 Morphological structure of the taro (<i>Colocasia esculenta</i> var. <i>esculenta</i>) plant (Paschoalin et al., 2021)	4
Figure 3 SEM images of the microstructure of taro corm chip under different magnifications; 500x on the left and 1800x on the right (Wibisono et al., 2019).	11
Figure 4 SEM of taro starch as individual and compound granules (A), potatoes starch granules (B), and cassava starch granules (C) (Njintang, Parker, et al., 2008; Szymonska et al., 2009)	11
Figure 5 Starch granules of <i>Xanthosoma</i> (A), <i>Colocasia</i> (B), and <i>Alocasia</i> (Havea, 1993)	12
Figure 6 Different forms of crystallinity in starch sources (Jojo et al., 2023)	15
Figure 7 HPLC chromatograms of <i>Colocasia esculenta</i> var. <i>esculenta</i> and fractions of A-chains and B-chains (BS and BL) (Hoyos-Leyva et al., 2017)	15
Figure 8 Photograph of the <i>C. esculenta</i> var. <i>Lau'ila</i> and <i>C. esculenta</i> var. <i>Holoitounga</i> corms and the cross-section of the raw corms	37
Figure 9 Standard curve for amylose determination	39
Figure 10 SEM micrographs of the raw corms of <i>C. esculenta</i> var. <i>Holoitounga</i> variety (A-D) and <i>C. esculenta</i> var. <i>Lauila</i> variety (E-H). In the raw parenchyma micrographs, starch granules are seen embedded in the cellular cytoplasm.	48
Figure 11 (a) Effect of cooking time on compression force of raw taro corms. (b) Enlargement of the 6-30 minutes cooking time region.	50
Figure 12 Flour samples after centrifuged at 4000xg for 40 minutes	64
Figure 13 Particle size distribution of the two flour samples studied	66
Figure 14 SEM images of flours viewed under 1100x, <i>Holoitounga</i> flours (A) and <i>Lau'ila</i> (B) and flours viewed under 2000x, <i>Holoitounga</i> flours (C) and <i>Lau'ila</i> flours (D).	67
Figure 15 Least gel concentration of <i>Holoitounga</i> (A) and <i>Lau'ila</i> (B), starting from 2 to 20 % m/v	73
Figure 16 Strain sweeps of taro flours and protein fortified systems. HTF represents the native <i>Holoitounga</i> flour, HTE for <i>Holoitounga</i> with egg white, HTP for <i>Holoitounga</i> with Pea protein, HTC for <i>Holoitounga</i> with Casein protein, LTF for the native <i>Lau'ila</i> flour, LTE	

for the Lau'ila with egg white, LTP for Lau'ila flour with pea protein, and LTC for the Lau'ila with casein protein.	78
Figure 17 Frequency sweeps analysis of taro-protein systems. HTF represents the native Holoitounga flour, HTE for Holoitounga with egg white, HTP for Holoitounga with Pea protein, HTC for Holoitounga with Casein protein, LTF for the native Lau'ila flour, LTE for the Lau'ila with egg white, LTP for Lau'ila flour with pea protein, and LTC for the Lau'ila with casein protein.	79
Figure 18 (A) Temperature sweeps analysis for heating of flours at 25-100 °C and (B) for cooling of flours at 100 – 25 °C. HTF represents the native Holoitounga flour, HTE for Holoitounga with egg white, HTP for Holoitounga with Pea protein, HTC for Holoitounga with Casein protein, LTF for the native Lau'ila flour, LTE for the Lau'ila with egg white, LTP for Lau'ila flour with pea protein, and LTC for the Lau'ila with casein protein.	82
Figure 19 Preparation of wheat-taro crackers	86
Figure 20 Preparation of shortbread cookies	87
Figure 21 PCA of the nutritional composition of wheat flour crackers	92
Figure 22 PCA of the puffiness and colour characteristics of wheat-taro crackers	95
Figure 23 Photographs of wheat-taro crackers after baking at different times	95
Figure 24 Hardness and fracturability of wheat-taro crackers	96
Figure 25 PCA biplot of the nutritional composition of wheat-taro shortbreads	98
Figure 26 Visual comparison of Holoitounga and Lau'ila shortbreads	99
Figure 27 Volume of shortbread on different substitution levels	100
Figure 28 Texture profile analysis of wheat-taro composite shortbread cookies	101
Figure 29 PCA biplot of the nutritional composition of bread	103
Figure 30 Physical properties of wheat-taro composite breads	105
Figure 31 Physical appearance of wheat-taro composite breads	105
Figure 32 PCA of wheat-taro composite bread crumb colour	107
Figure 33 Wheat-taro flour bread crumb	108
Figure 34 Textural profile analysis of wheat-taro composite breads	109

List of Table

Table 1 Proximate analysis of taro corms from different cultivars on a fresh weight basis (Onwueme, 1999)	10
Table 2 Starch granule size of different cultivars of <i>Colocasia esculenta</i> Schott var <i>esculenta</i> from different countries	12
Table 3 Water-related properties of taro from different regions	21
Table 4 Bakery formulations from taro flour	31
Table 5 Dry matter content, total starch content, total amylose and amylopectin content of taro corms from two different taro cultivars	44
Table 6 Proximate composition of freeze-dried taro powder	45
Table 7 Colour characteristics (L^* , a^* , b^* and ΔE) of fresh and stored (60 minutes) peeled corms from two different cultivars.	46
Table 8 Total water intake and total solid loss during the 30-minute cooking of taro corms from two different cultivars	51
Table 9 Texture profile parameters of cooked taro corms from two different cultivars	52
Table 10 Proximate compositions of the taro flour sample	62
Table 11 Bulk density, Water hydration indices and pH of the two taro flours studied	64
Table 12 Colour of taro flour.	65
Table 13 Particle size distribution of taro flours	66
Table 14 Gelatinization temperatures and enthalpy changes of the taro flours	68
Table 15 Pasting properties of taro flours	70
Table 16 Water absorption capacity and oil absorption capacity of taro flours	71
Table 17 The least gelling concentration of taro flours	72
Table 18 Foam capacity and stability of taro flours	74
Table 19 Emulsion capacity and stability of taro flours	75
Table 20 Nutritional composition of wheat-taro crackers per 100 g	91
Table 21 Puffiness and colour characteristics of wheat-taro crackers	93
Table 22 Nutritional compositions of wheat-taro shortbreads	97
Table 23 Nutritional Composition of wheat-taro breads	102

Chapter 1: Introduction

Tonga is a small developing nation located in the South Pacific with a population of 100,179 and a GDP per capita of \$6,708.86 (*Gross Domestic Product*, 2023). The country's economy is largely supported by agriculture, fishing, manufacturing, tourism, and services. However, much of its agricultural production remains primarily for domestic consumption. Tonga's key export commodities include root crops (33.1%), kava (20.2%), and fish (7.7%), with the remaining exports comprising live animals, base metals, and other products (39%). As of late 2024, Tonga recorded a 12.7% increase in its trade deficit compared to early 2024, reaching \$72.2 million (*International Merchandise Trade Statistics*, 2024). This alarming trend is exacerbated by the fact that food imports alone contribute approximately one-third of total imports. Such dependence on imported food highlights the underutilized of Tonga's agricultural resources. A contributing factor is limited research and innovation aimed at transforming local crops into value-added products, which could reduce import reliance and improve national food self-sufficiency.

As outlined in Tonga's long-term national development plan, achieving food security, improving nutrition, and promoting sustainable agriculture are key priorities. Tonga depends substantially on both fisheries and agriculture to meet its food security needs. However, seafoods remain among the most expensive commodities in local markets and consequently do not serve as the primary food source for most households. Conversely, agriculture, especially root crops and vegetables, provides staple foods that are more affordable and widely accessible. It is estimated that 60-80% of Tonga's cropped land is devoted to root crops, including cassava, taro, yams and sweet potatoes (Taufatofua & Mana'ia, 1995).

Among the major root crops, cassava occupies the largest area, followed by various types of taros. In Tonga, taro encompasses three genera: *Xanthosoma sagittifolium* (taro tarua), *Alocasia marorrhiza* (giant taro) and *Colocasia esculenta* (swamp taro) (Taufatofua & Mana'ia, 1995). These crops are sold mainly in fresh or frozen form, with about 60% of the supply traded domestically and 40% exported. Formal export channels account for approximately 40% of total exports, while the remainder is sent informally to Tongan communities and families abroad (Young & Wiseman, 2016). Cassava has undergone development into value-added products such as deep-fried chips, starch extraction, and flour, which are used in making bread, cakes, and desserts. Similar progress has been made with

coconuts and vanilla. However, despite being the second most cultivated root crop, taro has not undergone comparable value-added development. Although *Colocasia esculenta*, *Xanthosoma sagittifolium* and *Alocasia macrorrhiza* have been studied to some extent, their potential as flour-based ingredients remains largely unexplored. Havea (1993), for example, studied the functionality of taro starches for complementary feeding but did not extend the application to whole corm and flour.

1.1 Taro production and its socioeconomic importance in Tonga

Taro is one of the most important root crops cultivated in Tonga, both for its role in household food security and for its cultural economic significance. Among three genera, *Colocasia esculenta* ranks third after cassava and yam in terms of total cultivation area, accounting for approximately one-fifth of the country's annual root crop production in 2021 (Ha'unga & Taufatofua, 2021). Traditionally, swamp taro holds significant cultural value in Tonga, where it is regarded as a high-status crop and is reserved for royalty, gift-giving, ceremonial feasts, and the fulfilment of social obligations. The importance of taro is also represented by its inclusion as a design element on one of Tonga's currency coins (Onwueme, 1999).

In recent years, the cultivation of *Colocasia esculenta* has gained commercial traction, particularly for export to countries such as New Zealand and Australia. Since 2010, exports have averaged approximately 40 tonnes per month, peaking during July-August and November-December (Young & Wiseman, 2016). While this trend has led to increased production, the export market remains uncertain. A significant proportion of taro is exported through informal channels, which often results in products circulating back into the domestic market. When these goods are not sold, they contribute to postharvest loss and waste. This highlights the sector's continued underdevelopment and the broader issue of untapped economic potential. Limitations in research, postharvest innovation, and market diversification have hindered the advancement of taro beyond its traditional fresh or frozen forms, particularly in value-added product development.

1.2 Taro Botany

Taro (*Colocasia esculenta*) is one of the perennial plants that belongs to the Araceae family. It is believed to have originated in South Central Asia, probably India or the Malay Peninsula

and then spread eastward to the rest of South East Asia, China, Japan, the Pacific Islands and then later to West Africa (Onwueme, 1999). Globally, there are over 1,000 known cultivars of taro, which are generally classified into two main groups, Eddoe (*Colocasia esculenta* var. *antiquorum*) and Dasheen (*Colocasia esculenta* var. *esculenta*) (Okonkwo, 1993). These groups are distinguished primarily by their corm morphology. The dasheen type typically produces a large, singular central corm, while the eddoe type has a smaller central corm accompanied by several large lateral cormels (Figure 1) (Moorthy, 2004).

In Tonga, the dasheen cultivar is the predominant type grown. It features a large, cylindrical corm, typically reaching up to 30 cm in length and 15 cm in diameter, which constitutes the main edible portion of the plant (Onwueme, 1999). Taro plants generally grow to a height of 1 to 2 meters. Morphologically, the plant consists of a central corm just beneath the soil surface, from which large, heart-shaped leaves grow upwards. Roots grow downward, and additional corms or cormels develop laterally. The root system is fibrous and is concentrated primarily within the top one meter of soil (Figure 2).

Figure 1 *Colocasia esculenta* var. *esculenta* (dasheen) has a large central corm (A), and *C. esculenta* var. *antiquorum* (eddoe) has a small central corm with multiple relatively large cormels (Deo et al., 2009)

Taro is widely distributed across Tonga and is particularly suited to regions with high rainfall and remaining forest land, such as Vava'u, Tongatapu and 'Eua. Some varieties have also adapted to drier environments and are cultivated in other island groups. According to the National Biodiversity Stocktaking report, approximately 52 taro varieties are cultivated across Tonga (Prescott et al., 2004). Several of these varieties have been formally studied and released for cultivation by the Ministry of Agriculture, Food and Forests, with some dating back to the 18th century. However, factors such as disease and drought have led to the endangerment of certain traditional varieties. In response, ongoing breeding programs are focused on developing

new, more resilient cultivars capable of withstanding climate change and disease pressures (Ministry of Agriculture, Food and Forests Annual Report 2024).

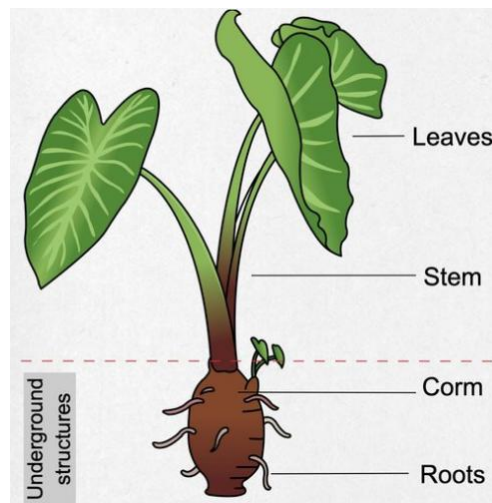


Figure 2 Morphological structure of the taro (*Colocasia esculenta* var. *esculenta*) plant (Paschoalin et al., 2021)

1.3 Food Application of Taro Corm

Industrial applications of *C. esculenta* var. *esculenta* (taro) have been widely reported, primarily due to their high starch content and small starch granule size. These properties make taro starch particularly suitable for complementary foods, especially for infants and individuals with gluten intolerance, as the starch is easily digestible (Boahemaa et al., 2024; Havea, 1993). Beyond starch extraction, whole taro corms have been suggested for use in deep-fried chips (Hollyer et al., 2000), as well as in ready-to-eat (RTE) products such as taro chunks and patties (Nip, 2023). Several other studies have also recommended converting taro corms into flour for use in a range of food applications, such as taro bread, taro cookies, extruded products, flavoured poi and other products (Aboubakar et al., 2008; Arıcı et al., 2016; Boahemaa et al., 2024; Kaur et al., 2013; Tu et al., 2023).

Among these value-added pathways, flour production stands out as a particularly promising use for corms that are unfit for fresh export or chip manufacturing. Currently, up to 30% of harvested taro is discarded due to its small size or irregular shape, making it difficult for mechanical peeling (Nip, 2023). Additionally, the textural quality of taro corms varies within the same corm, as the outer portions are not as starchy as the centre portions (Yu et al., 2022). This phenomenon poses a serious problem, especially when processing taro corm products that require uniform texture, such as RTE taro chunks and patty. Further, diversity in cultivar

morphology and composition also affects processing suitability and end-product quality. Given these challenges, it is essential to understand the specific characteristics of taro cultivars when selecting those most appropriate for flour production and product development.

In this study, two cultivars of *Colocasia esculenta* var. *esculenta*, Lau'ila and Holoitounga, are examined due to their prominence in Tongan agriculture. Both cultivars have been grown locally for more than 30 years and remain widely cultivated today. Lau'ila, the most popular cultivar, is valued for its white flesh and favourable sensory attributes (Prescott et al., 2004). When cooked in water, it develops a distinctive sticky, waxy texture, whereas Holoitounga exhibits a drier, more crumbly texture. These contrasting cooking characteristics, combined with their resilience to drought and disease and strong local consumer preference, provided the rationale for selecting these cultivars for investigation. Their continued importance in local production highlights their relevance for ongoing food product development in Tonga.

Current literature highlights several key characteristics of taro corms that significantly influence their food applications. These include physicochemical properties (such as starch, moisture, fibre content and amylose-amylopectin ratio), microstructural features (e.g. starch granule and morphology), and cooking behaviour (texture and cohesiveness)(Singh et al., 2005; Yu et al., 2022). Similarly, when taro is processed into flour, its quality is determined by both physicochemical and functional properties, which ultimately impact its performance in food formulations(Deguchi et al., 2021; Panyoo et al., 2014).

1.4 Research aims and significance

This study aims to characterize the corms and flours of two selected cultivars of *Colocasia esculenta* Schott var. *esculenta* in Tonga and to evaluate the potential of these flours as partial substitutes for wheat flour in bakery applications. This aim will be achieved by

- Evaluating the physicochemical characteristics, microstructural properties, cooking properties and textural properties of taro corms
- Evaluating the physicochemical and functional properties, as well as the rheological properties of taro flour
- Evaluating the potential of taro flour to partially substitute wheat flour in crackers, shortbreads and breads

The study serves as a model for exploring the broader potential of underutilized root crops in Tonga. A major limitation in advancing value-added processing lies in the limited understanding of the fundamental characteristics of local varieties. Different cultivars may exhibit distinct properties that influence their suitability for specific applications. Understanding these differences is critical to generate baseline information that will support more informed decisions in food formulation, contribute to the diversification of locally produced food items, and ultimately enhance national food security. Moreover, promoting the use of local root crops such as taro in processed food products has the potential to reduce dependence on imported staples, create new economic opportunities, and support Tonga's goals for agricultural sustainability and resilience.

1.5 Thesis outline

Chapter 2 Review of Literature This chapter provides the current research in *Colocasia esculenta* Schott var. *esculenta*, focusing on the characterization of its corms, flours, and food applications as reported in scientific literature. It examines the key properties that vary among taro cultivars and their influence on flour functionality in different food systems. This review establishes a baseline understanding of the typical characteristics of taro corms from various cultivars, which is essential for their appropriate selection, processing, and utilization in food applications, particularly in bakery products.

Chapter 3 Characterization of taro corms. This chapter presents the experimental characterization of taro corms used in this study. It details their physicochemical properties, including nutritional composition, starch content, and amylose-amylopectin ratio, along with their microstructural features, cooking behaviour, and the textural properties of cooked corms. These results provide insight into the inherent functionality of taro flour and form a foundation for evaluating its potential in novel food product development.

Chapter 4 Characterization of ungelatinized taro flours. This chapter examines the physicochemical and functional properties of the ungelatinized version of the flours derived from the taro corms studied in Chapter 3. These properties are critical for determining the suitability of the flours for specific food applications, as variations in composition and functionality influence their performance in different product types. Given that taro flour lacks gluten and has a relatively low protein content, which both contribute to the quality of many

baked products, this chapter also explores alternative approaches for protein fortification to enhance product quality.

Chapter 5 Applications of taro flour in bakery products. This chapter reports on the application of taro flour from different cultivars in crackers, shortbreads, and bread. As indicated in the literature, cultivars may vary in their performance within specific formulations. This chapter evaluates the partial substitution of wheat flour in each bakery product, assessing the resulting nutritional composition, physical characteristics, and textural properties to determine the optimal substitution levels for each cultivar.

Chapter 6 General discussion, Conclusion and Recommendations

Chapter 2: Review of Literature

2.1 Introduction

Colocasia esculenta (L) Schott var. *esculenta* is a tropical root crop of significant cultural, economic and nutritional significance across the Oceanic, African and South Asian regions. It is regarded as a perishable product, as it only lasts for 2 weeks at an ambient temperature. This is an addition to the 30% of edible aroids that are lost during storage, representing a significant post-harvest challenge (Rickard, 1991). This loss could be mitigated through preservation and processing, which would contribute to food security and promote economic growth in tropical countries. Several studies have highlighted the nutritional and health benefits of taro corms; however, only a few studies have examined their industrial potential for enhancing production and processing into a shelf-stable product (Huang et al., 2000; Simsek & El, 2012, 2015). Among various alternatives, conversion of taro corm into flour is a very promising and cost-effective solution, particularly for developing nations. However, characteristics of taro flour vary greatly depending on the cultivars, type of processing and storage conditions (Arici et al., 2016). As the cultivars possess distinct physicochemical and functional characteristics, their suitability for different food purposes is also variable (Kaur et al., 2006).

While taro flour can be further modified by thermal or chemical treatments, understanding its native ungelatinized form is essential, as it reflects the intrinsic physicochemical and functional properties of the corm before any structural alteration (Fatima, 2024). Establishing this baseline knowledge is critical for predicting its performance in various food systems and for designing appropriate processing strategies. Although studies have explored the application of taro flour from different regions in food applications, mostly in baked products, few have been successfully scaled up for commercialization (Ammar et al., 2009; Arici et al., 2021; Arici et al., 2020). This is largely due to limited knowledge on improving product quality, particularly because taro flour lacks key components, such as gluten, that are naturally present in cereal-based products (Calle et al., 2020). Considering these challenges, it is necessary to understand the properties of taro corms and flours, as this knowledge underpins their characteristics and guides their appropriate use in food formulations. This chapter, therefore, reviews the characteristics of raw taro corms, focusing specifically on ungelatinized taro flour and the potential of using taro flour to substitute taro flour in bakery products.

2.2 Characterization of taro corms

The corms of taro dasheen varieties differ in their physiological properties, such as the shapes, colour, and height, but they also exhibit variations in their chemical and morphological characteristics (Nagar et al., 2021). This section will review the characteristics of taro tubers that particularly influence the characteristics of derived products.

2.2.1 Nutritional composition of taro corm

The chemical composition of the taro corm has been documented in several studies, including those by Wang and Higa (1983), Aalbersberg (1990), Onwueme (1999), Temesgen and Retta (2015b), and Laxminarayana (2020). Table 1 presents the proximate composition of corms of taro from various sources on a fresh weight basis. Similar to other characteristics, the nutritional composition of taro varies depending on several factors, including the cultivar, growing conditions, maturity at harvest, post-harvest handling and processing methods (Wang & Higa, 1983). For instance, Nagar et al. (2021) found that between the 14-60 week maturity periods, the corm's starch increased from 10.7 to 30% and its moisture content dropped from 82% to roughly 62% (Himeda et al., 2012).

Like other root crops, taro corms are high in carbohydrates and low in fat and protein. The presence of symbiotic soil bacteria that raise the plant's nitrogen levels may be the reason why taro has a comparatively higher protein content than many other crops (Lucy et al., 2004). The high carbohydrate content in taro corm primarily consists of starch, fibre and small amounts of sugar. Starch accounts for 70-84.2% of the total carbohydrates (Arıcı et al., 2016; Simsek & El, 2012).

Taro possesses the highest levels of dietary fibre compared to other root crops, reported to reach up to 13.5g/100g for raw taro corms and 3.21 g/100g for cooked taro (Adane et al., 2013; Saxby, 2020). With this amount, it is estimated that 454 g of taro is needed to be consumed per day by Pacific Islanders to meet the recommended 25 g per day of dietary fibre (Saxby, 2020). However, the total crude fibre, representing the insoluble portion of the cell wall and found in a much smaller fraction (0.60-1.8%) (Onwueme, 1999). Fibre offers functional health benefits, including improved digestion, enhanced delivery of micronutrients, reduced intestinal transit time, and lower levels of LDL cholesterol and blood glucose (Temesgen & Retta, 2015b).

Table 1 Proximate analysis of taro corms from different cultivars on a fresh weight basis (Onwueme, 1999)

COMPONENT	CONTENT	COMPONENT	CONTENT
MOISTURE	63-85%	NIACIN	0.90 mg/100g
PROTEIN	1.4-3.0%	POTASSIUM	59 mg/100g
FAT	0.16-0.36%	CALCIUM	43 mg/100g
CARBOHYDRATE	13-29%	MAGNESIUM	33 mg/100g
CRUDE FIBRE	0.60-1.8%	SODIUM	11 mg/100g
ASH	0.60-1.3%	IRON	0.55 mg/100g
VITAMIN C	7-9 mg/100g	ZINC	0.23 mg/100g
THIAMINE	0.18mg/100g	MANGANESE	0.38 mg/100g
RIBOFLAVIN	0.04 mg/100g	COPPER	0.172 mg/100g

Numerous compositional studies of taro nutrition indicate that it contains not only essential macronutrients but also a range of micronutrients, including vitamins, calcium, phosphorus, magnesium, potassium, iron, zinc, copper and boron (Ferdaus et al., 2023; Huang et al., 2000; Nagar et al., 2021). In some cases, taro provides a higher level of these nutrients than other starchy crops, such as breadfruit (Huang et al., 2000). Additionally, taro corms contain notable levels of phenolic and flavonoid compounds, contributing to their antioxidant potential. Phenolic content ranges from 12 mg/100g in white fleshed cultivars to 20 mg/100 g in yellow-fleshed varieties (Lako et al., 2008).

2.2.2 Microstructure of taro corm and starch morphology

Taro corm's structure is generally like other tuberous crops, where micrographs of the parenchyma typically reveal well-preserved cell wall arrangements (Figure 3). However, there is limited availability of micrographs specifically illustrating the parenchyma of taro corms, while more detailed micrographs are available for taro starch following extraction (Aboubakar et al., 2008; Havea, 1993; Tu et al., 2023). The tuber cell wall is composed of lamella, which is primarily made up of pectic substances, and the primary cell wall is made up of cellulose, hemicellulose, glycans and pectin (Duarte-Correa et al., 2021; Salazar-Montoya et al., 2024). The microstructure of tubers and physicochemical properties of tubers provide critical information with regard to the behaviour of the corms when processed, such as deep-fried chips and making taro chunks and patties (Nip et al., 1994). Parenchyma with intact cell walls, high

starch content and dry matter content are the suitable properties fit for deep-fried chips(Bandana et al., 2016).

The cells in taro containing starch granules, showing variation of sizes, ranging from 0.5-5 μm and starch granules with a mixture of shapes, such as spherical or dome-shaped and split, oval, polygonal and irregular (Figure 4A) (Agama-Acevedo et al., 2011). Jane et al. (1992) explained that the shapes of the taro starches prove that they are compound starches, differing from conventional tuber starches such as potato and cassava, which typically exhibit rounded or oval shapes with smooth surfaces (Figure 4B and Figure 4C). Consequently, such starches exhibit a larger granule size distribution, typically from 7 to 85 μm , whereas taro starch granules are generally smaller in comparison. An earlier study presents that the starch granule shape for three genera of taro (*Alocasia*, *Colocasia*, and *Xanthosoma*) in Tonga is polygonal shapes (Figure 5); however, *Colocasia esculenta* (0.5-6 μm) is slightly larger than the *Alocasia* granules 0.5-3 μm (Havea, 1993).

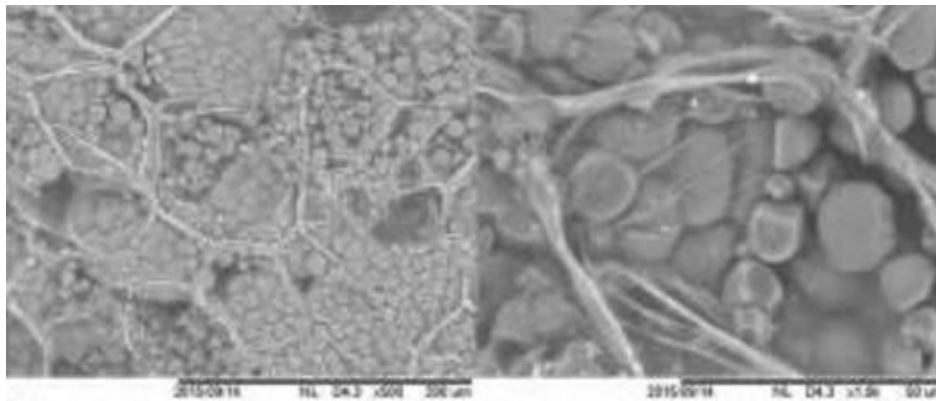


Figure 3 SEM images of the microstructure of taro corm chip under different magnifications; 500x on the left and 1800x on the right (Wibisono et al., 2019).

A

B

C

Figure 4 SEM of taro starch as individual and compound granules (A), potatoes starch granules (B), and cassava starch granules (C) (Njintang, Parker, et al., 2008; Szymonska et al., 2009)

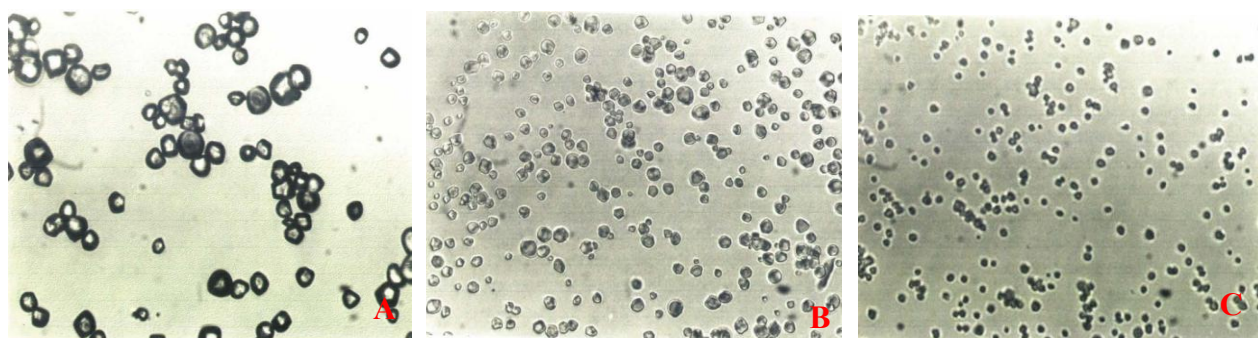


Figure 5 Starch granules of *Xanthosoma* (A), *Colocasia* (B), and *Alocasia* (Havea, 1993)

The variation in starch granules of *Colocasia esculenta var esculenta* varieties in Tonga has not been explored, yet there have been studies done on the popular varieties in Hawaii (Jane et al., 1992), Thailand (Anuntagool et al., 2006) and India (Sit et al., 2014). Jane et al. (1992) and Anuntagool et al. (2006) reported that starch granule size varies significantly among cultivars; these differences are often associated with the cultivation environment, maturity at harvest, and molecular structure of starch. The granule size distribution of many taro varieties spans a much wider size range compared to other starches (Havea, 1993). This characteristic could potentially influence the properties and behaviours of taro starch in various applications such as industrial use, processing, and cooking. Table 2 presents the size range of starches of different *C. esculenta* Schott var. *esculenta* varieties from different countries.

Table 2 Starch granule size of different cultivars of *Colocasia esculenta* Schott var *esculenta* from different countries

Varieties	Minimum (μm)	Maximum(μm)	Country	References
Bun long	2.55	3.08	Hawaii	(Jane et al., 1992)
Dasheen	3.69	4.26	Hawaii	
Hawaii White	2.85	3.27	Hawaii	
Niue	3.18	3.72	Hawaii	
Hawaii Red	2.94	3.40	Hawaii	
Bun-long	1.3	2.2	China	(Zeng et al., 2014)
Garu	1.9	4.2	India	(Sit et al., 2014)
Dog hoof	2.42	2.75	Taiwan	(Lu et al., 2008)
Mein	2.44	2.54	Taiwan	
KS01	2.37	2.79	Taiwan	
Lau'ila	0.5	6	Tonga	(Havea, 1993)
Not specify	2	5	Mexico	(Agama-Acevedo et al., 2011)

Due to the small size of taro starch granules, it has been recommended for use in baby food because of its high digestibility, as well as for various industrial applications, including the plastic and cosmetic industries (Havea, 1993; Jane et al., 1992). This information demonstrates that the sizes and shapes of starch granules significantly impact their physicochemical and functional properties, with larger granules tending to result in higher pasting viscosity.

2.2.3 Taro starch Structure

Starch is the major component of carbohydrates, accounting for approximately 70-85% of the taro corm dry weight. Notably, taro starch contains up to 50% resistant starch, making it a promising functional ingredient for reducing cholesterol and blood glucose levels due to its ability to bind bile acids and slow digestion (Nagar et al., 2021; Simsek & El, 2012). Beyond its nutritional significance, starch plays a critical role in determining the physicochemical and functional properties of taro corms.

Taro starch consists of two structurally distinct glucose polymers: amylose and amylopectin. Both are composed of α -D-glucopyranose units linked by α -1-4 linkages; however, amylopectin possesses a branched structure due to additional α -1-4 and α -1-6 linkages. The ratio of amylose to amylopectin is a key determinant of the functional properties of starches, thereby affecting the performance of taro flours in food applications (Havea, 1993). Understanding the molecular structure, chain length distribution, and weight of these two fractions is essential for evaluating their impact on rheological, viscoelastic, gelatinization, and retrogradation behaviours (Mua & Jackson, 1997). Previous studies have reported that the amylose content of the taro varieties from Mexico was 2.5% (Agama-Acevedo et al., 2011), China was 9.06% (Gaosong et al., 1997), Taiwan were 8.7-13.2 % (Lu et al., 2008), Thailand were 18.8 – 20.0% (Tattiyakul et al., 2007), Spain was 21.4% (Goñi et al., 1997) and Venezuela was 30.6% (Pérez et al., 2005).

During gelatinization, starch granules swell in the presence of heat and water. Amylopectin remains largely within the swollen granules, while the linear amylose chains leach into the surrounding medium to form a continuous phase. Waxy starches, which are low in amylose, typically swell more extensively than normal starches, as amylose acts as a constraint on granule swelling (Wang et al., 2015). Usually, amylose proportion is the governing factor for the quality attributes of taro starch. Studies revealed that amylose in native taro starch is approximately 17.12% comparable to cassava starch but lower than that of native potato starch (26.46%) and kidney bean starch (35.6%) (Wang et al., 2018). In a broader analysis of 315 taro

genotypes using iodine binding calorimetry and near infrared spectroscopy, the amylose content was reported to range from 10-49% (Lebot et al., 2009). Notably, amylose levels can be altered through modification techniques; for example, microwave treatment has been shown to increase the amylose content from 13.90 to 20.08% (Deka & Sit, 2016).

The amylose and amylopectin bond through inter- and intramolecular hydrogen as well as hydrophobic bonds, resulting in a water-insoluble particle (Wang et al., 2018). Amylose is composed of 490 units of glucose per molecule of composition whereas amylopectin is composed of 22 units of glucose per molecule. This is consistent with the higher average molecular weight of amylose (3 to 3.5×10^5 gmol^{-1}) than amylopectin (1.5 to 1.6×10^6 gmol^{-1}) measured from 7 varieties measured with poly-dispersion index ~ 1.2 and ~ 1.0 , respectively (Mweta et al., 2010). The high digestibility and functionality of taro starches may also be governed by the high molar weight of the amylose (2.5×10^7 g mol^{-1}) and amylopectin (5.7 to 13×10^8 g mol^{-1}) (Hoyos-Leyva et al., 2017).

Moreover, the amylose and amylopectin structures play a crucial role in the properties of taro starch. The crystallinity of amylopectin fractions is bonded through double helix linkages, which include the A-type that is mostly found in cereal starches, the B-type in tuber starches and the C-type in legume starches (Jojo et al., 2023). The differences between these starch types are the arrangement of their structures (Figure 6). The A-type starch is tightly packed in a monoclinic unit cell with eight water molecules, leaving a surface pore that facilitates the enzyme's access to the starch molecules, making it prone to enzymatic hydrolysis. In contrast, the B-type starch molecules are arranged in a hexagonal unit containing 36 water molecules, which makes them more resistant to hydrolysis. The C-type starch is a hybrid of the A- and B-types (Jojo et al., 2023).

Although taro is a tuber and believed to be classified as B-type starch, it is found to be dominated by short-chain amylopectin (A-chain) of approximately 80% gel, whereas the long-chain amylopectin (B-chain) only accounts for approximately 20% (Figure 7) (Hoyos-Leyva et al., 2017; Jane et al., 1992). These features influenced its X-ray diffraction pattern, revealing characteristics of A-type starch, which is associated with a more crystalline structure that is arranged in monoclinic units (Gupta et al., 2024).

Figure 6 Different forms of crystallinity in starch sources(Jojo et al., 2023)

Further, the ratio of the long chains and short chains of amylopectin molecules affects the packing of the molecules in the granule, which in turn determines the morphology and the size of the starch granule(Jane, 2007). Taro starch comprises very small irregular or polygonal forms, which have a larger surface area that allows for greater water absorption, swelling and viscosity (Jane et al., 1992). The starch granule morphology is viewed and measured under an electron microscope or laser diffraction.

Figure 7 HPLC chromatograms of *Colocasia esculenta* var. *esculenta* and fractions of A-chains and B-chains (BS and BL) (Hoyos-Leyva et al., 2017)

2.2.4 Cooking characteristics of taro corms

Cooking induces significant transformation in the physicochemical and textural properties of taro corms, influenced by the method and duration of heat treatment, and the corm's internal properties (Andersson et al., 1994). Boiling of taro in water and other media results in softening of corms, and that is due to changes such as the decrease in soluble proteins and resistant starch, and an increase in the degree of starch gelatinization, cell separation, soluble sugars, as well as starch hydrolysis (Aboubakar et al., 2009). These changes are crucial to prevent undesirable sensory attributes and nutritional losses.

Common cooking techniques include boiling, steaming, baking and frying, each influencing the degree and rate of starch gelatinization, and eventually the softening. The presence of the peel can slow heat transfer and prolong cooking, while peeling accelerates softening but may increase leaching (Bethke & Jansky, 2008). The starch characteristics in taro, particularly the ratio of amylose to amylopectin, can also influence the efficacy of the cooking (Bordoloi et al., 2012). High-amylose starches typically require longer cooking times due to their lower swelling power and resistance to gelatinization, whereas high-amylopectin starches gelatinize more readily and thus cook faster (Cornejo-Ramírez et al., 2018). Although no study has yet focused specifically on the boiling time of taro corms, Singh et al. (2005) reported that a high-amylose potato cultivar exhibited shorter cooking times compared to a low-amylose, high-amylopectin cultivar. These findings suggest that starch composition and total starch content influence cooking behaviours, including water uptake and solid loss. While data on water absorption and solute loss during the boiling of taro corms is lacking, studies on potatoes indicate that low-starch, mealy cultivars absorb more water and release more solids into the cooking medium (Singh et al., 2005).

Cooking time for taro and similar tubers can be measured using a compression force, which evaluates the force required to deform a piece of cooked parenchyma. For instance, Singh et al. (2005) determined the cooking time of potatoes by measuring compression force at 2-minute intervals over 30 minutes. A plateau in the compression force versus cooking time curve indicates the point of optimal doneness. Aboubakar et al. (2009) found that decreasing hardness during cooking was associated with starch gelatinization, and this was proposed as a proxy for cooking time. Although their study did not focus on taro, the plot showed a plateau at 15-20 minutes, suggesting that the studied taro corm was fully cooked within this time frame. However, this time can vary significantly among varieties.

2.2.5 Colour characteristics of taro parenchyma

Colour is an important parameter associated with consumer perception of corm freshness and suitability, playing a significant role in product development and marketing (Ivancic et al., 2003). Consumers typically associate a specific colour with particular products; thus, the colour of raw materials substantially affects the acceptance and marketability of the final product (Saxby et al., 2024). Additionally, the colour characteristics of taro corms provide valuable insights into their nutritional composition. For instance, yellow-fleshed taro corms have been reported to contain higher levels of beta-carotene compared to white-fleshed variants. Beta-carotene, a carotenoid, is recognized for its potential health benefits, including its role in reducing the risk of chronic diseases such as diabetes, cardiovascular diseases, and certain types of cancer (Kaushal et al., 2015).

2.3 Characterization of ungelatinized taro flour

Since taro corms have a short shelf life after harvesting, processing them into shelf-stable products such as flour can help reduce food loss and waste. While several studies have explored the extraction of taro starch for various food applications, converting taro tubers into flour offers greater potential for value addition and minimizing postharvest losses (Agama-Acevedo et al., 2011; Ahmed & Khan, 2013; Aprianita et al., 2014; Havea, 1993). However, limited research has been conducted on the physicochemical and functional properties of taro flour to ensure its optimal utilization in food systems.

2.3.1 Physicochemical properties

2.3.1.1 Chemical composition of flour

In the proximate analysis of taro flours, researchers commonly employ AOAC methods to determine protein, fat, moisture, ash and fibre contents (Aboubakar et al., 2008; Deguchi et al., 2021). The chemical compositions of taro flour differ from the taro tubers due to both processing techniques and intrinsic structural differences of the corms. While flour derived from grains or tubers is primarily composed of starch, raw tubers generally contain higher levels of moisture, typically ranging from 63% to 85% (wet basis)(Netam et al., 2022). Processing steps such as milling and drying substantially alter these proportions, leading to marked compositional differences between the raw material and the resulting flour(Deguchi et al., 2021).

According to Alcantara et al. (2013), the comparison of raw taro tubers and taro flours showed a slightly higher chemical composition of taro flours. The taro flours were prepared by slicing taro tubers and drying them at 60 °C for 24 hours. It was found that the crude ash and crude protein of the taro flour were significantly higher than the raw flour. The carbohydrate and crude fibre were marginally different, while the crude fat showed a significantly higher value for the raw taro compared to the flour. Additionally, taro is also known to contain oxalate and phytates, which cause an unpleasant acrid taste and irritation in the mouth and throat if consumed raw (Kristl et al., 2021). Taro corms are sometimes characterized by high levels of oxalate, with values up to 294-694 mg/100g DW reported for Japanese varieties cultivated in New Zealand and South Africa (Kristl et al., 2021; Lewu et al., 2010). Fortunately, the oxalates in taro corm are water-soluble and are often lost during boiling or significantly lost during processing. Alcantara et al. (2013) reported that converting taro corm into flour by peeling, washing with water, slicing and drying at 60°C for 24 hours significantly reduces the oxalate by 77%. Previous studies have reported that three cultivars of taro in Tonga contained 60 mg of oxalate per 100g fresh weight (Holloway et al., 1989), which is considerably lower than the 200 mg daily oxalate intake threshold recommended by the American Dietetic Association (2005). Therefore, while oxalate content remains a relevant nutritional consideration, it may not pose a significant health concern for taro consumption in Tonga. Further, the pH is an important characteristic in food as it can affect the food product's shelf life and can contribute to the loss of colour, flavour, and texture, all of which are important for sensory perception and customer acceptance. The pH of taro flour often falls within the range of 5.98-6.16 (Boahemaa et al., 2024).

2.3.1.2 Bulk Density (BD)

Bulk density is an important component of flour that needs to be known before food processing, as it reflects how much the flour will weigh for a given volume, impacting how it behaves when stacked and packaged (Boahemaa et al., 2024). Bulk density (g/mL) of flour is measured without any compression influence. Chandra et al. (2015) reveal that the bulk density depends on the flour's particle size, initial moisture content and processing conditions such as steaming or drying. The incorporation of different flours such as rice, green gram and potato flour with wheat flour tends to increase the bulk density (Du et al., 2014). The high bulk density of flour suggests a denser structure, making it ideal for mixing purposes, and suitable as a thickener in food products and preparations, as it helps reduce paste thickness, a crucial factor in

convalescent (Akpata & Akubor, 1999; Du et al., 2014). They can also provide better packaging benefits since more flour can be kept in a given space (S. R. Kumar et al., 2022). Conversely, low bulk-density flour would be less dense and could be beneficial in baby food formulation and extruded snacks (S. R. Kumar et al., 2022). However, some authors may not recommend the production of low bulk-density flours because of their low bulk density, high compressibility, high porosity/aerations and poor flow properties (Nkurikiye et al., 2023).

Previous studies have found that bulk density is positively correlated with the water absorption capacity, which is attributed to the increased starch gelatinization that also increases the density of the taro flour (Njintang et al., 2007; Tagodoe & Nip, 1994). Kaur et al. (2013) report that taro flour is the second, after potato, to have the highest BD in comparison with cereal and legume flour. The bulk density of taro flour is reported to have ranged from 0.57 – 0.71 g/mL by Njintang et al. (2007), 0.43-0.49 g/mL by Tagodoe and Nip (1994), and 0.48 – 0.55 g/mL (Boahemaa et al., 2024). Fatima (2024) reported that the bulk density increases to a higher range of 0.66-0.89 g/mL when taro corms are precooked with water, lemon, and steam, before milling into flour. Comparing the bulk density of taro to grain flours, wheat flours exhibited higher density, which typically ranged from 0.57-0.75 g/mL, indicating a higher water absorption capacity of taro than wheat flour (Bangladesh et al., 2022). Moreover, studies have also shown that the taro flour has higher tapped densities ranging from 0.57 to 0.82 g/mL (Boahemaa et al., 2024; Njintang et al., 2007).

2.3.1.3 Particle size distribution (PSD) of flour

Particle size distribution is a critical parameter influencing the physicochemical and functional properties of taro flour (Olakanmi et al., 2024). Milling taro corms into flour typically yields particles with heterogenous sizes, ranging from fine starch granules to larger fibrous fragments, depending on the milling technology, pretreatment and drying method and varietal characteristics of the corms (Deguchi et al., 2021). Deguchi et al. (2021) found that steaming of taro corms before milling into flour resulted in typically fine particles (<100 µm), whereas drying at 60 °C and 80 °C produced coarser sizes reaching up to 1000 µm. Scanning electron microscopy (SEM) further revealed that the coarser flours contained large agglomerates exceeding the typical size of compound starch granules (1-5 µm). This agglomeration was attributed to hydrophobic interactions arising from partial protein denaturation during the higher temperature drying process. When the three-dimensional structure of proteins is altered

by heat, hydrophobic amino acid residues become exposed, thereby increasing surface hydrophobicity and promoting intermolecular associations that lead to particle aggregation (Chanphai et al., 2015). Hoyos-Leyva et al. (2018) further reported that protein acts as an adhesive material facilitating the aggregation of starch granules in spray-drying microencapsulation. This suggests that protein adhered to the starch granules to form larger agglomerates during storage and resulting in higher particle sizes during storage. In contrast, other processing techniques, such as steaming, may induce more complete protein denaturation. Another study reported that taro flour with the highest moisture content tends to have a larger particle size ($> 100 \mu\text{m}$) as it occupies more pore volume. Whereas flour with a very fine particle size ($< 100 \mu\text{m}$) distribution can fill a smaller volume, which is a greater advantage in terms of packaging and transportation (Boahemaa et al., 2024).

2.3.1.4 Water absorption index, Water solubility index, and Swelling power

The water absorption and related properties of taro flour are commonly evaluated using three key indicators, namely the Water absorption index (WAI), Water solubility index (WSI) and Swelling power (SP). These properties reflect its hydration capacity, solubility and gel-forming ability, which directly influence processing behaviour, texture and suitability for different food applications (Ganongo-Po et al., 2018). The WAI, SP and WSI of taro flour have been widely documented across taro varieties and cultivation regions (Table 3). While values tend to fall within similar ranges regardless of geographic origin, taro flour generally has higher WAI and SP with low values of WSI.

WAI measures the specific volume occupied by swollen starch granules within flour after water absorption, reflecting how much water can be bound per unit weight of flour (Saxby et al., 2024). SP refers to the ability of starch granules to absorb and retain water during gelatinization, which involves the disruption of existing hydrogen bonds within the starch granules and the formation of new bonds with water molecules (Tester & Karkalas, 1996). These properties predict how flour will behave when hydrated, such as in dough preparation. Both WAI and SP are influenced by starch composition, particularly the amylose-to-amylopectin ratio, particle size and processing methods (Blazek & Copeland, 2008; Saxby et al., 2024). Ganongo-Po et al. (2018) further suggested that other compounds, different from starch, such as mucilage, are contributing significantly to the absorption of water in taro flours.

WSI, on the other hand, measures the amount of soluble molecules, such as leached amylose and amylopectin fragments, that diffuse into the water after starch granule rupture (Choi et al., 2012). The crystalline regions of starch granules break down when the temperature increases, leading to increased water absorption and eventually rupturing the granules. During cooling, the solubilized fragments can realign and form a gel structure, with the extent of leaching depending on flour type and starch granule integrity (Vamadevan & Bertoft, 2020).

The functional behaviour of starch is largely determined by its molecular composition. Amylopectin-rich flours like taro flour exhibit higher swelling power, water retention, and solubility due to their branched, less cohesive molecular structure, which is more easily disrupted (Friero et al., 2024). The high WSI leads to a slower retrogradation that is beneficial in maintaining a more stable texture in food products, potentially preventing the development of undesirable changes during storage. Pramodrao and Riar (2014) further suggested that shorter amylopectin chains in taro starch create a more open granule structure with increased surface area, enhancing the absorption and solubility compared to B-type starches like potato. In contrast, amylose forms more compact, lipid-complexed, and less soluble structures that inhibit granule swelling, increase rigidity, and lower WSI (Tester & Morrison, 1990).

From a product quality perspective, flours with high WAI and SP improve moisture retention, texture, and mouthfeel in products such as baked goods, gravies and puddings. Conversely, a combination of high WAI and SP with low WSI is desirable for high viscosity applications like thickening agents, pasta, noodles and bakery products, as it holds the dough together without excessive breakdown or water loss (Aidoo et al., 2022).

Table 3 Water-related properties of taro from different regions

Taro varieties	Cultivation country	WAI (g/g)	SP (g/g)	WSI (g/g)	References
Mana ulu, Tahitian, Bunlong, Kaua’I, Lehua	Hawaii	4.18-5.81	1.20-2.07	0.16-0.33	(Saxby et al., 2024)
White country, Ekona, RedIbo, Ngaoundere, Kwanfre	Cameroon	2.50-4.60		0.19-0.26	(Aboubakar et al., 2008)
Unspecified variety of taro flour	India	4.29		0.24	(Kaushal et al., 2012)

White varieties of taro tubers	Congo	1.45-4.00	2.17-4.36	0.11-0.15	(Ganongo-Po et al., 2018)
KA/019, BLM/SM/16 (Yeyanwoa)	Ghana	4.27-5.01	2.06-4.60	0.07-0.10	(Boahemaa et al., 2024)
Unspecified varieties	Inida	2.40-3.66		0.07-0.19	(Kumar et al., 2023)

2.3.2 Functional properties of taro flour

The functional properties of taro flour are critical determinants of the quality of the final products. These properties primarily depend on the flour's fundamental physicochemical properties. The compositions of taro flour play a crucial role in the functional properties of taro flour, with different constituents contributing variably to its functionality. Some exert major effects while others have only minor influence. Starch, for example, is mainly responsible for gelatinization, browning, dextrinization, gelation and others. Fat contributes to emulsification, aeration and shortening, whereas proteins influence foaming, browning, emulsification, coagulation and denaturation. Although the functional properties are largely determined by the compositions, other factors, including microstructure, molecular conformation, and processing method, may play a critical role in the functional properties of flour (Zubair et al., 2023).

2.3.2.1 Thermal behaviour of taro flour - Differential Scanning Calorimetry (DSC)

Starch granules are insoluble in cold water and become soluble only upon heating. During this process, they absorb water and swell many times their original size. Initially, only a small amount of water penetrates and saturates the intercellular spaces within the granules. As heating continues, the granules expand progressively until reaching a critical temperature, where they undergo irreversible swelling up to 25-30 times their original size (Havea, 1993). This phenomenon, known as gelatinization, involves the breakdown of molecular order within the granules and is characterized by the leaching of amylose, which contributes to a substantial increase in viscosity (Berk, 2013). Upon cooling, starch molecules release into a more ordered, crystalline structure, forming a gel-like substance in a process referred to as retrogradation.

The gelatinization of starch in flours occurs within certain temperatures, typically reported in the literature as intervals due to natural variability in starch characteristics (Bringhurst et al., 2022). These temperature ranges are influenced by the physical and chemical structure of the starch granules, including granule size, configuration, and the nature of intermolecular bonding (Fredriksson et al., 1998). For example, A-type starch granules such as those found in taro flour, are generally more accessible and tend to gelatinize at lower temperatures, whereas B-type granules are more compact and require higher thermal energy (Bathgate et al., 1973). However, some A-starch granule exhibits higher gelatinization temperatures and gelatinization enthalpies, due to variations in crystallinity and internal structure (Liang et al., 2025). The degree of crystallinity in starch granules is directly related to the strength of the intermolecular forces, which are influenced by factors such as the amylose-to-amylopectin ratio, molecular weight distribution, degree of branching, and the conformation and length of amylopectin chains (Leach, 1965).

Differential Scanning Calorimetry (DSC) is a standard method used to assess the thermal transitions of starches and flours, including gelatinization and retrogradation (Zobel, 1984). This technique measures endothermic reactions by tracking heat absorption during starch transition phases (Nguimbou, 2012). DSC typically identifies three key temperatures: onset temperature (T_o), which signals the beginning of starch swelling; peak temperature (T_p), associated with the highest rate of gelatinization; and the conclusion temperature (T_c), marking the end of the process. These thermal parameters vary depending on starch structure and composition, such as the amylose and amylopectin content, crystallinity and morphology, and granule size (Coronell-Tovar et al., 2018; Elmi Sharlina et al., 2017). Higher amylose content is associated with increased peak temperatures due to greater water absorption demands and stronger internal bonding (Coronell-Tovar et al., 2018).

Comparative studies have highlighted significant differences in the gelatinization behaviour of taro flours and starches across regions and cultivars. A research in Hawaii reported that the gelatinization temperatures of taro flours (72.3-79.0 °C) were higher than those of their starches (69.1-74.0 °C) (Jane et al., 1992). This discrepancy is attributed to the presence of mucilage and complex polysaccharides like arabinogalactans in the flour, which may compete with starch for water, raising the gelatinization threshold. Also, the presence of lipid in flour may complex with amylose, even in small quantities, and may delay the gelatinization process (Nguimbou, 2012). Similarly, Ganongo-Po et al. (2018) reported gelatinization temperatures ranging from 72.35-81.5 °C for five taro varieties from Congo. In contrast, flours

from Cameroon showed lower gelatinization temperatures (58.99 – 69.75 °C), with no significant difference between the onset and peak gelatinization temperature of the starches and flours (Aboubakar et al., 2008). Moreover, taro flours exhibit distinct thermal properties even when cultivars are grown under similar conditions (Aboubakar et al., 2008; Ganongo-Po et al., 2018). Compared to other tubers, taro flour (74.32 °C) has higher gelatinization temperatures than yam (78.70 °C) and sweet potato (73.57 °C), suggesting a greater thermal stability of its starch crystallites (Aprianita et al., 2009).

2.3.2.2 Pasting and gelling characteristics

When flours suspended in water are continuously heated and stirred, they gradually develop viscosity, a process referred to as the pasting properties of flours. Upon cooling and storage, some of these flour pastes can transform into a gel, a viscoelastic solid in a liquid colloid that maintains a defined shape without flowing (Tabilo-Munizaga & Barbosa-Cánovas, 2005). The pasting and gelling properties of flours are the two important functional attributes that are primarily influenced by their starch, interactions of starch and other constituents such as protein, fibre and lipid, particle size distribution and degree of starch damage (Chávez-Murillo et al., 2018; Hasjim et al., 2013). The pasting happens after gelatinization, and it involves granular swelling and leaching of amylose molecules when heating at a higher temperature. Pasting leads to the formation of a thick gel, and changes in viscosity can be observed based on rheological principles (Batey, 2007).

Several techniques could be used to assess the pasting properties of flours, including the Rapid Visco Analyzer (RVA), amylograph, and a dynamic rheometer equipped with a starch pasting cell (Yuan et al., 2021). Among these, RVA has become the preferred instrument as it is more sensitive, repeatable, and versatile (Zhang & Hamaker, 2005). This RVA simulates the cooking process of flours by subjecting a flour-water suspension to a controlled cycle of heating, cooling and holding temperature (Balet et al., 2019). As the temperature increases during the heating stage, the gelatinization temperature of amylopectin is reached, resulting in a peak in paste viscosity. At this stage, starch granules absorb water and swell, releasing amylose and smaller amylopectin molecules. During the subsequent holding phase at high temperature, the viscosity typically decreases due to granule integration and molecular (Balet et al., 2019). During the cooling period, viscosity increases again as soluble amylose retrogrades, forming a gel that contains gelatinized starch granules (Balet et al., 2019).

The amylose content is inversely proportional to the peak viscosity of flours, meaning that flours with low amylose content, such as waxy flours, exhibit higher peak viscosities, lower final viscosity and pasting temperatures (Anuntagool et al., 2006). The more amylose present during heating, the higher the tendency for amylose molecules to form a more rigid gel network, hindering the granule from swelling, which limits the viscosity development (Yuan et al., 2021).

The pasting properties of taro flour have been well documented (Anuntagool et al., 2006; Boahemaa et al., 2024; Falade & Okafor, 2015). Taro flour is reported to have different ranges of viscosity depending on the cultivars and country of cultivation. The peak viscosity of reported from Thailand ranged from 3168-5292 cP (Anuntagool et al., 2006), India was 1958cP (Kaur et al., 2013), Nigeria were 1187.52-1611.96cP (Falade & Okafor, 2015), and Ghana were 1406.25-2773.34 (Boahemaa et al., 2024). The pasting time also ranged from 5-11 minutes, and the pasting time from 78-92.53 °C (Anuntagool et al., 2006; Boahemaa et al., 2024; Falade & Okafor, 2015).

In comparison with other commercial flours, taro flour has higher pasting viscosity than the wheat flour, arrowroot flour, soya, corn, pea, lentil, white rice, rye, quinoa, and other flours, but lower than potato flour (Buzera et al., 2023; Kaur et al., 2013; Yuan et al., 2021). This high pasting viscosity of taro flour makes it a good body-providing agent and can be used as a gelling agent or thickening agent in food products. Kaur et al. (2013) found that the paste formed by taro flour remained stable when cooled, as shown by its lower setback viscosity, making it beneficial in formulations of food products that require starch stability at low temperatures.

The gelling properties of flours are often assessed using the least gelation concentration (LGC) method (Emmanuel et al., 2010). In this regard, the higher the gelling properties of flour, the lower the least gelation concentration. LGC is the minimum quantity (g) of flour that, when put in 100ml of water, allows it to form a stable gel after boiling. This parameter is pivotal for determining the texture and viscoelasticity of food products, and it is known to be inversely correlated with the swelling power and water absorption capacity (Friero et al., 2024). The formation of gel largely depends on the starch and protein in flour. Since taro is mainly made up of starch, starch is responsible for the amorphous gel, which is more or less rigid after gelatinization and the formation of starch pastes when subjected to cool water.

Flours with higher amylopectin content (waxy flour) require a small amount of flour per unit of water(LGC) to form a stable gel, due to their branched structure that traps water inside,

forming the gel (Cornejo-Ramírez et al., 2018). However, Tian et al. (2023) explain that due to the small size and low steric hindrance of amylose molecules, it exhibit fluidity gels, but during gelatinization, they leach out of the starch granules and twist together to form a network of gel that is more compact and stronger. Additionally, the drying processing of the taro chips may also be altering the gelling behaviour of taro. (Himeda, Njintang, et al., 2014) found that the flours made from sun-dried taro generally exhibited lower LGC values compared to those that were electrically dried. This suggests that the latter highly hinders the ability of the flour to form a gel and probably through the Maillard reaction. It is believed that Maillard reaction contributes to the densification of the flour, which reduces its ability to absorb water and consequently affects its gel-forming ability.

The least gelation concentration of taro was reported by Calix-Rivera et al. (2023), Kaushal et al. (2012) and Emmanuel et al. (2010). The taro flour was reported to form a soft gel at 2 %w/v and a firmer gel at 4%w/v (Calix-Rivera et al., 2023), which was lower than LGC reported by Kaushal et al. (2012) and Emmanuel et al. (2010) where it ranges from 6-8%. The LGC of taro flour was found to be lower than that of normal wheat flour, which exhibited gel at 10% w/v, pigeon pea flour at 12%w/v, and cassava flour at 4-6%w/v (Emmanuel et al., 2010).

2.3.2.3 Water absorption capacity (WAC) and Oil absorption capacity (OAC)

The capacities of flour to absorb water and oil are critical functional properties that influence its suitability for various food applications. Both WAC and OAC are closely related to texture, mouthfeel, and the flour's ability to interact with other ingredients during formulation. They refer to the amount of water and oil that flour can physically absorb and retain under ambient (non-heated) conditions (Awuchi et al., 2019).

WAC represents the optimal water level required for dough development before it becomes overly sticky and difficult to handle. Hydration occurs when starch and other flour constituents, such as protein, pentosan, and fiber, interact with water molecules through hydrogen bonding and hydrophilic interactions. Several studies have reported the WAC of taro flours from different varieties and regions. Taro cultivated in Ghana exhibited WAC values ranging from 1.71 to 1.35 g/g (Boahemaa et al., 2024), Hawaii were 0.93 to 3.48 g/g (Saxby et al., 2024), Nigeria were 2.1-3.6 g/g, India ranged from 1.34 to 2.45 g/g (Kaushal et al., 2012), Cameroonian varieties were 2.42-3.21 g/g (Njintang, Parker, et al., 2008), and an earlier study from Hawaii was 1.50-1.80 g/g (Tagodoe & Nip, 1994). Saxby et al. (2024) suggested that the

differences in WAC among the taro varieties may be attributed to the starch content of the flours. In excess water, the crystalline structure of starch is disrupted, allowing water molecules to bind to exposed hydroxyl groups of amylose and amylopectin via hydrogen bonding, leading to increased granule swelling and solubility. Varieties with high WAC are believed to also have more hydrophilic food components, such as non-starch components, such as mucilage, fibre, and cellulose may influence the WAC of taro flour (Kaushal et al., 2012).

OAC is primarily governed by the interaction between oil and the non-polar side chains of protein and the surface hydrophobicity of the flour matrix. High OAC is advantageous in food applications, where flavour retention, mouthfeel, lipid-based nutrient fortification, and shelf-life extension are important (Awuchi et al., 2019; Kaushal et al., 2012). Saxby et al. (2024) also noted that the small granule size and polygonal morphology of taro starch may contribute to both WAC and OAC. Reported OAC values for taro flours vary across regions and varieties. Taro from Ghana exhibited values between 1-1.15 g/g (Boahemaa et al., 2024), Hawai'i varieties ranged from 1.25 to 3.15 g/g (Saxby et al., 2024), Nigerian samples showed values between 2.50 and 3.35 g/g (Falade & Okafor, 2015), Indian varieties ranged from 1.04 to 2.51 g/g (Kaur et al., 2013), and Cameroonian flours ranged from 1.74 to 1.86 g/g (Njintang, Mbofung, et al., 2008).

2.3.6.5. Foam capacity (FC) and foam stability (FS)

Foaming capacity and stability of flour are crucial functional properties of flour, particularly in baking, as they impact the texture, consistency, and overall quality of the final product (Saxby et al., 2024). Foaming capacity reflects the flour's ability to incorporate air, while foam stability measures how well the air is retained in the foam over time. These properties are essential for achieving desirable characteristics, such as a light, airy texture, in food products like baked goods.

The foaming capacity of taro flour was found to range from 4.67-28.33 mL/100mL (Saxby et al., 2024), 18-27 mL/100mL for taro cultivated in Cameroon (Njintang, Mbofung, et al., 2008), 29-31 mL/100 mL for taro cultivated in Hawai'i (Tagodoe & Nip, 1994) and 9 mL/100 mL and 4.46-18.28 mL/100mL for those cultivated in India and Nigeria (Falade & Okafor, 2015; Kaur et al., 2013). Saxby et al. (2024) reported that the foaming capacity of taro flours is correlated with other texture and flavour-improving properties such as oil absorption capacity and bulk density. The foaming of flour can be attributed to proteins forming a continuous cohesive film

around the air bubbles within the foam, thereby lowering the surface tension at the water-air interface (Kaushal et al., 2012). Another study reported that foaming capacity is higher than other tuber flours, such as cassava 3.66-7.33%, sweet potato flour 12.47%, and potato were 12.92-17.60% (Chandra et al., 2015; Giri et al., 2022; Zainol, 2020). The high foaming capacity of taro flour may have been due to the high mucilage content of taro flour (Tagodoe & Nip, 1994).

The foaming stability for the taro flour may be attributed to the proteins and polysaccharides and which are good emulsifiers that may reduce surface tension and prevent coalescence (Arici et al., 2016; Badia-Olmos et al., 2023). The solubility, structure and amino acid composition of proteins present in flour greatly influence its foaming stability, but proteins that are more hydrophobic and less soluble at neutral pH may result in poor foaming stability (Badia-Olmos et al., 2023). Varieties with higher protein content are reported to have higher foaming stability, ranging from 95-98.7% than those who have lower protein content (Saxby et al., 2024). Boahemaa et al. (2024) also reported a higher foaming stability (92.57%) for the KA/019 taro variety that has higher protein content, with 85.50% for the BL/SM/16 that has the lower protein content. The protein in taro is believed to act as a binding agent during spray drying, forming unique spherical aggregates by cross-linking; however, if the taro protein is removed, irregularly shaped starch will aggregate (Hoyos-Leyva et al., 2018). With these, the high foaming stability of taro flour varieties may serve as foam-enhancing or whipping agents in the formulation of various products.

2.3.6.6. Emulsifying activity (EA) and emulsifying stability (ES)

Emulsifying activity and stability of flours are crucial for various food applications, influencing texture, appearance, and shelf life. Emulsifying activity refers to a flour's ability to stabilize an emulsion, a mixture of oil and water, while emulsion stability indicates how well the emulsion resists separation over time. These properties are primarily determined by the flour's protein and lipid components, which act as emulsifiers, helping to bind oil and water together (Nawaz et al., 2021).

The emulsifying activity of taro varieties from Hawaii reported by Saxby et al. (2024) ranged from 19.3 to 36.7% and emulsifying stability ranged from 12.7-32.7%. Their result was consistent with a previous study that reported that taro flour from India was 40 % and 42.3 % for the emulsifying activity and stability, respectively (Kaushal et al., 2012). Although studies

have determined that protein is the key determinant for the Emulsion properties of flours, Saxby et al. (2024) found that the Tahitian variety has the lowest protein content, but it exhibited the highest oil absorption capacity, foaming capacity and stability and emulsification activity and stability. It is suspected that the presence of mucilage in taro, such as gum and arabinogalactan, may have aided in stabilizing the emulsion along with the Tahitian taro proteins through their amphiphilic structures. These polysaccharides possess characteristics that can be beneficial for food processing to enhance flavour by entrapping flavouring compounds like vanillin (Tari & Singhal, 2002). The increasing EA and fat binding during food processing can prove beneficial for various food products, highlighting that taro can be a valuable additive for stabilizing fat emulsions, particularly in the production of soups, cakes and sausages (Saha & Bhattacharya, 2010).

2.3.6.7. Rheological properties of taro flour

The viscoelastic properties of flours are fundamental to understanding and optimizing dough structure, particularly in bakery applications. Since taro lacks gluten, analyzing its rheological behaviour is essential for understanding how it interacts within dough systems and influences processing performance and final product quality. Rheological measurements describe how a dough deforms and flows under stress and are essential for predicting handling properties, baking behaviour, and sensory attributes of the finished product. These assessments enable the development of improved formulations, tailored processing techniques, and consistent product outcomes.

While previous studies have investigated the rheological behaviour of taro flour in composite formulations, these often involve interactions with other ingredients that can mask the inherent functional properties of the flour (Panyoo et al., 2014). Therefore, evaluating taro flour in a simplified flour-and-water system provides a clearer understanding of its fundamental rheological characteristics. Salvador et al. (2006) emphasized that analyzing such simplified systems is crucial for determining the intrinsic mechanical properties of dough. Techniques such as small amplitude oscillatory shear testing allow simultaneous characterization of the dough's elastic (G') and viscous (G'') moduli, offering insights into its frequency and strain-dependent viscoelastic behaviour (Khatkar & Schofield, 2002).

Panyoo et al. (2014) reported that a 10% (w/v) dispersion of taro flour in water exhibited a sharp increase in storage modulus (G') at around 83 °C, indicating gelatinization due to starch

granule swelling and network formation (Vasanthan, 1996). Similarly, viscoelastic measurements showed that flour from peeled taro corms yielded higher G' values than unpeeled ones, suggesting greater gelatinization and water retention capacity. Additionally, in composite doughs, increasing the proportion of taro flour in gluten-free formulations has been shown to raise both G' and G'' values, indicating a strengthening effect on dough structure. This improvement is attributed to the high starch content (70-80%) with fine granule size and the presence of mucilage (approximately 9.1%), which contributes to the cohesive and elastic properties of taro-based doughs (Hong & Nip, 1990). These findings support the potential of taro flour as a functional ingredient for enhancing the rheological performance of gluten-free bakery products.

2.4 Applications and technological challenges of taro flour in bakery products

2.4.1 Use of taro flour in bakery formulations

Taro flour has been used in various food products, primarily for bakery formulations. Table 4 summarizes the bakery products that have been investigated using taro flour, which include cookies, bread and cake. While a few studies have explored its use in gluten-free formulations, the majority have focused on the partial substitution of wheat flour with taro flour.

The use of taro flour for gluten-free cookie formulations has shown that other gluten-free flours, such as quinoa and corn flour are need to be added with up to 50% shortening to gain better acceptability of the product (Dilek & Bilgiçli, 2021). For the partially substituted cookies, different substitution levels were recommended depending on the formulations; however, some studies recommended up to 50% of substitution (Nip et al., 1994). The differences in the substitution levels recommended in the literature are attributed to the different interactions of taro flour with the other ingredients, such as the shortening, water and hydrocolloids and the different characteristics of taro varieties (Boahemaa et al., 2024). Moreover, the utilization of taro flour for cake making has been explored and has recommended the substitution of up to 40%. The increased portion of taro flour was found to significantly increase the stiffness and rigidity of the cake batter; however, it improves the dietary content, ash content and resistance in the cake (Arıcı et al., 2021).

Further, bread is a popular bakery product that has been investigated for the potential of taro flour to substitute wheat flour. Most studies have recommended the substitution of up to 10% however, some recommended the use of enzymes such as endoprotease to improve bread specific volume and alcalase-type protease for increasing crumb softness (Calle et al., 2020). Previous studies suggested the addition of other additives such as proteins, fibres, and hydrocolloids and other ingredients such as fat sources and sweeteners to increase the volume of gluten-free breads (Djeukeu et al., 2024; Mir et al., 2016). Proteins such as whey protein, albumin and rapeseed protein isolate have been shown to increase volume and pore density of gluten-free bread (Korus et al., 2021; Pico et al., 2019). Hydrocolloids such as xanthan gum, hydroxypropyl methylcellulose, psyllium and guar gum are typically used to improve the cohesive and viscoelastic behaviour of dough by stabilizing gas cells and serving as water binders; the polysaccharides could enhance dough expansion and delay starch retrogradation (Renzetti & Rosell, 2016). Calle et al. (2020) had explored the effectiveness of mixing enzymes and hydrocolloids in bread making; they found a great improvement in bread volume and crumb softness. However, there has never been a study based on the effectiveness of adding protein to improve the textural and sensory properties of wheat-taro flour breads. The substitution of wheat flour with taro flour in bread is reported to have decreased the protein content significantly, which will possibly decrease the energy (calories) of the final product as well. This could be beneficial for those who are in weight management, but the low protein content could be affecting consumer acceptability. Fortifying bread with protein to improve quality would also be beneficial in increasing protein content, hence increasing the nutritional value of the final products.

Table 4 Bakery formulations from taro flour

BAKERY PRODUCTS	GLUTEN-FREE FORMULATIONS OR SUBSTITUTION OF WHEAT FLOUR	ACCEPTABLE SUBSTITUTION LEVEL	REFERENCE
COOKIE (BISCUIT)	50% substitution of wheat flour and gluten-free formulation	Substituting up to 50% was highly acceptable, followed by 100% taro flour cookies	(Nip et al., 1994)
COOKIE	Gluten-free formulation	20% taro flour with corn flour, with 50%	(Dilek & Bilgiçli, 2021)

		shortening, gained better acceptability	
BISCUITS	Substitution of wheat flour at 5, 10, 15, 20, 25, and 30%	10% substitute with taro flour, only 15% with egg-like taro flour	(Himeda, Njintang Yanou, et al., 2014)
COOKIE	Substitution of wheat flour (10, 20 and 30%)	Substituting up to 30%	(Alflen et al., 2016)
CAKE	Substitution of wheat flour at 10,20,30, and 40%	40% of the substitution level showed physical properties like wheat cake	(Saklani et al., 2021)
CAKE	Substitution of wheat flour (20, 20, 30 and 40%)	Substitution with 40% taro flour	(Saklani et al., 2021)
CAKE	Wheat flour substitution (3.15, 6.30, 12.50, 18.70 and 25%)	The addition of taro flour up to 25% provided similar quality attributes to the wheat cakes	(Arıcı et al., 2021)
BREAD	Gluten-free formulation and substitution of wheat flour at 3.15, 6.30, 12.30, 18.70 and 25%	12.50% of wheat flour blended with 18.70% of taro flour	(Arıcı et al., 2020)
BREAD	Gluten-free formulation blended with hydrocolloid and enzymes	Gluten-free bread with endoprotease allowed developing breads with higher specific volume, but the alcalase-type protease increases crumb softness	(Calle et al., 2020)
BREAD	Substitution of wheat flour (5, 10, 15 and 20%)	Substitution up to 10%	(Ammar et al., 2009)
BREAD	Substitution of wheat flour (5, 10, 15, and 20%)	Substitution with 10% taro flour produced bread like the control.	(Nigam & Tomar, 2022) & (Nigam & Tomar, 2022)

BREAD	Substitution of wheat flour (10, 20 and 30%)	Substitution of wheat flour in bread making should not exceed 10% (Hossain, 2016)
BREAD	Substitution of wheat flour (30, 40 and 50%)	30% substitution was rated with the highest scores in colour, while 50% substitution had the highest rating in texture (Sanful, 2011)

2.4.2 Physical and sensory characteristics

The incorporation of taro flour into baked products significantly influences their physical characteristics, including colour, texture, volume and spread ratio. Due to its high starch content and lack of gluten, taro flour tends to produce baked goods with a denser structure and lower loaf volume compared to those made entirely with wheat flour (Saxby et al., 2024). The absence of gluten restricts gas retention during proofing, leading to compact crumb structures and reduced specific volume in bread formulations (Elgeti et al., 2015). In cookies and biscuits, taro flour has been reported to increase hardness and reduce spread, attributed to the higher water absorption capacity and low fat-binding properties of the flour. Colour parameters are also affected; taro flour often imparts a slightly grey or purple hue, which may reduce visual appeal depending on consumer preferences (Dilek & Bilgiçli, 2021; Nip et al., 1994).

Despite these physical changes, the sensory acceptance of taro-based baked goods remains generally positive, especially when taro flour is used in moderate substitution levels. Studies have shown that incorporating taro flour at levels of 10-30% into bread and cookies can maintain acceptable sensory properties, including taste, aroma and mouthfeel (Dilek & Bilgiçli, 2021). Panelists have noted a mild, nutty flavour associated with taro, which can enhance product uniqueness. However, higher substitution levels may lead to increased firmness and altered mouthfeel, which can negatively affect overall acceptability (Ammar et al., 2009). Texture and flavour modifications can often be mitigated through formulation adjustments, such as the addition of protein, fats, sugars, hydrocolloids or enzymes to improve softness and palatability (Calle et al., 2020). Therefore, while taro flour poses some technological challenges, it offers an opportunity for developing culturally relevant and nutritionally enriched baked products with acceptable sensory attributes.

2.4.3 Nutritional impacts

The incorporation of taro flour into bakery products has the potential to enhance their nutritional profile, particularly by increasing dietary fibre, resistant starch, and micronutrient content (Arici et al., 2020; Saklani et al., 2021). Taro corms are known to contain appreciable levels of complex carbohydrates, including non-digestible polysaccharides, which contribute to lower glycemic responses compared to refined wheat flour. According to Nurilmala et al. (2024), the 100% substitution of wheat flour with taro flour had reduced the glycemic index of cookies by 7.86 and the glycemic load by 2.87, indicating improved postprandial glucose responses. In addition, taro flour is a source of other minerals such as potassium, magnesium, calcium and essential vitamins such as vitamin C and several B-complex vitamins (Calle et al., 2020). The inclusion of taro flour in baked products may also improve the fibre content by 14% compared to wheat flour, which supports digestive health and satiety, thus making it a viable ingredient in the formulation of functional foods with potential health benefits (Nurilmala et al., 2024).

However, substituting wheat flour with taro flour can lead to a decrease in protein content due to taro's lower inherent protein level, which may impact the nutritional balance, particularly in products where protein fortification is desirable. Taro flour generally contains 1.4-3.0 g/100g of protein, which is lower than the 10-13 g/100g typically found in wheat flour (Arici et al., 2020). The protein content of wheat flour may have been helpful for the quality of baked products when substituted with taro flour. Despite this, the absence of gluten in taro makes it suitable for gluten-free product development, especially for individuals with celiac disease or gluten sensitivity (Arici et al., 2020). Moreover, the lower fat content of taro flour compared to some cereal-based flours contributes to reducing the overall caloric value of bakery products (Njintang, Mbofung, et al., 2008). Thus, while the addition of taro flour may necessitate adjustments in formulation to maintain nutritional adequacy, it offers a promising means of diversifying the nutritional characteristics of baked goods.

2.5 Research gaps and rationale

Despite extensive studies documenting the nutritional, physicochemical, and functional properties of taro corms and flour, and their potential application in bakery products, significant gaps remain in identifying the best cultivars for bakery products. While research has provided substantial insights into the individual characteristics of taro corms and taro flour, variations

stemming from different cultivars, processing methods, and geographic origins indicate an ongoing need for in-depth investigations tailored specifically to local varieties and conditions.

One critical research gap identified in this review is the limited understanding of the fundamental physicochemical and microstructural properties of taro corms that link to the functional properties of taro flour and eventually influence taro-based products. Most studies have focused primarily on the nutritional and starch composition of taro corms; however, a lack of studies has been the investigation of the microstructure and cooking properties, which are critical for expanding value-added products for taro. This can be important to explore the potential of taro in broader food applications, such as taro chips and others.

Additionally, extensive studies have focused on the characterization of starch extraction and taro flours; however, few properties have not been explored, such as the microstructure of taro flours from different varieties. The microstructure of taro flours may exhibit unique characteristics that may be linked to the functional properties of the flour. This limitation hinders the ability to effectively predict and optimize taro flour's performance in real-world bakery applications.

Also, while existing studies have explored the applications of taro flour in bakery products, they often remain at the experimental or laboratory scale, with limited commercial success. One of the primary challenges contributing to this limitation is the technological constraint posed by taro flour's lack of gluten, resulting in products with reduced loaf volume, denser textures and altered sensory characteristics. There is a pronounced scarcity of research dedicated to overcoming these technological limitations. This may be achieved through systematic studies on formulation strategies such as fortification with proteins, ingredient interactions and processing optimizations aimed at enhancing the quality and acceptability of taro-based baked products.

Therefore, the rationale for this literature review lies in addressing these identified gaps by synthesizing existing knowledge on the physiochemical and functional characteristics of taro corms and ungelatinized flour, while specifically highlighting the opportunities and challenges for their application in bakery products. The outcomes of this review will inform future studies aimed at improving taro flour's functionality and overcoming existing technological constraints, thus supporting its broader utilization and commercialization as a valuable ingredient in food systems, contributing to food security, economic development and nutritional diversification.

Chapter 3: Characterization of taro corms

3.1 Introduction

The characteristics of taro-based products are closely linked to the intrinsic properties of taro corms and can vary significantly across different cultivars (Saxby et al., 2024). Given that taro is predominantly composed of starch, the physicochemical attributes of its starch, particularly the amylose-to-amylopectin ratio, as well as the granule shape and size, play a central role in determining the physical, chemical, thermal, morphological and functional properties of taro corms, which can be explored for varied applications. (Nagar et al., 2021). Taro corms are generally low in amylose and rich in amylopectin compared to other tuberous plant starches (Zeng et al., 2014). However, those with lower amylose content are classified as waxy varieties and often have a smaller starch granule size (Jane et al., 1992) . High amylose or mealy varieties typically exhibit a dry, crumbly, and powdery mouthfeel due to their lower moisture retention (Havea, 1993).

While sensory evaluation by trained panelists is commonly used to assess mealiness, microstructural analysis of parenchyma tissues can also provide valuable insight. Singh et al. (2005) differentiated different potato varieties through observing the microstructure of the parenchyma by assessing the granule size, cell wall structure, and the density of granule packing within the cells. These microstructural characteristics also directly influence the textural attributes of plant-based foods (Singh et al., 2005). Understanding the textural properties requires thorough knowledge of the food's microstructure and its mechanical response to external forces. When a force is applied to the cellular network, rupture occurs at the point of least resistance, depending on the strength of the middle lamella, the failure may result in either intercellular separation or cell rupture (Aguilera & Stanley, 1999). Typically, raw parenchyma tissues tend to rupture under pressure, whereas thermal processing often results in cell separation due to the weakening of pectic substances (Singh et al., 2005). The changes in taro texture during cooking are primarily associated with starch gelatinization and retrogradation, processes that are heavily influenced by thermal treatment.

From a nutritional perspective, taro corm is a valuable source of carbohydrates, dietary fibre, and minerals (Fufa et al., 2023). It is notable for its high essential micronutrients, including potassium, magnesium, and vitamin C, but is generally considered a low-protein food. However, its protein content is higher than that of many other root crops, such as cassava and yams (Koffi et al., 2020). Moreover, while taro corms are rich in micronutrients such as anthocyanins and carotenoids, their colour is directly associated with their characteristic pigmentation.

Since no single taro variety is universally suitable for all food applications, cultivar-specific analysis is essential to evaluate their suitability for various processing conditions and product qualities. Accordingly, this chapter focuses on the physicochemical and textural characterization of the corms of *C. esculenta* var. *esculenta* Holoitounga and *C. esculenta* var. *esculenta* Lau'ila, aiming to assess their potential for specific food applications.

3.2 Method and Materials

3.2.1 Materials

The two-taro cultivars selected for this study are the *C. esculenta* var. *Holoitounga* and *C. esculenta* var. *Lau'ila*, who are commonly known as Holoitounga and Lau'ila. These cultivars are among the very few that were first introduced to Tonga in the 1980s and are still widely grown to date (Prescott et al., 2004). They have distinctive features and consumers perceive them differently in terms of their colour, flavour, and mealiness. Figure 8 shows the photograph of the corms and the cross-section of the corms at their fresh, raw stage. Holoitounga appears to have dark, thick pink fibre, but Lau'ila has a lighter colour texture, with pale cream thin fibre.

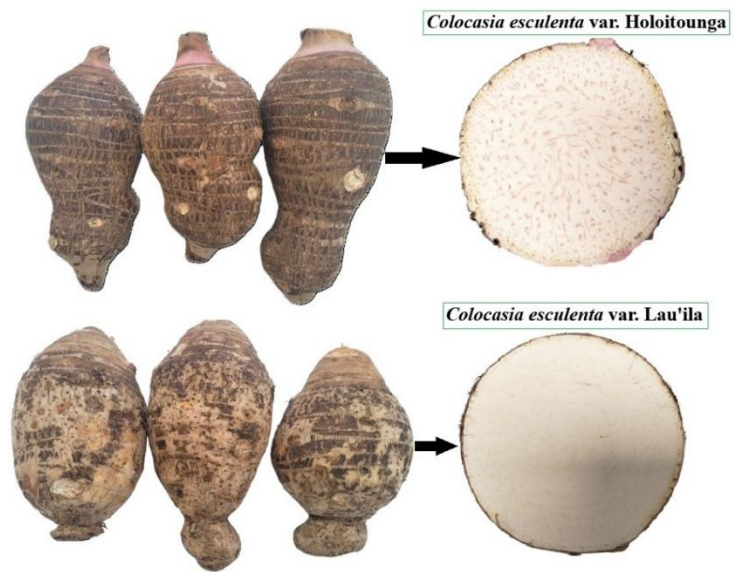


Figure 8 Photograph of the *C. esculenta* var. *Lau'ila* and *C. esculenta* var. *Holoitounga* corms and the cross-section of the raw corms

The corms of the Holoitounga and Lau'ila were freshly harvested after nine months of planting from two private plantations in the Eastern District of Tongatapu. They were freshly chopped off from the leaves and branches, cleaned with potable water and dried at room temperature before being air freighted to Palmerston North, New Zealand, which arrived within the same day of shipment. Within 24 hours of arriving at Massey University's Food Technology Laboratory, random corms were selected for freeze drying of taro corms, while the rest were used to produce taro flour.

3.2.2 Methods

3.2.2.1. Freeze drying of taro corms

The corms were peeled, cleaned and chopped into 5 x 5 mm pieces and immediately immersed in frozen liquid nitrogen and subsequently stored at -20 °C to freeze-drying. The chopped pieces were obtained from the inner parenchyma region of the corm. The lyophilized samples were then ground using a coffee grinder and sieved through a No. 70 (British Sieve Standards). Portions of the freeze-dried pieces were stored for microstructure imaging.

3.2.2.2. Dry matter, starch, amylose and amylopectin content

The dry matter content of taro corms was determined using the AACC Method 44-15.02 (AACC, 1999) with an adjustment to the temperature. The corms were peeled, cleaned, sliced into 2mm thickness and dried at 105 °C for 24 hours. The moisture content was determined in triplicate.

The total starch content of freeze-dried taro powders was determined using a Total starch assay kit (K-TSTA, Megazyme International, Ireland), following the AOAC Method 996.11.

The amylose content of freeze-dried taro powders from two taro cultivars was determined following the rapid calorimetric method described by Williams (1970). Approximately 20 mg of flour was weighed and mixed with 10 ml of 0.5 mol L⁻¹ potassium hydroxide (KOH) solution. The mixture was thoroughly dispersed and transferred to a 100 ml volumetric flask, to which 5 ml of 0.1 mol L⁻¹ hydrochloric acid (HCl) and 0.5 ml of iodine reagent were sequentially added. The mixture was then diluted to 50 ml with distilled water. The absorbance of the resulting solution was measured at 625 nm using a spectrophotometer. Amylose content was calculated based on a standard curve prepared from known concentrations of amylose and amylopectin.

Standard solutions were prepared by mixing 2, 4, 6, 8, 10 mg of amylose and 8, 16, 24, 32, 40 and 48 mg of amylopectin, each with 10 mL of 0.5 M KOH. The solution was transferred to 100 mL volumetric flasks and diluted to the mark with distilled water. From each test solution, a 10 mL aliquot was transferred to a 50 mL volumetric flask, followed by the addition of 5mL of 0.1 molL⁻¹ HCl and 0.5 mL of iodine reagent. The volume was made up to 50 mL with distilled water. Absorbance was measured at 625 nm after 5 minutes. The best-fitted curve is plotted in Figure 9.

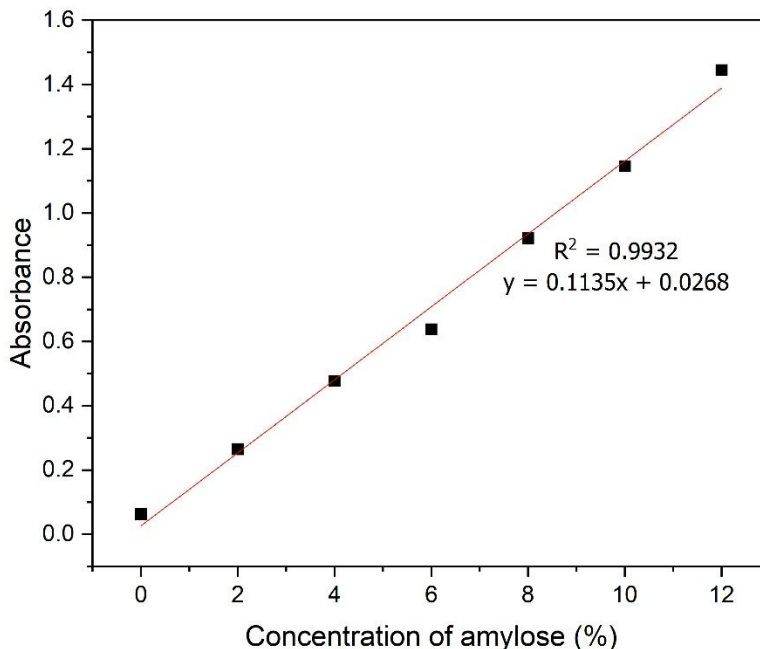


Figure 9 Standard curve for amylose determination

3.2.2.3. Proximate composition

The freeze-dried taro powder was used to determine the proximate composition of the taro corms from the two cultivars following established methodologies reported in previous studies. Moisture content was determined according to the AOAC Method 930.15 (*Official methods of analysis of the Association of Official Analytical Chemists*, 1980). The ash content was determined by incinerating 2g of powder in a furnace at 550 °C for 5 hours (Thiex et al., 2019). The crude protein content was determined based on total nitrogen content, which was measured using the Kjeldahl method ("AACC 46-12.01 Crude Protein—Kjeldahl Method, Boric Acid Modification," 2011). A 0.5g samples were accurately weighed into a digestive tube and mixed with 3g of K₂SO₄ and CuSO₄ catalyst and concentrated sulphuric acid. The mixture was then digested at 420 °C for 45

minutes or until clear and then distilled with boric acid using the Kjeltec 2100 system (Tecator, Sweden) before titrating with 0.1M HCl. The Kjeldahl nitrogen (N%) was calculated using Equation 1.

Equation 1

$$\% \text{ Nitrogen} = \frac{(A \times B) \times 14 \times 100}{1000 \times C}$$

Where A is the volume in ml of the HCl used in the titration, B is the molarity of the HCl used, and C is the weight (g) of the original sample used. The total nitrogen was then converted to crude protein by multiplying by 6.25.

The crude fat content was determined using the Ether extraction method (Mojonnier) as described by Lynch et al. (2020). Approximately 2g of the sample was mixed with concentrated ethanol and HCl (25 ml of concentrated HCl and 11 ml of water) and subsequently heated for 30 minutes. The mixture was then transferred into a Mojonnier extraction tube, where diethyl ether and petroleum were added to extract the fat. The solvent layer was carefully decanted into a pre-weighed flask and evaporated on a steamer to remove the bulk of the solvents. The final drying was carried out in an air oven at 100 °C for 90 minutes. The crude fat was calculated based on the mass difference, using Equation 2.

Equation 2

$$\% \text{ fat} = \frac{w_2 - w_1}{w_3} \times 100$$

Where W_1 is the weight of the empty flask (g), W_2 is the weight of the flask and fat (g), and W_3 is the weight of the sample taken (g).

The total carbohydrates were calculated using the difference method, subtracting the sum of other proximate compositions (on a dry basis) from 100, as described by Banti et al. (2025). The crude fibre was determined using the AOAC 962.09/978.10, employing a fibre determinator. The dietary fibre content was measured using a Megazyme kit following AOAC 991.43 (*Official methods of analysis of the Association of Official Analytical Chemists*, 1980).

3.2.2.4. Colour characteristics

The colour characteristics of raw corms from the two taro varieties were evaluated using a colourimeter (Minolta Chroma meter CR-400, Minolta Ltd., Osaka, Japan) on the CIE L*, a*, and b* colour space system. The instrument was calibrated against a standard white reference tile (L*=94.72, a*=-0.40, b*=3.61) before measurement. Each corm was divided into three sections (top, middle and basal), and colour measurements were obtained from the inner parenchyma tissue of each section. Additionally, cut pieces from each cultivar were assessed for discolouration development after 60 minutes of storage at room temperature. The changes in L*, a* and b* values during 60 minutes storage ($\Delta L = L^*_{60} - L^*_0$, $\Delta a = a^*_{60} - a^*_0$, $\Delta b = b^*_{60} - b^*_0$, where L*_0, a*_0, b*_0 represent the reading at time zero and L*_60, a*_60, b*_60 represent the reading at 60 minutes after storage) were calculated before calculating ΔE using Equation 3.

Equation 3

$$\Delta E = \sqrt{\Delta L^2 + \Delta a^2 + \Delta b^2}$$

3.2.2.5. Microstructure

The samples were taken from the inner parenchyma regions, freeze-dried, and their fractured surface examined and photographed using a scanning electron microscope (JEOL JSM-6610 LA SEM, Japan) at different magnifications and representative images were chosen. An accelerating voltage of 20 kV was used during micrography acquisition.

3.2.2.6. Cooking characteristics of taro corms

Cooking time of taro corms

The optimum cooking time of taro corms was determined by cooking uniform-sized peeled tubers (10 x 10mm) in boiling water (99 ± 1 °C). The pieces were removed from the boiling water after every 2 minutes of cooking, cooled down to room temperature for 2 minutes and then immediately subjected to the texture analyzer for analysis. Tuber pieces were cut from the inner middle sections of the corms of the two taro cultivars of the same size to ensure consistency.

The textural properties of each sample piece were measured using a texture analyzer (TAXT Plus, Stable Microsystem, Surrey, UK) equipped with a flat cylindrical probe (35 mm diameter) and a 5 kg load cell. The probe compressed the samples to 50% of their original height at a crosshead

speed of 0.83 mm/s. The optimum cooking time was defined as the time required to reach the minimum compression force during the 50% compression of the sample.

Water intake and total solid loss during cooking

The total water intake and total solids loss during cooking were determined by pre-weighing cylindrical pieces that were cooked in boiling water for 30 minutes. The cylindrical pieces were then removed, drained, rinsed with distilled water, and then redrained for 2 minutes. The cooked cylindrical pieces were weighed for the determination of water uptake (%). The rinse water was collected in a pre-weighed Erlenmeyer glass beaker and placed in an air oven at 110 °c for 24 hours. The residue was weighed and recorded as total solid loss (percentage weight of the cylindrical piece of taro).

3.2.2.7. Texture profile analysis of cooked taro corms

The texture profile of the cooked taro corms was determined by cutting taro corms from the inner parenchyma region of the taro and cooking them in boiling water for 30 minutes. The cylindrical pieces were then removed and analyzed using a texture analyzer (TAXT Plus, Stable Microsystems, Surrey, UK). The sample was compressed with a cylindrical probe 35 mm in diameter using a 5 kg loading cell. The sample was analyzed with a pre-test speed of 1.00 mmsec⁻¹, test speed of 0.83 mmsec⁻¹, and deformed at 50% of the original sample height. The analysis was performed in triplicate for each cultivar.

3.2.2.8. Statistical analysis

Statistical analysis was performed using Origin Pro software from OriginLab Corporation, Northampton, Massachusetts, USA. Analysis of Variance (ANOVA) was performed on the set of data from two cultivars, and a difference is considered significant only at a confidence level of more than 95% ($p \leq 0.05$).

3.3 Results and Discussion

3.3.1 Dry matter content, total starch content, total amylose and amylopectin content of taro corms

The analysis of the two cultivars studied revealed significant differences ($p \leq 0.05$) in their dry matter content and starch composition. Table 5 shows that Holoitounga has the highest dry matter content and amylose content. In contrast, Lau'ila demonstrated a lower dry matter content but with a higher total starch content and the greatest amylopectin content. Despite these differences, the dry matter content of both cultivars is within the typical range reported for taro corms cultivated in South Pacific island countries (<30%) (Rogers et al., 1992) and is considerably higher than values reported from Nigeria (22.53 %) (Fufa et al., 2023), and New Zealand (22 %) (Bussell & Goldsmith, 1999).

The higher dry matter content in Holoitounga cultivar suggests a firmer and drier texture, which could be advantageous in food processing that requires reduced moisture content, such as drying or flour production (Tu et al., 2023). Moreover, earlier studies have indicated that differences in moisture content among taro cultivars are associated with eating quality, with drier and firmer corms generally being more desirable compared to those with higher water content (Lebot et al., 2004).

The different starch contents of Holoitounga (66.93 %) and Lau'ila (68.40%) suggest variations in functional characteristics, which may exhibit different potential applications in food processing and product development. The total starch contents in this study were lower than those reported from Hawaii, which ranged from 73-76% (Jane et al., 1992) but higher than those reported from China (43.84-60.79%) (Yu et al., 2022).

Moreover, the amylose content (9.45%) in this study was lower than that reported by Havea (1993) for Lau'ila (13.6%). This discrepancy may be attributed to differences in sample preparation, as Havea (1993) analyzed amylose and amylopectin content from extracted starch, whereas the present study used freeze-dried flour, which contains non-starch components that may interfere with the measurement. Nevertheless, the amylose content reported here (9.45-12.75 %) remains within the range observed for taro cultivars in China (9.34-34.19 %) reported by Tu et al. (2023).

The higher amylose content in Holoitounga may confer a dry, fluffy, crumbly texture and slower digestibility, which can benefit applications targeting glycemic control (Tu et al., 2023). In contrast, the higher amylopectin in Lau'ila may result in a moist, firm and cohesive texture with improved frozen-thaw stability, making it more suitable for ready-to-eat frozen products (Singh et al., 2005). Considering the differences in dry matter content and starch composition between the two cultivars, it can be inferred that Holoitounga exhibits more floury characteristics. In contrast, Lau'ila displays properties more typical of a waxy cultivar.

Table 5 Dry matter content, total starch content, total amylose and amylopectin content of taro corms from two different taro cultivars

Cultivars	Dry matter content (%)	Total Starch (% dry weight basis)	Total amylose (% dry weight basis)	Total amylopectin (% dry weight basis)
Holoitounga	38.43 ^a	66.93 ^b	12.75 ^a	87.25 ^b
Lauila	37.23 ^b	68.40 ^a	9.45 ^b	90.55 ^a

Values are a means of triplicate measurements. Means in the same column with different superscripts are significantly different ($p \leq 0.05$).

3.3.2 Proximate Composition

The proximate composition analysis of freeze-dried powder from two taro cultivars studied, Holoitounga and Lau'ila revealed significant differences ($p \leq 0.05$) in several components (**Table 6**). The moisture content of Lau'ila was significantly higher than Holoitounga. Although the absolute moisture levels were relatively low due to the effects of freeze drying, the observed difference suggests that Holoitounga possess a greater potential for long-term storage due to its lower hygroscopicity (Onwuka, 2005). The ash content, indicative of total mineral presence, was significantly higher in Holoitounga, indicating that it may contain higher levels of essential micronutrients such as calcium, magnesium, iron, zinc and potassium (Mergedus et al., 2015).

Lau'ila exhibited significantly higher crude protein than Holoitounga. Although taro is not typically a high-protein crop, it still has higher protein content compared to other root crops such as cassava, sweet potato and yam (Temesgen & Retta, 2015a). Nevertheless, the crude protein content of both cultivars was lower than the values reported for Ethiopian taro cultivars, which

varied from 03-9.28% (Banti et al., 2025), but slightly higher than those in an earlier study, which ranged from 1.4-3.0% (Onwueme, 1999). The crude protein in taro corms is believed to be made up of all essential amino acids, particularly phenylalanine and leucine, but low in histidine and lysine (Del Rosarlo et al., 1999).

Similarly, although taro is not typically higher in crude fat, both cultivars exhibit higher crude fat contents than those previously reported for other taro varieties (0.160-1.23%) (Banti et al., 2025; Onwueme, 1999). In this study, Holoitounga showed a significantly higher crude fat content compared to Lau'ila, suggesting a slight difference in their flavour and energy density of food formulations using these cultivars.

The crude fibre and dietary fibre were also significantly higher in Holoitounga compared to Lau'ila, highlighting the potential role of Holoitounga to promote digestive health, satiety and glycaemic control, as dietary fibre is associated with these benefits (Chandrasekara, 2018). The crude fibre in this study was both lower than the reported values, which ranged from 2.96 to 5.06% (Banti et al., 2025), but aligned with an earlier study on taro cultivars in the Pacific, which reported a range from 0.60-1.18 % (Onwueme, 1999). Similarly, the dietary fibre of the studied cultivars was also similar to that reported from cultivars grown in Papua New Guinea, which ranged from 1.4-5.4 % (Wills et al., 1983).

Further, carbohydrate content, which dominated the composition of both cultivars, was significantly higher in Holoitounga compared to Lau'ila. Given that taro is a staple root crop in Tonga, this confirms its role as the primary source of energy, which is highly important in food security due to its energy density and adaptability.

Table 6 Proximate composition of freeze-dried taro powder

Cultivars	Moisture content (g/100g)	Ash content (g/100g)	Crude protein (g/100g)	Crude fat (g/100g)	Crude fibre (g/100g)	Carbohydrates (g/100g)	Dietary fibre (g/100g)
Holoitounga	1.78 ^a	3.31 ^a	2.63 ^b	1.76 ^a	1.23 ^a	89.29 ^a	4.54 ^a
Lauila	2.13 ^b	2.90 ^b	3.49 ^a	1.33 ^b	1.13 ^b	89.02 ^b	3.63 ^b

Values are a means of triplicate measurements. Means in the same column with different superscripts are significantly different ($p \leq 0.05$).

3.3.3 Colour characteristics of raw taro corms

Colour is a critical indicator of visual quality, influencing consumer perception and the behaviour of tubers during processing (e.g. drying, milling), particularly due to discolouration caused by enzymatic and chemical browning. Measurements of CIE L^* , a^* , and b^* lab scale values for the corms' parenchyma varied considerably among the two studied cultivars. Lauila showed consistently higher lightness values (L^*) than Holoitounga at 0 minutes and 60 minutes of storage, indicating that Lau'ila corms were significantly lighter or brighter in appearance ($p \leq 0.05$).

Regarding the redness/greenness, Holoitounga exhibited positive a^* values, indicating a slight red tint, while Lau'ila had negative a^* values, reflecting a slightly greener appearance. The significant difference between cultivars ($p \leq 0.05$) suggests inherent genetic differences in pigmentation, possibly related to anthocyanin or chlorophyll content (Kapoor et al., 2022). Importantly, neither cultivar exhibited a marked change in a^* values during the 60-minute storage period, suggesting relative stability of colour after peeling.

Holoitounga exhibited higher yellow-blue axis (b^*) values than the Lau'ila, although both cultivars showed high b^* values indicative of yellowish shades (Moscetti et al., 2018). However, Holoitounga's yellowish tones decreased slightly over time during the 60-minute storage, while the Lau'ila remained constant, reflecting its ability to retain colour along the b^* axis. Assessment of overall colour change (ΔE) revealed low values for both cultivars, indicating minimal colour change during the 60-minute storage period. As ΔE values below 2.0 are generally considered barely perceptible to the human eye, indicating that short-term exposure after peeling is unlikely to negatively affect visual quality in either cultivar (Minaker et al., 2021).

Table 7 Colour characteristics (L^* , a^* , b^* and ΔE) of fresh and stored (60 minutes) peeled corms from two different cultivars.

Cultivar	L^*		a^*		b^*		ΔE
	L_0	L_{60}	a_0	a_{60}	b_0	b_{60}	
Holoitounga	82.70 ^b	82.38 ^b	1.77 ^a	1.57 ^a	12.71 ^a	12.18 ^a	1.289 ^a
Lauila	88.86 ^a	89.50 ^a	-1.69 ^b	-1.69 ^b	11.96 ^b	11.96 ^a	1.67 ^a

Values are a means of triplicate measurements. Means in the same column with different superscripts are significantly different ($p \leq 0.05$).

3.3.4 Microstructural properties of raw taro corms

Observing the microstructure of cells helps to determine how the tuber behaves under mechanical damage, thermal and chemical conditions, thereby directly affecting food quality, processing outcomes, and consumer acceptance (Kaur, 2004; Zúñiga et al., 2009). The SEM images (Figure 10) of the parenchyma tissues of Holoitounga (A-D) and Lau'ila (E-H), reveal distinct microstructural features, especially in their cell arrangements, cell walls, pack density of the starch granules and overall structural organization.

The parenchyma cells of Holoitounga corms exhibited a more porous structure, with well-defined cell walls. The surface texture appeared moderately smooth, with deposits of slightly larger granules attached to the inner surfaces of the cell walls. Holoitounga starch granules are loosely distributed and individually dispersed, with minimal agglomeration or clumping. Granules are spatially separated, indicating a lack of compact packing or cohesive binding among particles. These characteristics reflect a mealy texture, which is indicative of floury behaviour consistent with the high amylose content of this cultivar (Singh et al., 2005).

In contrast, the parenchyma cells of Lau'ila corms exhibited a denser and more compact arrangement. The cells appeared larger and more irregular in shape, with rougher cell walls that were extensively covered with smaller starch granules that appeared more densely packed compared to those in Holoitounga. This compact and irregular structure is associated with its higher starch content and corresponds to a waxier texture upon cooking. Also, the slightly smaller granule size and denser packing may indicate a structural adaptation to limit moisture loss (Do et al., 2020; Gavgani et al., 2022). Furthermore, the higher degree of fracturing and deformation may be attributed to dehydration or mechanical stress.

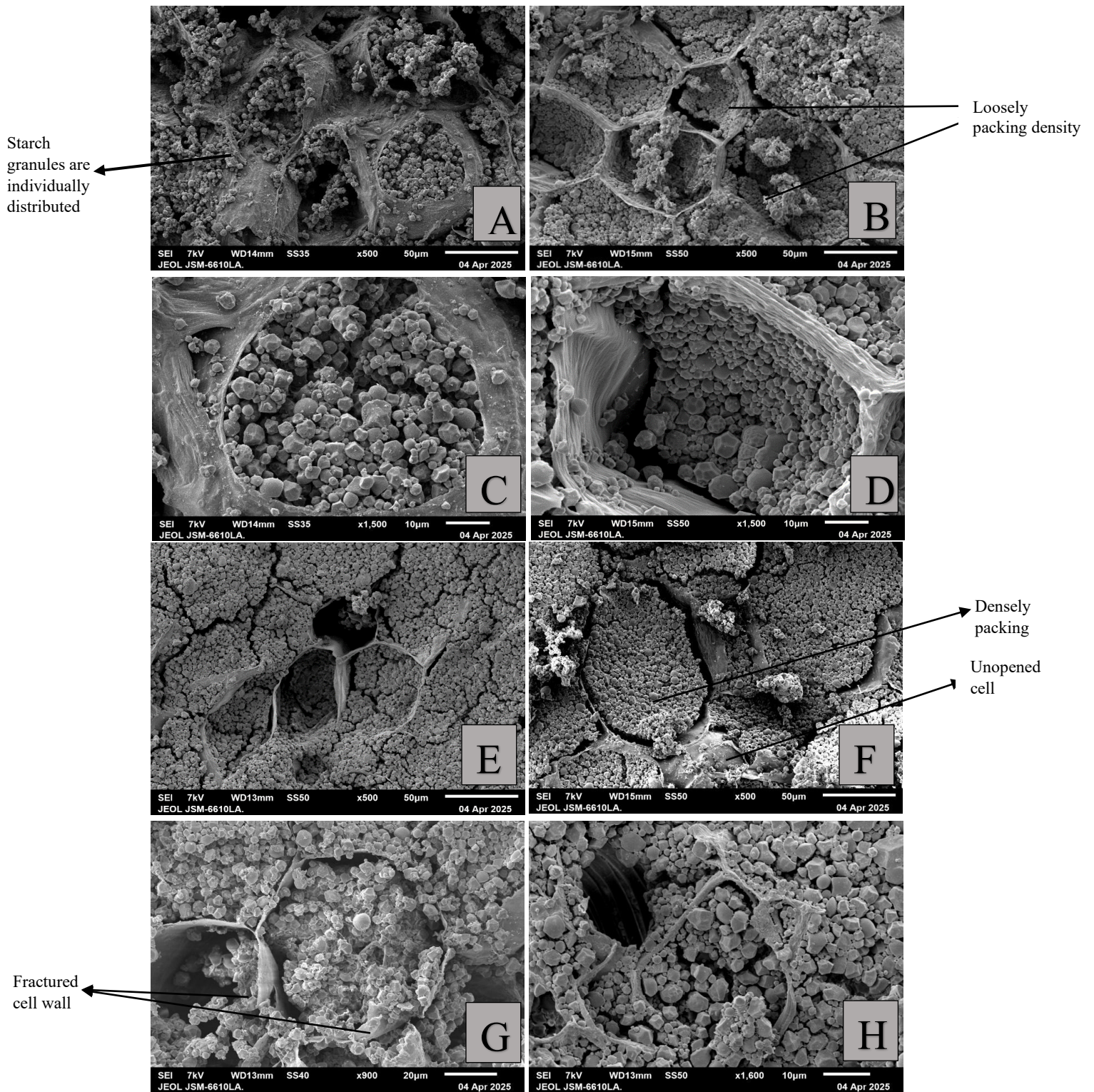


Figure 10 SEM micrographs of the raw corms of *C. esculenta* var. *Holoitounga* variety (A-D) and *C. esculenta* var. *Lauila* variety (E-H). In the raw parenchyma micrographs, starch granules are seen embedded in the cellular cytoplasm.

3.3.5 Cooking characteristics

Cooking time of taro corms

The cooking time of the two varieties, Holoitounga and Lau'ila, was determined by measuring their compression force over a 30-minute cooking period. Figure 11 revealed the distinct softening behaviours between the two, which can be attributed to their underlying physicochemical compositions, particularly their starch and amylose/amylopectin content, as well as their microstructure properties.

As seen in Figure 11a, both varieties exhibited an initial sharp decrease in compression force within the first 4 minutes of cooking, dropping from approximately 570-580 N to below 60 N. This steep decline corresponds to the early stage of cooking, during which the breakdown of the cell wall and middle lamella due to starch gelatinization and pectin solubilization, leads to the softening of the taro corms (Tian et al., 2018).

Following the initial phase, a further decline in compression force was observed from 6 to 30 minutes (Figure 11b) for both cultivars. However, Lau'ila consistently maintained a higher compression force throughout the cooking process compared to Holoitounga, indicating that it has a firmer texture over the cooking period. This could be explained by its high starch content and the dense structure of starch granules (Figure 10), which may have delayed the softening, considering it has high amylopectin content. In contrast, the softer texture of the Holoitounga corm may be attributed to the less densely packed starch, forming a crumbly texture.

Moreover, Holoitounga exhibited the lowest cooking time of 12-14 minutes, whereas Lau'ila is 14-16 minutes. The fast-cooking time of Holoitounga may be associated with the large and porous structure of its parenchyma cells, as well as its lower starch content, which allows for better water and heat penetration. Whereas the dense, compact tissue in Lau'ila resists water penetration and heat diffusion, thereby increasing its cooking time. This study is consistent with a previous study that reported a plateau in the hardness of taro corm during cooking at 15-20 minutes (Aboubakar et al., 2009).

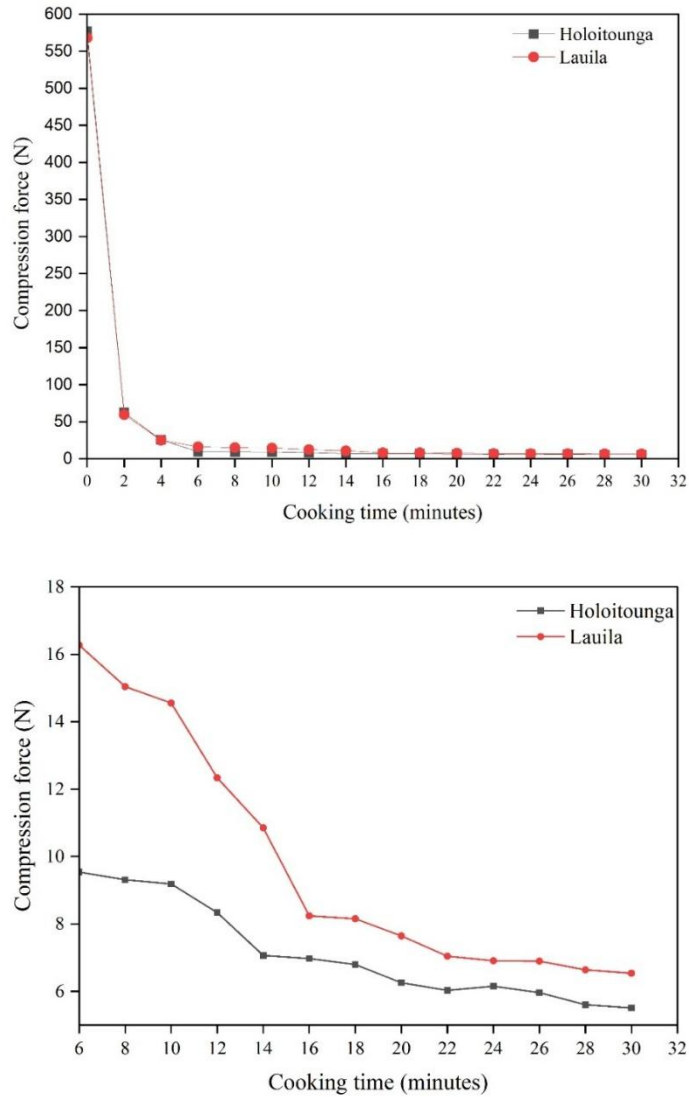


Figure 11 (a) Effect of cooking time on compression force of raw taro corms. (b) Enlargement of the 6-30 minutes cooking time region.

Water intake and total solid loss during cooking

The cooking performance of taro corms, particularly in terms of water intake and solid loss, is a critical parameter affecting both nutritional retention and consumer acceptability. As shown in Table 8, the water intake of taro corms showed significant differences ($p \leq 0.05$) between the two cultivars. Such differences can be attributed to the cellular structure, starch composition and amylopectin to amylose content, which affect gelatinisation and water binding (Genet, 1992; Tran et al., 2020).

Holoitounga shows a higher water uptake compared to Lau’ila, indicating that Holoitounga corms have a higher capacity to absorb water during cooking. The open and porous structure in the Holoitounga’s parenchyma cells likely facilitates more efficient water penetration during cooking, contributing to its significantly higher water uptake. Further, the high water uptake may also be due to the mucilages in Holoitounga, as the polysaccharides are likely to act like sponges and increase apparent water intake (Do et al., 2020). The higher total solid loss observed in Holoitounga may be attributed to its porous structure and high amylose content. The amylose content results in starch granules that hydrate and swell during boiling, exerting pressure on the cell wall and middle lamella. This pressure causes cell separation, cell collapse and disintegration, which releases more solids into the boiling water(Kaur et al., 2002).

In contrast, Lau’ila parenchyma showed a denser, more compact arrangement with more densely packed starch granules, which explained the limitation of water movement within the cells, leading to a lower water intake during boiling. Additionally, the lower total solid loss observed in Lau’ila may also be attributed to its higher amylopectin content, which promotes greater cohesiveness and swelling without extensive solubilization. Amylopectin-rich starches tend to form gels that help maintain structural integrity and reduce the migration of soluble compounds into the cooking water (Yongqiang Gong et al., 2024).

Table 8 Total water intake and total solid loss during the 30-minute cooking of taro corms from two different cultivars

Cultivars	Water intake (%)	Total solid loss (%)
Holoitounga	28.77 ^a	0.19 ^a
Lauila	27.35 ^b	0.05 ^b

Values are a means of triplicate measurements. Means in the same column with different superscripts are significantly different ($p \leq 0.05$).

3.3.6 Texture profile analysis of the cooked taro corms

Texture profile analysis quantitatively measures the mechanical properties like hardness, Fracturability, adhesiveness, springiness, cohesiveness, gumminess and chewiness to simulate the mastication behaviour of cooked taro corms. As presented in Table 9, the two cultivars demonstrated significant differences across all measured texture parameters ($p \leq 0.05$).

The high compression force of Lau'ila, as seen in Figure 11 may also explain the high hardness observed in the textural profile of its corms. This firm texture is likely associated with its tightly packed starch and cells that provide mechanical resistance, increasing hardness and ease of breaking under stress. Additionally, the high negative adhesiveness of Lau'ila may be associated with the gelatinization of starch granules in which they are swollen, break and release amylose and amylopectin, forming a thick sticky paste that adheres to surfaces such as plates or utensils during consumption. Amylopectin, in particular, contributes significantly to adhesiveness due to its highly branched structure and ability to form viscous, cohesive gels (H. Han et al., 2019). The high amylopectin in Lau'ila, may explain why it has higher adhesiveness and cohesiveness than Holoitounga. Similarly, the high springiness, gumminess and chewiness of Lau'ila may also be explained by the ability of the high amylopectin content to form a strong gel, making the texture more resilient and springy (Boahemaa et al., 2024).

In contrast, Holoitounga exhibited the highest fracturability, reflecting its high dry matter content, which leads to loose cell structure and weak intercellular adhesion after cooking (Kaur et al., 2002). Also, during boiling, the high amylose content in Holoitounga swells and gelatinises, increasing internal pressure and causing the cells to separate easily, resulting in a crumbly, mealy texture that is very brittle (Chen, 2020).

Table 9 Texture profile parameters of cooked taro corms from two different cultivars

Cultivars	Hardness (N)	Fracturability (N)	Adhesiveness (g. sec)	Springiness (m)	Cohesiveness	Gumminess (N)	Chewiness (g.sec)
Holoitounga	11.57 ^b	23.53 ^a	-459.62 ^a	0.27 ^b	0.11 ^b	1.77 ^b	0.57 ^b
Lauila	20.52 ^a	10.42 ^b	-2140.69 ^b	0.81 ^a	0.16 ^a	2.59 ^a	1.51 ^a

Values are a means of triplicate measurements. Means in the same column with different superscripts are significantly different ($p \leq 0.05$).

3.4 Conclusion

In conclusion, the cooking and textural characteristics of corms from two different taro cultivars were found to be strongly linked to their chemical compositions and microstructural characteristics. Holoitounga with higher dry matter, amylose with a loosely packed cell arrangement, larger cells, and more intact cell walls showed a lower cooking time and higher water intake and total solid loss during boiling. Also, it has a soft, crumbly texture that correlates with its high fracturability. In contrast, Lau'ila with lower dry matter, higher starch content and amylopectin with tightly packed starch granules and cell arrangement with vulnerable cell walls to heating and mechanical stress showed a firmer texture with higher adhesiveness, springiness, cohesiveness, gumminess and chewiness with longer cooking time.

Chapter 4: Characterization of ungelatinized taro flours

4.1 Introduction

Taro (*Colocasia esculenta*) is regarded as one of the perishable crops due to its high water content that significantly limits its marketability and storage life (Aboubakar et al., 2008). Conversion of taro corms into flours extends product longevity and opens opportunities for diversification into a wider range of food products such as gluten-free baked goods, snacks, and reconstituted products (Boahemaa et al., 2024). However, the successful utilization of taro flour in food systems requires a clear understanding of its physicochemical and functional properties, which govern its performance during processing and determine its suitability for specific applications (Wang et al., 2020). Properties such as moisture content, proximate analyzes, swelling capacity, water and oil related properties, gelatinization behaviour, pasting and emulsion characteristics influence how taro flour behaves under different processing conditions. These characteristics are highly dependent on the cultivar, growing environment, and processing method and therefore must be thoroughly evaluated (Wang et al., 2020).

Taro flour is naturally gluten-free, which presents challenges in its application to food products, particularly in baked goods, where gluten plays a crucial role in the dough structure and eventually the quality of the final products (Arici et al., 2020). However, the incorporation of protein concentrates has been shown to mimic the functional properties of gluten, enhancing structure, moisture retention, and the overall eating quality of gluten-free products (Aprodu et al., 2016; Ozgolet et al., 2025; Ziobro et al., 2016). Egg white albumen and milk-derived proteins have been particularly effective in improving the rheological properties and volume of gluten-free formulations (Ziobro et al., 2016). From a sustainability perspective, plant-based proteins such as pea protein have also demonstrated potential to enhance both the nutritional and functional qualities of gluten-free products, improving consumer acceptance (Sahagún et al., 2018). However, most of these studies have focused on other gluten-free flours such as cassava starch, corn, and rice flour, with limited to no research conducted on taro flour.

This chapter aims to evaluate the physicochemical and functional properties of flour derived from two Tongan taro cultivars analyzed in Chapter 3, Holoitounga and Lau'ila, focusing on their ungelatinized forms. By characterizing these properties, this study seeks to identify their unique functional behaviours and highlight potential food applications. Specifically, the objectives of this study are

- To analyze the physicochemical and functional characteristics of ungelatinized taro flours from the two cultivars
- To assess the rheological properties of taro flour samples and investigate the effect of incorporating proteins such as egg albumin, whey milk protein (casein) and pea protein on their rheological behaviour with comparison to wheat flour

Through this analysis, the study contributes to the body of knowledge required for the development of taro-based food products and supports efforts toward sustainable crop utilization and food innovation in Tonga.

4.2 Materials and Methods

4.2.1 Preparation of ungelatinized taro flours

The two *C. esculenta* var. *esculenta* cultivars characterized in Chapter 3, Holoitounga and Lau'ila corms, were peeled and washed thoroughly with tap water and sliced into 2mm thickness using a stainless benchtop slicer machine. The slices were then placed on aluminium trays with holes and dried in an electric dryer with convection air for 24 hours at 45 °C. The drying temperature of 45 °C was selected based on the reported gelatinization temperature of 80 °C for the Lau'ila cultivar, as identified by Havea (1993) and further confirmed by preliminary differential scanning calorimetry (DSC) analysis conducted on the freeze-dried powder samples. Maintaining low drying temperatures (45 °C) over an extended period ensured that the starch granules in the taro flours remained ungelatinized, which was essential for the objectives of this study.

After drying, the chips from each batch were milled using a Milling machine (HDC, China). The milled flours were then sieved through 212 µm (No. 70 US) mesh and packed in a plastic bucket, sealed and stored in the Massey Product Development Lab (Riddet Complex East Wing) dry storage for further analysis and product development.

4.2.2 Physicochemical Characterizations

4.2.2.1. Proximate analysis

The ungelatinized taro flours were analyzed in triplicate for moisture, crude protein, crude fat, and ash using approved methods 925.10, 923.03, 922.06, and 920.87 of the *Official methods of*

analysis of the Association of Official Analytical Chemists (1980). The difference method was used to calculate the carbohydrate content by subtracting the sum of moisture, protein, ash, fat and fibre from 100. Also, the energy (E) was determined by taking the sum of multiplying the protein by 4, carbohydrates by 4, and fat by 9 (Boahemaa et al., 2024).

4.2.2.2. Bulk density (BD)

The bulk density of the two pre-gelatinized flours was analyzed using the method described by Kaur et al. (2013). Flour was filled to 10 mL in a pre-weight graduated cylinder. The weight of the flour and the cylinder was noted. BD was calculated from the weight and volume of the flour in the cylinder. Tapped density was measured by tapping the bottom of the cylinder several times until there was no further diminution of the sample level. The new volume was noted. Measurements were made in triplicate. The bulk density and tapped density were calculated following Equations 1 and 2, respectively.

Equation 4

$$\text{Bulk density } \left(\frac{g}{mL}\right) = \frac{\text{Weight of sample (g)}}{\text{Volume before tapping (mL)}}$$

Equation 5

$$\text{Tapped density } \left(\frac{g}{mL}\right) = \frac{\text{Weight of sample (g)}}{\text{Tapped volume (mL)}}$$

4.2.2.3. Water absorption index (WAI), water solubility index (WSI), and swelling power (SP)

A modification method of Boahemaa et al. (2024) was used to determine the WAI, WSI and SP of the ungelatinized taro flours. A suspension of 2.5g of flour in 30 mL of distilled water was heated in a water bath at 90 °C for 15 min. After cooling, the paste was centrifuged (Thermo Fisher Scientific Centrifuge, Germany) at 4000xg for 40 minutes. The supernatant was dried overnight at 110 °C, and the sediment was weighed. All measurements were performed in triplicate. WAI, WSI and SP were calculated using Equation 6, Equation 7, and Equation 8, respectively.

Equation 6

$$\text{WAI } \left(\frac{g}{g}\right) = \frac{\text{Weight of sediment (g)}}{\text{Weight of sample (g)}}$$

Equation 7

$$WSI \left(\frac{g}{g} \right) = \frac{\text{Weight of dissolved solids in supernatant (g)}}{\text{Sample of weight (g)}}$$

Equation 8

$$SP \left(\frac{g}{g} \right) = \frac{\text{Weight of sediment (g)}}{\text{Sample weight (g) - weight of dissolved solids in supernatant (g)}}$$

4.2.2.4. Colour characteristics

The colour characteristics of flour from different cultivars were measured in triplicate using a Chroma meter CR-400 calorimeter (Konica Minolta, Japan) based on L*, a* and b*. The instrument was calibrated against a standard white coloured reference tile (Y=86.6, X=0.3162, y=0.3232). The flour samples were filled in small plastic petri dishes and placed on top of the measuring head, covered with a black protection tube, before the measurements were taken.

4.2.2.5. pH of flour

The pH of the flour samples was measured in triplicate using an Orion 3 Star pH benchtop meter (Thermo Electron Corporation). A 10g flour sample was homogenized in 50 mL of distilled water before measuring the pH for each cultivar.

4.2.2.6. Particle size distribution

The particle size distribution of the flour samples was analyzed using a laser particle size analyzer (Mastersizer S, Malvern Instruments, France). Each sample was dispersed in absolute ethanol. Five measurements were made for each of the flour samples. The particle size distributions were characterized by Dv10, Dv50, and Dv90 values, which are the equivalent volume diameters at 10%, 50% and 90%, respectively.

4.2.2.7. Microstructure

The samples were taken from the inner parenchyma regions, freeze-dried, and their fractured surface examined and photographed using a scanning electron microscope (JEOL JSM-6610

LA SEM, Japan) at different magnifications and representative images were chosen. An accelerating voltage of 20 kV was used during micrography acquisition.

4.2.3 Methods for Functional Characterization

4.2.3.1. Thermal properties

The thermal properties of the ungelatinized flours were analyzed using Differential Scanning Calorimetry (DSC), following the method of Aboubakar et al. (2008). DSC thermograms of taro flours were recorded on a DSCQ2000 (TA Instruments, USA). Approximately 18.0mg of flour was mixed with distilled water in a 1:3 (w/v) ratio, sealed hermetically in aluminium pans, and allowed to equilibrate for 1 hour. An empty sealed pan was used as the reference.

The samples were heated from 25 – 98 °C at a rate of 5 °C/min. The instrument was calibrated for temperature and enthalpy using indium. The onset temperature (T_o), peak temperature (T_p), and conclusion temperature (T_c) of gelatinization were determined from the thermograms by the intersection of tangents at the baseline and the inflection points of the peak. Heat capacity and enthalpy of gelatinization (ΔH) were calculated using the instrument's software. All measurements were performed in triplicate.

4.2.3.2. Gelling properties – Least gelation concentration (LGC)

The least gelation concentration of the taro flour samples was determined using the modified method of Coffman and Garciaj (1977). Sample suspensions ranging from 2% to 20% (m/v), were prepared by dispersing the flour in 10 mL of distilled water in test tubes. The tubes were heated in a gently boiling water bath for 1 hour and then cooled rapidly at room temperature for 2 hours. After cooling, each tube was inverted. The LGC was recorded as the lowest concentration at which the samples did not fall or slip upon inversion.

4.2.3.3. Pasting properties

The pasting properties of taro flour samples were determined using a Rapid Visco Analyzer (RVA, 4500 Model, Perten Instrument, US) in accordance with AACC International Method 76.2101, ICC Standard No. 162, as described by Yuan et al. (2021). A 3.0 g of flour sample was weighed into an RVA canister, and 25 mL of distilled water was added to obtain a

dispersion at a concentration of 14% moisture. During the measurement, the sample was equilibrated at 50°C for 1 minute, then heated to 95 °C at a heating rate of 6 °C/min. The temperature was held at 95°C for 5 minutes, followed by cooling back to 50 °C at the same rate. The temperature was then held at 50°C for an additional 2 minutes.

RVA measurements were performed at two different temperatures (50 and 90 °C). The paddle speed was set to 960 rpm for the initial 10 seconds to ensure complete suspension, then reduced to 160 rpm for the remainder of the run. The pasting properties, including the peak viscosity (PV), holding strength (HS), breakdown viscosity (peak viscosity minus the holding strength), final viscosity (FV) and setback viscosity (final viscosity minus the holding strength), were recorded from temperature versus the viscosity curve. All measurements were conducted in triplicate.

4.2.3.4. Water absorption capacity (WAC) and oil absorption capacity (OAC)

The water absorption capacity and oil absorption capacity of taro flours were determined using the method described by Kaur et al. (2013). The WAC was determined by dispersing 3.0g of taro flour in 25 ml of distilled water in a pre-weighed centrifugation tube. The dispersion was stirred intermittently and allowed to stand for 30 minutes. It was then centrifuged at 3000xg for 25 minutes. The supernatant was decanted, and the tube was inverted and drained at 50 °C for 25 minutes before reweighing.

For OAC, 0.5g of taro flour was mixed with 6 mL of palm oil in a pre-weighed centrifuge tube. The mixture was stirred for 1 minute using a thin brass wire to ensure uniform dispersion, then allowed to stand for 30 minutes. It was centrifuged at 3000xg for 25 minutes, after which the separated oil was removed with a pipette. The tubers were inverted and allowed to drain for 25 minutes before reweighing. All measurements were performed in triplicate. The WAC and OAC values were expressed as grams of water or oil absorbed per gram of dry sample.

4.2.3.5. Foaming capacity (FC) and foam stability (FS)

The capacity and stability of foams were determined following a method of Lin et al. (1974) with slight modifications. A 3% (w/v) dispersion was prepared by mixing 50 mL of taro flour suspension in distilled water. The mixture was homogenized using a high-speed blender for 3 minutes. The homogenized sample was immediately transferred to a 100 mL graduated

cylinder. The blender was rinsed with an additional 10 mL of distilled water, which was also added to the cylinder. The total volume was recorded before and immediately after whipping. Foaming capacity was calculated as the percentage increase in volume due to whipping. Foam stability was assessed by measuring the foam volume in the graduated cylinder at storage intervals of 20, 40, 60 and 120 minutes. All measurements were performed in triplicate.

4.2.3.6. Emulsion capacity and stability

Emulsion capacity and stability were determined following the method of Boahemaa et al. (2024), with slight modifications. In a centrifuge tube, 1.0 g of taro flour was mixed with 10 mL each of distilled water and soybean oil. The mixture was homogenized and centrifuged using a refrigerated centrifuge (Multifuge X4R Pro, Thermo Fisher, Germany) at 2000 x g for 30 minutes. Emulsion capacity was calculated as the ratio of the height of the emulsified layer to the liquid layer's height and expressed as a percentage. For emulsion stability, the prepared emulsion was heated in a water bath at 80 °C for 30 minutes, cooled to 25 °C, and then centrifuged at 2000 × g for 15 minutes. Emulsion stability was similarly calculated as the percentage ratio of the height of the emulsified layer to the total height of the liquid layer. All measurements were performed in triplicate.

4.2.4 Rheological analysis of taro flour and its protein fortified blends in a powder-and-water system

The rheological properties of taro flour and its protein fortified blends were determined using a controlled stress Rheometer (Physica MCR 301, Anton Paar, Austria) using a 40mm parallel plate system with a 1mm gap. The dough was prepared with a 1:1 ratio of powder to water, considering the moisture content in each powder. The protein isolates, including egg white, pea protein and milk protein concentrate (casein), were fortified with 10w/w of taro flour. Each dough samples were subjected to strain, frequency and temperature sweeps.

The strain sweeps were performed at 1 Hz from 0.01 to 10 Pa at 25 °C to determine the linear viscoelastic region of the samples, which were all found to be 0.01%. The frequency sweeps were running from 0.01 Hz to 10 Hz at 25 °C. The temperature sweep tests were performed by heating doughs from 25 °C to 100 °C and cooling from 100 °C to 25 °C at 5 °C/min heating

rate with a fixed strain of 0.2% and frequency of 1 Hz. The tests were performed in triplicate. The values of the storage modulus (G'), the loss modulus (G'') and the damping factor ($\tan \delta$) were recorded as a function of strain, frequency and temperature sweeps.

4.2.5 Statistical Analysis

Statistical analysis was performed using Origin Pro software from Origin Lab Corporation, Northampton, Massachusetts, USA. Analysis of Variance (ANOVA) was performed on the set of data from two cultivars, and a difference is considered significant only at a confidence level of more than 95% ($p \leq 0.05$).

4.3 Results and Discussions

4.3.1 Physicochemical Characteristics

4.3.1.1 Proximate Composition

The proximate composition of Holoitounga and Lau'ila flours reveals notable differences in their nutritional profiles (Table 10). As expected, the results showed that carbohydrates is the most important chemical component in flours while the proteins and fats was very limited. The carbohydrate levels varied from 85.71 – 86.72 g/100g, which consistent with those reported by Boahemaa et al. (2024) (83.5-86.6 g/100g) but lower than taro flours reported by Aboubakar et al. (2008) (90.5-95.5 g/100g). Carbohydrates were marginally higher in Holoitounga compared to Lau'ila, contributing to its higher caloric density. The observed carbohydrate content of Holoitounga, coupled with its significantly higher crude fat, contributed greatly to its more energy-dense compared with the Lau'ila.

Lau'ila flour exhibited the highest moisture content compared to the Holoitounga flour ($p \leq 0.05$), suggesting that the two flours may require different storage conditions. Specifically, Lau'ila may need stricter storage conditions to prevent clumping or mould growth (Zulfa et al., 2023). These differences in moisture content could be due to residual water trapped within the densely packed starch granules in Lau'ila (Chapter 3).

Crude protein content was significantly higher ($p \leq 0.05$) in Lau'ila (3.59 g/100g) than in Holoitounga (2.64 g/100g). This distinction may have implications for the nutritional quality of the flour and functional properties such as oil absorption, emulsion, foaming and rheology

(Hasmedi et al., 2021). In contrast, Holoitounga exhibited a higher crude fat (1.72 g/100g) than Lau'ila (1.33 g/100g), suggesting that the functional properties and taste of the two flours may differ considerably. Holoitounga flour may enhance flavour richness and mouthfeel in products like cookies and shortbreads but may be susceptible to oxidative rancidity compared to Lau'ila. However, crude fat in taro is still relatively lower than other gluten-free flours (1.4-6.6%) (González et al., 2025).

Ash content, a proxy for total mineral content, was comparable between the two flours, indicating similar mineral availability. Compared to the taro corms (Chapter 3), the ash content of the flours was relatively lower than the native taro corms. This may be due to loss of minerals during the preparation of the flour, such as washing, drying and milling of flours (Aricı et al., 2016).

Table 10 Proximate compositions of the taro flour sample

Flour samples	Moisture content (g/100g)	Crude protein (g/100g)	Crude fat (g/100g)	Ash content (g/100g)	Carbohydrates (g/100g)	Energy (kCal)
Holoitounga	6.97 ^b	2.64 ^b	1.72 ^a	1.95 ^a	86.72 ^a	372.92 ^a
Lau'ila	7.40 ^a	3.59 ^a	1.33 ^b	1.97 ^a	85.71 ^a	369.17 ^b

Values are a means of triplicate measurements. Means in the same column with different superscripts are significantly different ($p \leq 0.05$).

4.3.1.2. Bulk density (BD), Water absorption index (WAI), water solubility index (WSI), swelling power (SP), and pH

The bulk density and hydration properties of flours are critical, particularly for their potential usage in food applications. Table 11 shows a significant difference between the Holoitounga and Lau'ila taro varieties in terms of BD, WAI, WSI, SP, and pH.

Bulk density is an important parameter for the packaging, transporting and reconstitution behaviour of flour (Augustin et al., 2003). Holoitounga exhibited a significantly higher bulk density and tapped density ($p \leq 0.05$) compared to Lau'ila. The higher densities observed in Holoitounga may be attributed to its lower moisture content and finer particle size. Such properties may be favourable in applications requiring higher solid content and compactness, such as in noodle or pasta production, where denser flours can contribute to firmer textures.

In contrast, the higher density of Lau'ila flour is attributed to its high moisture content and coarser particle size. This characteristic is advantageous for products where lightness and aeration are desired, such as baked goods and extruded snacks and also for the production of weaning foods, as low bulk implies food that may contain other nutrients apart from fibre (Akubor, 2007; Boahemaa et al., 2024). This study is consistent with Boahemaa et al. (2024) where BD and TD for taro flours were ranged from 0.48 to 0.55 g/mL and 0.75 to 0.82 g/mL, respectively.

The ability of flour to absorb water and swell is crucial in determining its behaviour during cooking and processing. Holoitounga's significantly higher WAI ($p \leq 0.05$) reflects its stronger capacity to absorb and retain water, likely due to high amylose starch granules that are more compact and crystalline, therefore, it requires more water to penetrate and disrupt the structure, leading to greater swelling and water uptake during heating (Singh et al., 2003). This is consistent with Boahemaa et al. (2024), where the taro cultivar (BL/SM/16) with the slightly highest amylose content has a higher water absorption capacity.

Conversely, Lau'ila exhibited a significantly higher WSI, and marginally elevated SP compared to Holoitounga. These higher values may be attributed to an increased content of phosphate groups on amylopectin. The electrostatic repulsion between the adjacent phosphate groups enhances hydration by weakening the bonding within the crystalline regions of the starch granules (Singh et al., 2003). Additionally, the higher WSI of Lau'ila corresponds with the thick gel-like layer observed on top of the flour in Figure 12, suggesting a greater release of soluble components such as damaged starch, sugars, or short-chain polysaccharides. The clear yellow colour in the water phase in the Holoitounga samples may be attributed to the high level of flavonoid (flavones) in its taro corms. These flavonoids may be contributing to the various health benefits of taro corms, including the antioxidant and anti-inflammatory properties (Lebot & Legendre, 2015; Ouédraogo et al., 2023). Further, the pH of Holoitounga was significantly higher than Lau'ila ($p \leq 0.05$). The pH is an important characteristic in food because it can affect a food product's shelf life. It can contribute to the loss of colour, flavour, and texture, all of which are important for sensory perception and consumer acceptance (Boahemaa et al., 2024).

Table 11 Bulk density, Water hydration indices and pH of the two taro flours studied

Flours	Bulk density (g/mL)	Tapped density (g/mL)	WAI (g/g)	WSI (g/g)	SP (g/g)	pH
Holoitounga	0.59 ^a	0.90 ^a	4.70 ^a	0.19 ^b	5.52 ^a	6.53 ^a
Lau'ila	0.47 ^b	0.78 ^b	3.96 ^b	0.30 ^a	5.64 ^a	6.13 ^b

Values are a means of triplicate measurements. Means in the same column with different superscripts are significantly different ($p \leq 0.05$).



Figure 12 Flour samples after centrifuged at 4000xg for 40 minutes

4.3.1.3. Colour characteristics

Colour is a critical quality attribute of flour, influencing both consumer perception and the suitability of the flour for specific food applications. The colourimetric values for the taro flours, expressed as L*, a* and b*, differed significantly ($p \leq 0.05$) (Table 12).

The L* value indicates the lightness of the flour, with higher values corresponding to a lighter appearance. Lau'ila flour exhibited a significantly higher L* value than Holoitounga, indicating that Lau'ila is visually lighter and more appealing for products where a white, pale colour is desirable, such as bakery products and noodles. The lower L* value of Holoitounga suggests a comparatively darker flour, which could result from higher levels of residual pigments and phenolic compounds (He et al., 2021).

The a* values measure the red-green balance, with negative values indicating a greenish hue and positive values indicating a reddish hue. Holoitounga flour had a slightly negative a* value, while Lau'ila was near neutral, and the difference was statistically significant. The greenish tint in Holoitounga may be attributed to the presence of certain pigments, such as chlorophyll or other compounds. In contrast, Lau'ila's near-zero a* value suggests a more neutral colour

profile, which is generally preferred in flour-based products as it does not impart any unwanted colour tones to the final product.

Furthermore, the b^* value reflects the yellow-blue balance, with higher values indicating greater yellowness. Holoitounga has a significantly higher b^* value compared to Lau'ila, indicating a more pronounced yellow hue. Overall, the differences in the colour values of the taro may also be attributed to their biological origin, temperature during the growing season, and soil type and moisture (Singh et al., 2003)

Table 12 Colour of taro flour.

Flours	L*	a*	b*
Holoitounga	89.55 ^b	-0.31 ^b	8.84 ^a
Lau'ila	92.55 ^a	0.03 ^a	5.43 ^b

L =lightness from dark, +a*/-a* =redness/greenness, b* =yellowness/blueness. Values are a means of triplicate measurements. Means in the same column with different superscripts are significantly different ($p \leq 0.05$).*

4.3.1.4. Particle size distribution

As shown in Table 13, significant differences ($p \leq 0.05$) were observed between the particle size of flour samples across all measured particle size indices. Holoitounga exhibited a bimodal distribution (Figure 13), with a major peak around 120 μm and a secondary shoulder between 10-30 μm , and a median particle size of 55.67 μm . This heterogeneity in particle size may be attributed to mechanical resistance during milling (Toozandehjani et al., 2017). The presence of a significant proportion of finer particles may enhance water absorption and swelling capacity, potentially improving viscosity; however, it may also lead to increased dustiness or lumping during rehydration (Dayakar Rao et al., 2016; Del Gaudio et al., 2013).

In contrast, Lau'ila presented a unimodal distribution (Figure 13), with a prominent peak between 70-90 μm with a median particle size of 84.98 μm (Table 13), indicating coarser particles and relatively uniform particle size. This sharp distribution curve suggests consistent grinding or a more homogenous structural composition of the Lau'ila corm, which may result in predictable behaviour during mixing and hydration processes. A narrow particle size range is often associated with better packing ability, reduced segregation in dry blends, and consistent pasting properties (Boahemaa et al., 2024; Toozandehjani et al., 2017). The coarser particles

of Lau'ila flour may also be attributed to its higher starch content and higher amylopectin content, result in a slower rate of moisture loss and a more gradual change in texture, which can lead to a denser, tougher and less brittle chip that resists fracturing during drying, and therefore more difficult to mill (Basiev et al., 2021). Conversely, Holoitounga flour, with its higher amylose content and porous microstructure, produces more brittle textures. This brittleness makes the dried chips easier to break and consequently easier to grind into finer flour particles.

Table 13 Particle size distribution of taro flours

Flour sample	Particle size distribution			
	D(0.1), μm	D(0.5), μm	D(0.9), μm	D [4,3], μm
Holoitounga	6.284 ^b	55.673 ^b	174.473 ^b	74.084 ^b
Lau'ila	9.156 ^a	84.975 ^a	211.637 ^a	99.538 ^a

D(0.1), D(0.5), and D(0.9) represent the particle sizes below which 10%, 50%, and 90% of the sample particles fall, respectively. D[4,3] represents the volume-weighted mean diameter. Values are the means of triplicate measurements. Means in the same column with different superscript letters are significantly different at $p \leq 0.05$.

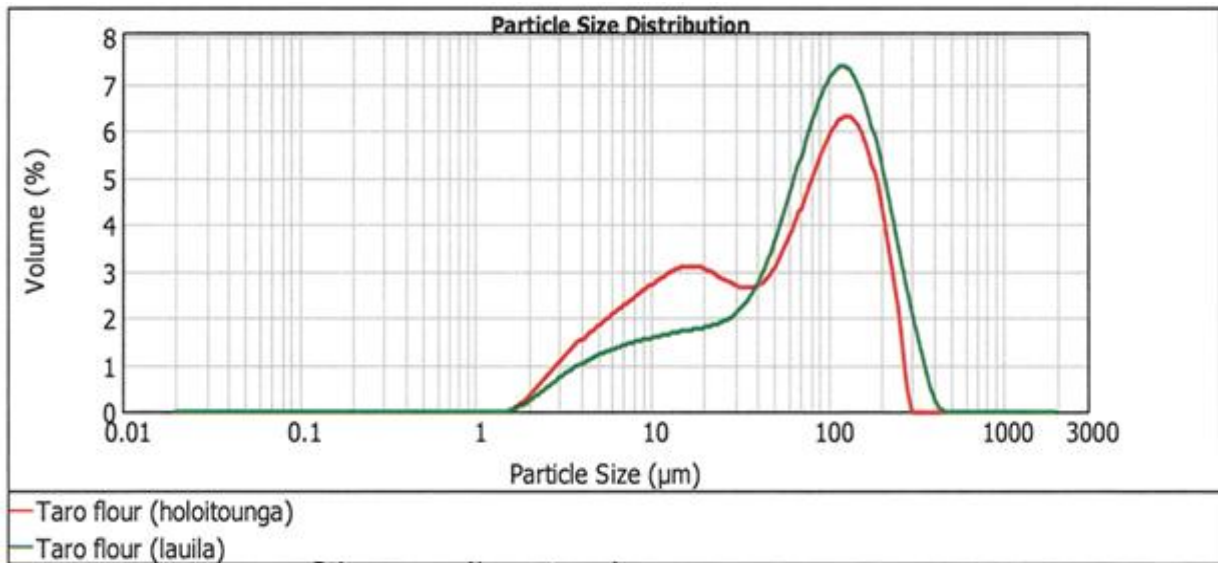


Figure 13 Particle size distribution of the two flour samples studied

4.3.1.5. Microstructural properties

The microstructure of the two taro flours reveals distinct microstructural profiles that align with known taro morphology while exhibiting variety-specific differences in granular arrangement and aggregation patterns (Figure 14).

The irregular polygonal shape of starch granules observed in both Holoitounga and Lau'ila flours corresponds with established morphological characteristics of taro starch (Nagar et al., 2021). However, the two varieties diverge in granular packing density and boundary definition. Holoitounga's loose aggregation with visible void spaces contrasts sharply with Lau'ila densely packed matrix. Such structural differences may correlate with variations in water and oil absorption capacity and paste viscosity. Also, the loose aggregation is reflected by the unimodal population and its fine particle sizes. Conversely, densely packed granules in Lau'ila could restrict water diffusion, resulting in slower hydration and altered rheological profiles (Zhang et al., 2022). Such densely aggregated starch granules may also explain their coarser particle sizes seen in Table 13.

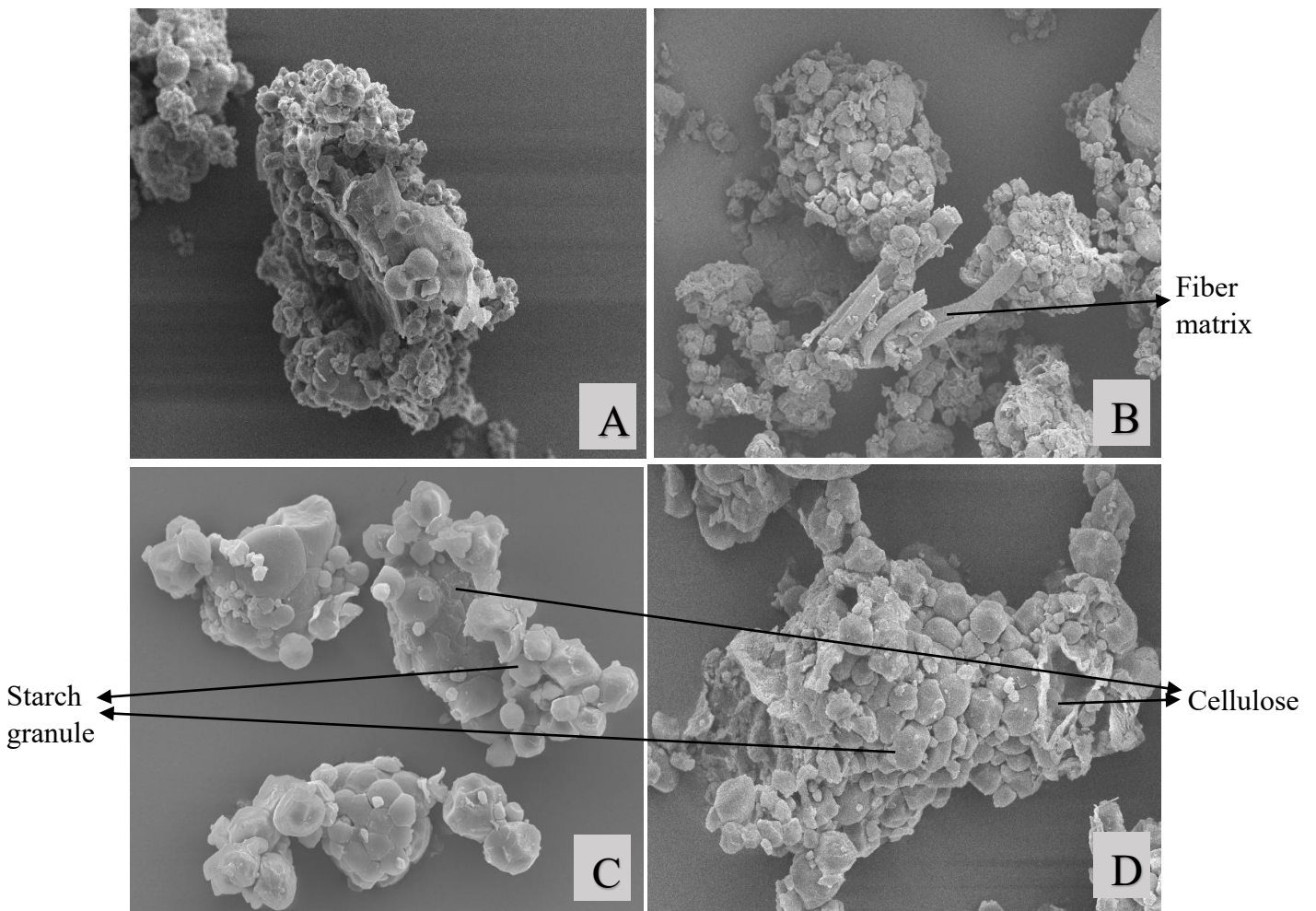


Figure 14 SEM images of flours viewed under 1100x, Holoitounga flours (A) and Lau'ila (B) and flours viewed under 2000x, Holoitounga flours (C) and Lau'ila flours (D).

4.3.2 Functional Characteristics

4.3.2.1. Thermal properties

The DSC results reveal a significant difference ($p \leq 0.05$) in the gelatinization behaviour between Holoitounga and Lau'ila taro flours, indicating distinct functional properties and crystalline organization. Table 14 shows that Holoitounga flour has significantly higher ($p \leq 0.05$) gelatinization temperatures, suggesting greater thermal stability of its starch crystallites. The differences may be attributed to variations in starch crystallinity, granule structure, and amylose-to-amylopectin ratios between the two cultivars. Higher gelatinization temperatures are typically associated with more ordered and stable crystalline regions within the starch, which resist thermal disruption (Singh et al., 2003). Conversely, Lau'ila's lower gelatinization implies weaker crystalline organization, which could correlate with its higher amylopectin content (Table 14). Amylopectin promotes the swelling of starch granules and the disruption of their ordered crystalline structure (Vamadevan & Bertoft, 2020). The gelatinization temperatures for both cultivars align with previous studies, which varied from 72 °C to 87.13°C (Aprianita et al., 2009; Havea, 1993; Jane et al., 1992).

In addition, Holoitounga showed a wider gelatinization temperature range of 20.26 °C, compared to 18.97 °C for Lau'ila. A broader gelatinization range often reflects greater heterogeneity in starch granule composition or differences in molecular arrangement (Cai et al., 2014). Furthermore, the enthalpy change required for gelatinization was significantly greater in Holoitounga than in Lau'ila, indicating a higher energy demand for disrupting crystalline regions in the former. This suggests that Holoitounga starch may possess a more stable or compact crystalline structure, potentially influenced by higher amylose content or more extensive hydrogen bonding (Liu et al., 2024).

Table 14 Gelatinization temperatures and enthalpy changes of the taro flours

Flour samples	Onset temperature	Peak temperature	Conclusion temperature	$T_c - T_o$ (°C)	ΔH (J/g)
	T_o (°C)	T_p (°C)	T_c (°C)		
Holoitounga	74.90 ^a	78.92 ^a	95.15 ^a	20.26 ^a	4.47 ^a
Lau'ila	73.75 ^b	76.86 ^b	92.72 ^b	18.97 ^b	3.95 ^b

Values are a means of triplicate measurements. Means in the same column with different superscripts are significantly different ($p \leq 0.05$)

4.3.2.2. Pasting properties

The pasting characteristics of Holoitounga and Lau'ila flours determined by RVA are presented in Table 15. Significant differences were observed between the two flours tested in their behaviour during heating and cooling cycles under excess water conditions. The pasting temperature indicates the point at which starch granules begin to swell and leach amylose, marking the onset of gelatinization (Mauro et al., 2023). Holoitounga flour exhibited a significantly higher pasting temperature compared to Lau'ila flour ($p \leq 0.05$). This suggests that Holoitounga flour requires more heat energy to initiate gelatinization, potentially due to differences in granule structure and amylose content. Higher pasting temperatures are often associated with greater resistance to swelling and may reflect a more crystalline starch structure (Jane et al., 1992).

Peak viscosity (PV) reflects the maximum swelling capacity of starch granules before they rupture due to shear or temperature (Mauro et al., 2023). Holoitounga flour exhibited a significantly higher peak viscosity than Lau'ila, indicating a greater ability to absorb more water and swell to a greater extent, resulting in a thicker paste. This enhanced swelling behaviour may be attributed to several factors, including protein and starch content, including amylopectin/amylose ratio, molecular structure and branching pattern of amylopectin, as well as granule size and morphological characteristics (Kaur et al., 2007; Li et al., 2022). This finding is consistent with Jane et al. (1992), where the taro flour with a high amylose content exhibited the highest viscosity and pasting temperature compared to taro flours with low amylose content. It was suggested that such a result may be attributed to the high mucilage content in taro corms. Also, the amylopectin fraction in Holoitounga may have more short chains, which tend to collapse when in water, leading to high breakdown viscosity (Lu et al., 2008).

Trough viscosity represents the minimum viscosity after the peak, reflecting the stability of the starch paste under heat and shear (Kumar & Khatkar, 2017). Holoitounga flour had higher trough viscosity than Lau'ila. Similarly, the breakdown, calculated as the difference between peak and trough viscosities, was also significantly higher for Holoitounga. A higher breakdown value indicates that Holoitounga is relatively stable under heat and shear, meaning it maintains some structural integrity during different processing conditions (Ide et al., 2019).

Further, final viscosity measures the ability of starch to retrograde or reassociate during cooling, which is important for the formation of gels and the texture of finished products. Both

flours showed no significant difference in final viscosity. Correspondingly, the setback, the increase in viscosity from trough to final, reflects the tendency of starch molecules to reassociate and form a gel upon cooling. Both flours had similar setback values, suggesting comparable retrogradation tendencies.

Table 15 Pasting properties of taro flours

Flours	Pasting temp (°C)	Peak viscosity (cP)	Trough viscosity (cP)	Final viscosity (cP)	Breakdown	Setback
Holoitounga	82.28 ^a	4952.33 ^a	2238 ^a	3474.33 ^a	2714.33 ^a	1236.33 ^a
Lau'ila	80.7 ^b	4399.67 ^b	2134 ^b	3217.33 ^a	2265.67 ^b	1083.33 ^a

Values are a means of triplicate measurements. Means in the same column with different superscripts are significantly different ($p \leq 0.05$).

4.3.2.3. Water absorption capacity (WAC) and oil absorption capacity (OAC)

Understanding the flour's water and oil absorption capacity is crucial for optimizing dough functionality and ensuring consistent product quality in baking and food processing (Awuchi et al., 2019). These functional properties provide critical insights into the appropriate amount of liquid required to form a cohesive dough, influence dough development and textural attributes, and ultimately affect the sensory and structural quality of baked products.

As shown in Table 16, Holoitounga exhibited significantly higher ($p \leq 0.05$) water absorption capacity and oil absorption capacity than Lau'ila, indicating enhanced hydrophilic and lipophilic binding capacities. These characteristics are advantageous in food formulations that demand high moisture and fat retention. The high WAC of Holoitounga is consistent with its high peak viscosity (Table 15), supporting its greater capacity to absorb water during thermal processing compared to Lau'ila. However, this finding contrasts with findings from a previous study, where a taro cultivar with a higher amylopectin content demonstrated greater WAC (Boahemaa et al., 2024).

The WAC values obtained in this study are consistent with previously reported values for taro flours from Ghana, Hawaii, and Cameroon, which vary from 76-180 g/100g (Aboubakar et al., 2008; Boahemaa et al., 2024; Tagodoe & Nip, 1994). Variations in WAC among cultivars are generally influenced by differences in starch content, the degree of starch damage during

milling and the presence of non-starch polysaccharides such as pentosan and fibre (Boahemaa et al., 2024).

Oil absorption capacity reflects a flour’s ability to bind and retain oil, a characteristic that is critical in baking and cooking as it affects mouthfeel, consistency, flavour retention, and overall acceptability of the final product (Tsegay et al., 2024). The significantly higher OAC observed in Holoitounga may be attributed to the presence of non-polar amino acid side chains, despite taro’s inherently low protein content (Adebowale & Lawal, 2004; Tsegay et al., 2024). Additionally, the fine and dense starch granules in taro may offer a larger surface area for oil interaction, while the presence of mucilage could further enhance oil-binding capacity (Kaur et al., 2013). The OAC values reported in this study are lower than those of taro cultivars from India, Cameroon and Hawaii, which vary from 104-315 g/100g (Kaur et al., 2013; Njintang et al., 2007; Saxby et al., 2024).

Table 16 Water absorption capacity and oil absorption capacity of taro flours

Flour samples	Water absorption capacity (g/100 g)	Oil absorption capacity (g/100g)
Holoitounga	94.614 ^a	92.51 ^a
Lau’ila	89.58 ^b	86.42 ^b

Values are a means of triplicate measurements. Means in the same column with different superscripts are significantly different ($p \leq 0.05$).

4.3.2.4. Least Gelation Concentration (LGC)

The least gelation concentration is a critical functional property that reflects the minimum concentration of flour required to form a self-supporting gel under defined conditions. It is an indicator of the gel-forming ability of flours, which in turn is influenced by their starch and protein composition, particle size, temperature and interaction with water (Chang et al., 2021). As shown in Table 17 and Figure 15, both Holoitounga and Lau’ila flour exhibited no gel formation at lower concentration (2% m/v), with the samples displaying viscous consistency, indicating insufficient solids to establish a continuous gel network. Gelation onset for Lau’ila was observed at 4 % m/v, forming a weak gel whereas Holoitounga remained viscous at this concentration but start gelation at 6% m/v. This suggests that the slightly higher amylose content in Holoitounga forms a stronger gel network, which requires a higher concentration to

reach the critical point of gelation, while the higher amylopectin of Lau'ila exhibited a less rigid structure allows for gel formation at a lower concentration.

As the concentration increased to 6-10%, both flours progressively developed weak to moderate gels. Notably, at 10% w/v, Holoitounga achieved moderate gel consistency, while Lau'ila was still in the weak gel stage. This indicates that Holoitounga's gel network forms more rapidly and strengthens earlier in concentration build up.

Both flours produced moderate gels at higher concentration (12-14% m/v), which leads to a firmer gel at 16% m/v with minimal syneresis and stable structure, showing that higher solids content allowed for full gelatinization and network entanglement.

At concentrations of 18%, both flours form firm gels. Notably, Holoitounga maintained firm gel status a 20%, while Lau'ila's gel firmness dropped to moderate gel. The strong formed ability of Holoitounga may be attributed to its higher amylose content compared to the higher amylopectin content of Lau'ila. This is due to the branched structure of amylopectin which hinders the formation of strong, stable networks like those formed by the linear amylose (Durrani & Donald, 1995).

Table 17 The least gelling concentration of taro flours

Concentration % (m/v)	Holoitounga flour		Lau'ila flour	
2	(-)	Viscous	(-)	Viscous
4	(-)	Viscous	(±)	Very weak gel
6	(±)	Very weak gel	(±)	Very weak gel
8	(±)	Weak gel	(±)	Very weak gel
10	(+)	Moderate gel	(+)	Weak gel
12	(+)	Moderate gel	(++)	Moderate gel
14	(++)	Moderate gel	(++)	Moderate gel
16	(++)	Firm gel	(++)	Firm gel
18	(++)	Firm gel	(+++)	Firm gel
20	(+++)	Firm gel	(++)	Moderate gel

Viscous consistency was characterized by a visible gelatinous mass suspended above a fluid layer. A very weak gel refers to a loosely formed gel layer adhering to the bottom of the test tube, which readily detaches upon inversion. A slightly thicker gel layer was referred to as a weak gel. A moderate gel denotes a semi-structured gel layer with minimal syneresis, evidenced by a small amount of liquid flowing along the tube walls upon inversion. A firm gel was defined by a well-formed, stable gel matrix that retains its structure and position when the tube is inverted, showing no observable flow.

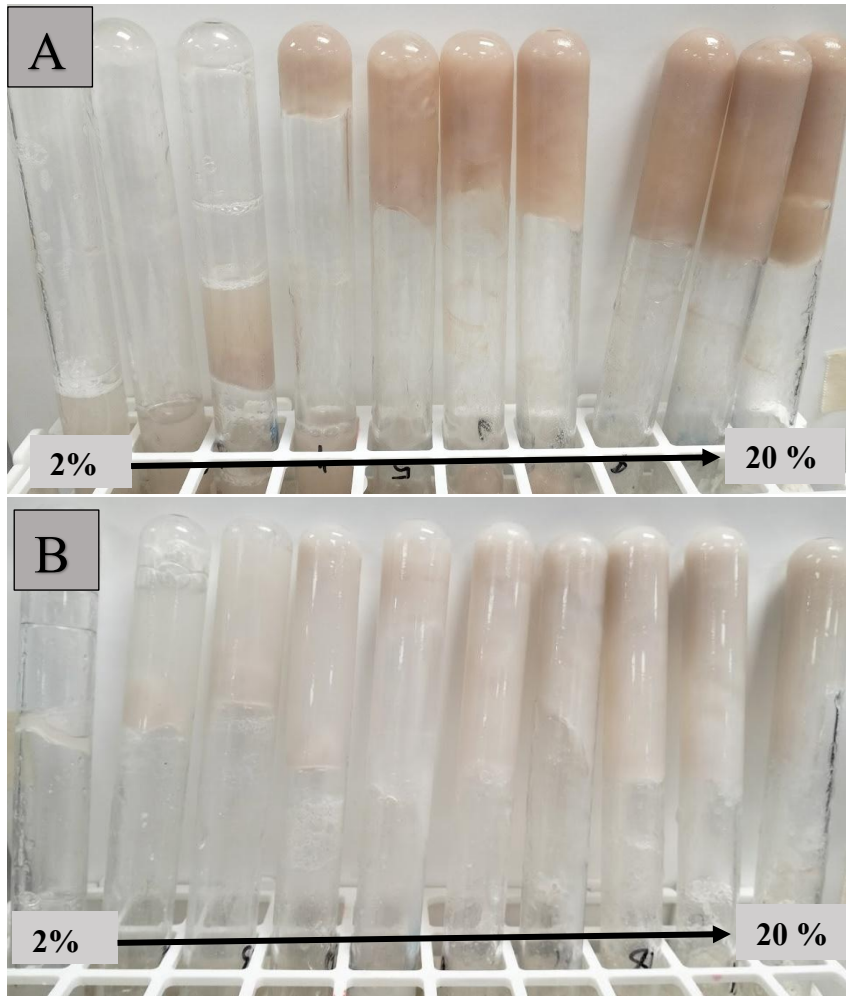


Figure 15 Least gel concentration of Holoitounga (A) and Lau'ila (B), starting from 2 to 20 % m/v

4.3.2.5. Foam capacity and stability

Foam is an important parameter that helps improve the texture, consistency and appearance of foods (Akubor, 2007). The foam capacity between the two taro flours showed that Lau'ila has significantly higher foam capacity ($p \leq 0.05$), whereas the Holoitounga taro flours have higher foaming stability. The differences in the foaming capacity of the taro flours may have been due to proteins that form a continuous cohesive film around the air bubbles in the foam (Kaur et al., 2013). The high crude protein content of Lau'ila explained its higher foaming capacity, which aligns with the positive correlation of foaming capacity and the protein content in taro reported by Kaur et al. (2013). Compared to other flours such as legume, corn flour, soya and potato flour, Taro exhibited the least foaming capacity, and that is because of its lack of protein (Kaur et al., 2013). The foaming capacity of this present study is both lower than the taro varieties of previous studies (ranging from 9.75 – 16.98%) (Amon et al., 2011; Boahemaa et al., 2024; Kaushal et al., 2012).

Conversely, Holoitounga demonstrated superior foam stability at 95.61%, significantly higher ($p \leq 0.05$) than Lau'ila's 93.33%, indicating that the foam formed by Holoitounga is more resistant to collapse over time. These differences highlight the influence of taro cultivar on functional properties, which could be critical in determining their suitability for specific food formulations. Since foaming stability is governed by the ability of the film formed around the entrapped air bubbles to remain intact without training, it follows that stable foams can only be formed by highly surface-active solutes. The good foam stabilities of flours suggest that the native proteins that are soluble in the continuous phase are very surface active in these flours (Kaushal et al., 2012). The foaming stability of these varieties is consistent with the taro varieties reported in previous studies, 85.50-98.50% (Boahemaa et al., 2024; Kaushal et al., 2012).

Table 18 Foam capacity and stability of taro flours

Flour samples	Foam capacity (%)	Foam stability (%)
Holoitounga	5.13 ^b	95.61 ^a
Lau'ila	7.69 ^a	93.33 ^b

Values are a means of triplicate measurements. Means in the same column with different superscripts are significantly different ($p \leq 0.05$).

4.3.2.6. Emulsion capacity and stability

The emulsifying characteristics of flours rely heavily on protein as the surface active agents that stabilized the emulsion by creating electrostatic repulsion on the oil droplet surface (Kaushal et al., 2012). Taro is not traditionally known as a strong emulsifier compared to other legume flours due to being very low in protein content, but it does exhibit more emulsion-related properties depending on other factors, including starch, particle size and fibre content (Jane et al., 1992).

This present study showed that Holoitounga taro flour has significantly higher emulsifying ability and stability. This result may reflect its considerably small granule size, which further enhances its interfacial coverage capacity, contributing to the moderate emulsification properties despite its lower protein content than Lau'ila. Adding to that, the high-water absorption capacity of Holoitounga may increase the viscosity of the continuous phase in an

emulsion, which can prevent the separation of oil and water droplets, thus improving emulsion stability.

Table 19 Emulsion capacity and stability of taro flours

Flour samples	Emulsion Capacity (%)	Emulsion Stability (%)
Holoitounga	6.25 ^a	3.13 ^b
Lau'ila	3.13 ^b	1.88 ^a

Values are a means of triplicate measurements. Means in the same column with different superscripts are significantly different ($p \leq 0.05$).

4.3.3 Rheological properties of taro flour-protein systems

4.3.3.1. Strain sweeps – Linear viscoelastic region (LVER)

From the strain sweeps graphs in Figure 16 **Error! Reference source not found.**, the LVER is defined as the strain interval where a material's stress response is directly proportional to its strain (Marin, 1988). Wheat dough remained linear to 0.3 - 0.4 % strain, after which G' decreased and $\tan \delta$ rose, indicating the onset of network disruption. Holoitounga based doughs showed the broadest LVERs, holding linearity to 0.4-0.5%, whereas Lau'ila based doughs tended to yield earlier, with LTF beginning to deviate at around 0.2-0.3%. Within the LVER, all samples exhibited $G' > G''$ and $\tan \delta < 1$, confirming elastic dominance and an intact viscoelastic matrix.

These differences suggest that Holoitounga systems possess a slightly more resilient primary network, reflecting much stronger starch-water interactions or a higher effective amylose contribution, which tolerates greater deformation before nonlinearity and structural breakdown. In contrast, the earlier onset of nonlinearity in Lau'ila systems points to a more fragile network that is prone to microstructural rearrangement at lower strains. Technologically, a wider LVER is advantageous for processing steps that impose low to moderate deformations such as mixing, sheeting and early proofing (Faubion & Hosney, 1990). This implies better shape retention and gas cell stability prior to baking. The steeper post LVER decline of G' and the rapid rise in $\tan \delta$ in Lau'ila doughs anticipate earlier yielding under mechanical load, which may translate to softer handling properties and greater risk of degassing or spread if processing strains exceed 0.3 %.

The fortification of egg white, casein and pea protein into taro flour systems altered the extent of the LVER, reflecting changes in the structural resilience and deformation tolerance of the dough network. In Holoitounga flour systems, the addition of egg white protein (HTE) and casein (HTC) generally maintained or slightly extended the LVER compared to the native HTF, indicating improved network stability. Egg white is rich in globular proteins (e.g. ovalbumin) that readily denature and form strong intermolecular bonds during mixing, contributing to a more cohesive and elastic matrix (Mine, 1995). Casein, with its flexible, open-chain structure, can act as a filler and network enhancer by interacting with starch granules, thereby delaying the onset of structural breakdown (L. Kumar et al., 2022). In contrast the addition of pea protein (HTP) showed a slightly narrower LVER, suggesting that while pea protein may contribute to network formation through hydrogen bonding and limited hydrophobic interactions, its particulate morphology and lower solubility can lead to weaker integration with the continuous dough phase (Zhao et al., 2024).

For Lau'ila flour systems, all protein additions improved the LVER relative to the unfortified Lau'ila flour. Egg white (LTE) extended the LVER to 0.3-0.4 % strain, and casein (LTC) achieved similar improvements, both indicating a reinforcement of the viscoelastic structure. Pea protein (LTP) also improved deformation tolerance compared to LTF but remained less effective than egg white and casein, consistent with its more limited compatibility with the starch network.

4.3.3.2. Frequency sweeps analysis

The frequency sweep test provides insight into the viscoelastic behaviour of flour systems under oscillatory stress, simulating how dough responds to deformation at varying rates. The storage modulus (G'), loss modulus (G''), and damping factors ($\tan \delta$) were examined to characterize the strength, rigidity, and elastic-viscous balance of the samples Figure 17 **Error! Reference source not found..**

Across all samples, both G' and G'' increased with frequency, indicating that the samples dissipate more energy as heat at faster oscillatory deformation. Among the samples tested, Holoitounga taro flour (HTF) exhibited the highest G' values across the frequency range, indicating a dominant elastic character and a rigid gel network. This behaviour is attributed to the high amylose content in HTF, which promotes the formation of a dense three-dimensional network capable of storing mechanical energy (Wang et al., 2024). In contrast, the LTF showed

moderate G' and G'' values that are lower than HTF, indicating a viscous behaviour but rigid than wheat flour. The wheat flour exhibited consistently low G' and G'' values, with very high $\tan \delta$ values, suggesting a viscous or liquid-like behaviour that does not resist deformation effectively. Consequently, the dough is soft, loose, or poorly developed. This behaviour could have been due to the excess amount of water added to the sample as (Kaur et al., 2013)

The addition of protein isolates had varying effects on the rheological behaviour of both HTF and LTF. For HTF, the addition of egg white protein (HTE) led to a significant reduction in G' and G'' compared to HTF alone, but the system maintained a strong elastic structure with a $\tan \delta$ similar to HTF. This suggests that egg white protein contributes to enhanced flexibility without significantly compromising gel strength, supporting its role as a network-forming agent in gluten-free matrices. Pea protein (HTP) and casein (HTC) also contributed to the viscoelasticity of HTF, but to a lesser extent. HTP maintained moderate G' and G'' values with a slightly higher $\tan \delta$, indicating a somewhat less rigid but still elastic structure. In contrast, Lau'ila taro flour (LTF) and its protein blends exhibited significantly lower G' and G'' values across all frequencies, comparable to the protein fortified system of HTF. However, if closely comparing the $\tan \delta$ of the two taro fortified systems, LTF protein blends showed slightly lower values throughout the studied frequencies, indicating a stronger and stable elastic network.

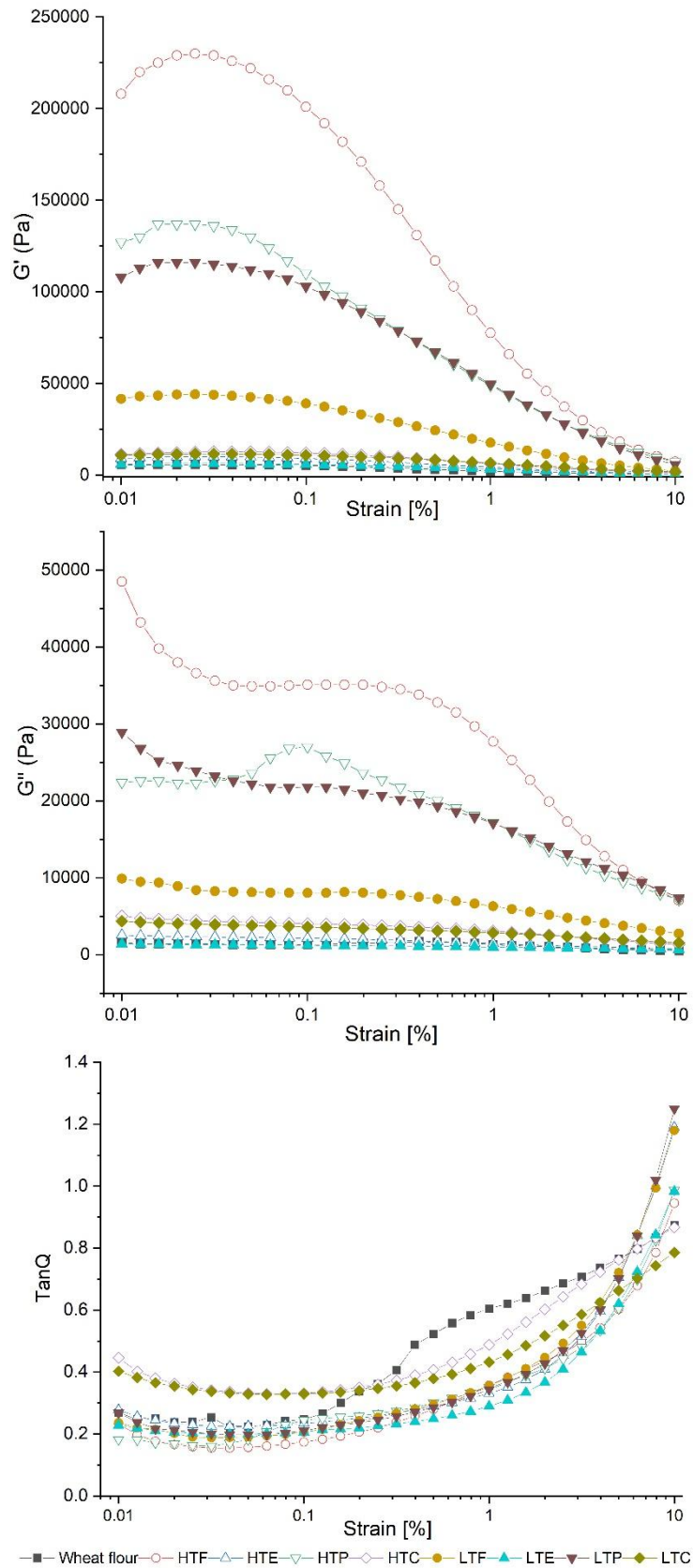


Figure 16 Strain sweeps of taro flours and protein fortified systems. HTF represents the native Holoitounga flour, HTE for Holoitounga with egg white, HTP for Holoitounga with Pea protein, HTC for Holoitounga with Casein protein, LTF for the native Lau'ila flour, LTE for the Lau'ila with egg white, LTP for Lau'ila flour with pea protein, and LTC for the Lau'ila with casein protein.

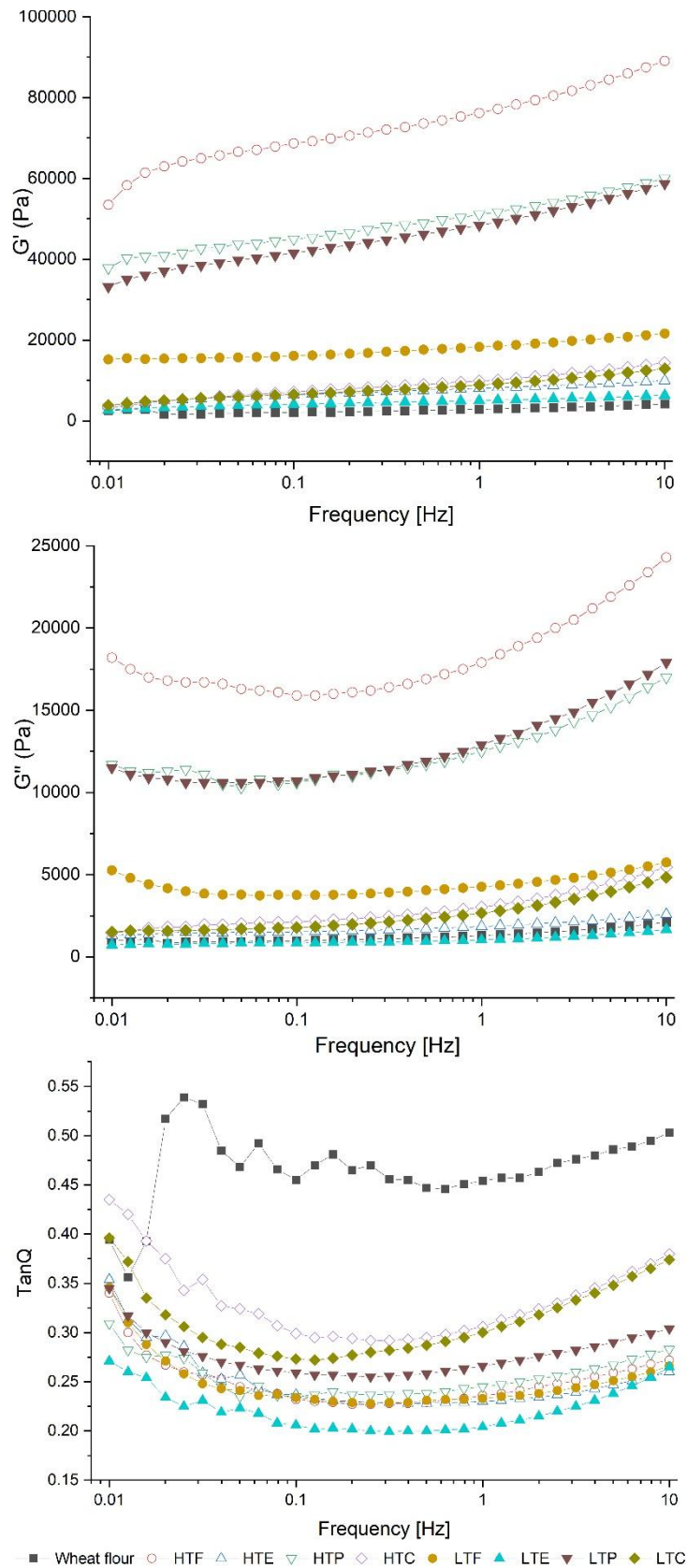


Figure 17 Frequency sweeps analysis of taro-protein systems. HTF represents the native Holoitounga flour, HTE for Holoitounga with egg white, HTP for Holoitounga with Pea protein, HTC for Holoitounga with Casein protein, LTF for the native Lau'ila flour, LTE for the Lau'ila with egg white, LTP for Lau'ila flour with pea protein, and LTC for the Lau'ila with casein protein.

4.3.3.3. Temperature sweeps analysis

Temperature sweep rheology was conducted to evaluate the viscoelastic transitions of wheat, Holoitounga and Lau'ila taro flours, along with their blends with three protein isolates. The heating phase (15- 100 °C) simulates starch gelatinization and network formation, while the cooling phase (100- 25 °C) captures retrogradation and gel setting behaviour. Changes in the storage modulus (G'), loss modulus (G'') and damping factor ($\tan \delta$) provide insight into the structure-forming potential and thermal stability of the flour systems (Figure 18(A) and Figure 18(B)).

Heating phase: Gelatinization and network formation

During heating, all samples exhibited a typical rise in both G' and G'' as the temperature increased to 85-90 °C, indicating thermal transitions associated with starch gelatinization and protein denaturation. HTF sample alone exhibited a higher G'' value compared to other formulations, suggesting more viscous and less elastic behaviour. The LTF sample exhibited a moderate G' and G'' with similar $\tan \delta$ values to the HTF, indicating a more balanced viscoelastic behaviour.

The addition of protein isolates further influenced the gelation behaviour of the taro flours. Notably, the HTE sample recorded the highest peak G' , surpassing both unfortified HTF and wheat flour. This indicates a synergistic effect between amylose and albumin protein, likely involving denaturing of albumin, exposing hydrophobic regions that interact with amylose, forming a more robust gel network (Ishigaki et al., 2023). Pea protein (HTP) and casein (HTC) also contributed to gel strength, though to a lesser degree, with moderate increases in viscoelastic moduli. The differences suggest that the effectiveness of protein fortification depends on the protein's structural and interactive compatibility with starch (Scott & Awika, 2023). In contrast, Lau'ila taro flour (LTF) and its protein blends displayed lower G' and G'' values during heating. The viscoelastic transitions were more gradual and less defined, consistent with the waxy starch characteristics of Lau'ila, which contains minimal amylose. Although the addition of egg white protein (LTE) enhanced G' relative to LTF alone, the overall moduli remained far below those of HTF-based systems, indicating limited network formation.

Wheat flour, used as a control, exhibited a broad increase in G' and G'' at lower temperatures compared to taro flours. This is attributed to a combined effect of early starch gelatinization and gluten network development (Kaur et al., 2013). While its moduli were lower than taro

flours, the wheat sample displayed a more balanced viscoelastic response, reflective of a continuous and extensible gluten-starch structure.

The $\tan \delta$ trends during heating further highlighted differences in gel formation, although all samples showed a decrease in $\tan \delta$ values with the increase in temperature. Such observations may have been attributed to a viscous and weakly structured network before starch gelatinization, but after gelatinisation, a stronger elastic network forms, leading to a gel-like behaviour. HTF and its protein blends, particularly HTE, exhibited consistently low $\tan \delta$ values, confirming strong elastic dominance and effective gelation. A similar trend is observed for LTE in contrast to LTF and other protein blends, in which they maintained higher $\tan \delta$ values, indicating more viscous, weaker gels. Wheat flour showed a transient increase in $\tan \delta$ around 60- 70 °C, likely due to early starch swelling and protein unfolding, followed by a decline as the gel network formed.

Cooling phase: Retrogradation and Gel stabilization

During cooling from 100 °C to 25 °C, retrogradation and network organization processes became apparent. Wheat flour maintained consistent G' and G'' values during cooling, suggesting that the dough does not stiffen or weaken much as it cools, showing good thermal stability. Native taro flours showed lower G' and G'' values compared to wheat flour, suggesting a thermally stable dough; however, $\tan \delta$ of Lau'ila increased at below 30 °C, suggesting a shift from a strong elastic gel to a viscous dominant behaviour. This could be attributable to its higher amylopectin, which has limited crystalline structure formation on cooling, and thus does not develop a strong elastic gel (Y. Gong et al., 2024).

Egg white blends with both Holoitounga and Lau'ila showed consistently higher G' and G'' values that increased as the temperature dropped. The $\tan \delta$ values were consistently lower than other formulations but slightly higher than the wheat flour. These results show that egg white fortification strengthens the taro flour matrix, leading to a firmer, more elastic and thermally stable gel network compared to other samples.

The casein fortified samples showed a consistent G' and G'' throughout the cooling temperatures, with higher $\tan \delta$ compared to wheat flour and egg-white blends. Pea protein fortified samples, especially with Lau'ila flour, showed the least viscoelastic behaviour and more unstable gel structures. However, both cultivars showed small differences in terms of the fortifications, but looking closely, HTF has slightly better viscoelastic behaviour and a stable gel network.

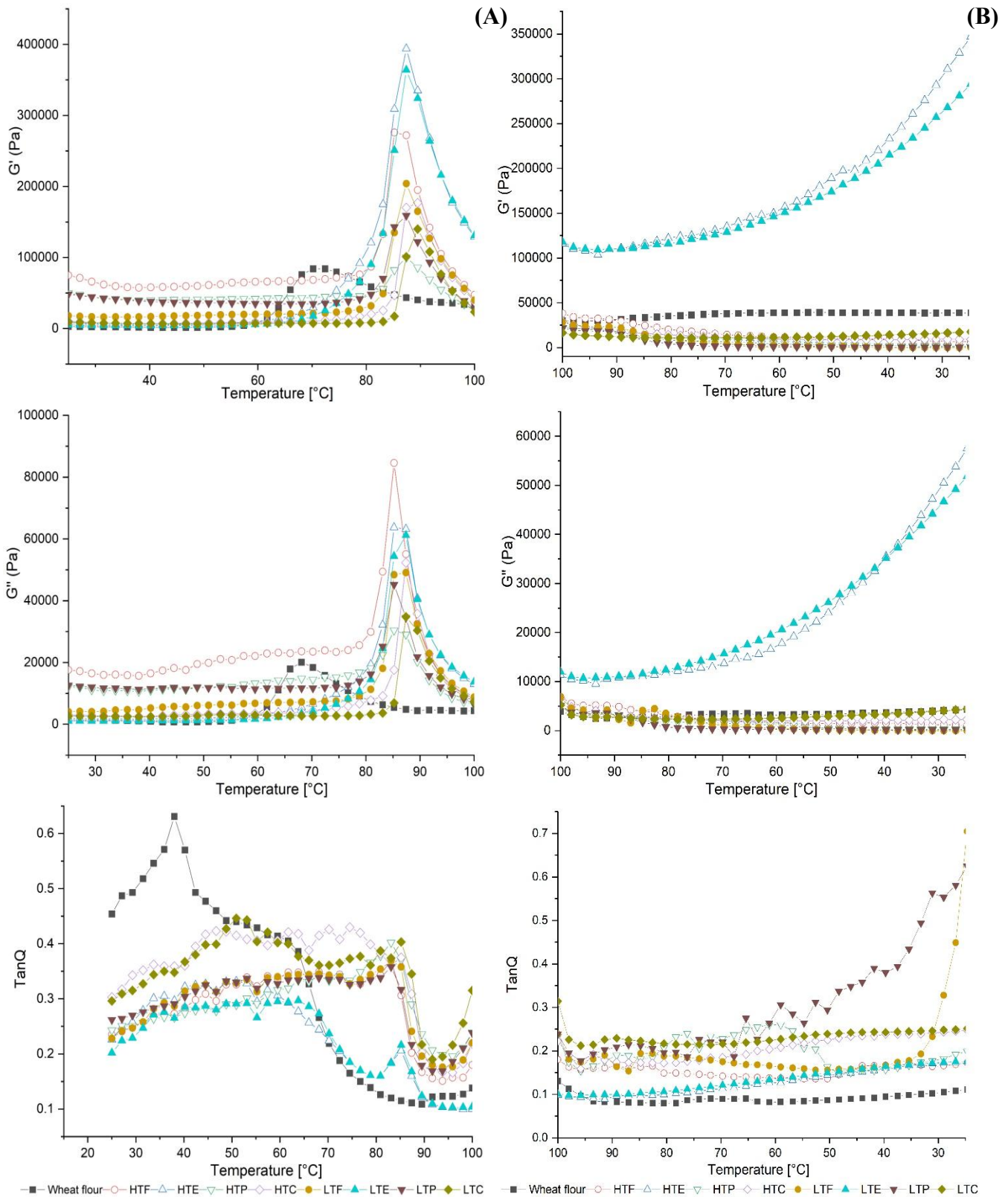


Figure 18 (A) Temperature sweeps analysis for heating of flours at 25-100 °C and (B) for cooling of flours at 100 – 25 °C. HTF represents the native Holoitounga flour, HTE for Holoitounga with egg white, HTP for Holoitounga with Pea protein, HTC for Holoitounga with Casein protein, LTF for the native Lau’ila flour, LTE for the Lau’ila with egg white, LTP for Lau’ila flour with pea protein, and LTC for the Lau’ila with casein protein.

4.4 Conclusion

To conclude, the physicochemical and functional properties of ungelatinized taro flours demonstrated distinct varietal differences aligned with their starch composition, discussed in Chapter 3. Holoitounga flour, characterized by higher amylose content, finer particle size and elevated levels of carbohydrates, fat and ash contents, exhibited superior functional attributes, including higher water and oil absorption capacities, emulsion and foaming stability and lower least gelation concentration. These traits reflect its floury nature and contribute to its high gelatinization temperature and peak viscosity. Conversely, Lau'ila flour, with its waxy starch profile, larger and more agglomerated granules, and slightly higher protein content, displayed greater swelling power and solubility but weaker gel-forming and viscoelastic behaviour.

Rheological assessments further confirmed that Holoitounga flour, particularly when fortified with egg white protein, closely approximated the viscoelastic characteristics of wheat flour, showing enhanced elasticity, structural integrity, and thermal stability. In contrast, Lau'ila systems remained structurally limited despite modest improvements with protein supplementation. Collectively, these findings underscore the potential of high amylose taro flour, especially when combined with functional proteins like egg white, as a viable gluten-free alternative in bakery applications, offering both improved technological functionality and enhanced nutritional value.

Chapter 5: Application of ungelatinized taro flour in bakery products

5.1 Introduction

Tonga remains heavily reliant on imported flour to meet demand for bakery products. In 2024 alone, the country imported approximately 4,235 tonnes of wheat and cereal flours at a value of NZD 6.40 million, marking an increase from 4,022 tonnes in 2023 (*International Merchandise Trade Statistics*, 2024). This rising trend highlights the significant role flour plays in Tonga's food supply, particularly in the production of bread, cookies, pastries and other baked goods. Although the Tonga government has expressed interest in import substitution as a strategy to improve food security and reduce reliance on imports, there is limited research and technical knowledge regarding the use of locally available resources, such as taro, as alternative flour sources in bakery applications.

Substituting wheat taro flour entirely in bakery products presents considerable challenges. Wheat flour has long been valued for its unique functional and sensory properties, including its gluten content, which is essential for dough structure and texture (Ooms & Delcour, 2019). Consequently, consumers are accustomed to its performance and flavour profile, and achieving similar quality with non-wheat flours often requires significant formulation adjustments. A practical and more feasible approach is partial substitution, which can help maintain consumer acceptability while incorporating local ingredients.

Holoitounga taro flour offers a floury behaviour, and Lau'ila taro flour, with waxy characteristics, examined in Chapter 4, offers a promising option for partial substitution. Crackers, a staple breakfast item and affordable bread alternative in many Tongan households, along with cookies commonly used as a treat at family celebrations, present accessible entry points for exploring taro flour substitution. Bread, the most widely consumed baked product, remains the most technically challenging due to the structural role of gluten, which is absent in taro flour.

Previous studies have indicated that partial substitution of wheat flour with taro flour up to 10 – 15% may be acceptable in bread formulations (Ammar et al., 2009; Hegazy, 2019; Hossain, 2016; Shubhangi et al., 2023). However, with such a small substitution, it will only reduce a small portion of the imported flours, exploring a potential to increase substitution to a higher

percentage, such as 25-50% would be more economically efficient. To address the limitations of gluten-free flours, researchers have proposed incorporating hydrocolloids and protein isolates such as egg white (albumin), whey milk (casein), and plant-based proteins to mimic the binding and elasticity provided by gluten, thereby enhancing dough strength and product structure (Piluk et al., 2025; Rodriguez Furlán et al., 2015; Storck et al., 2013; van Riemsdijk et al., 2011). Fortifying the wheat-taro flour system with protein for enhancement of textural properties would also be advantageous for improving the protein content of the products, as taro has a very negligible amount of protein that is reduced when the substitution level increases (G. Abera et al., 2017). To date, no study has investigated the use of protein-fortified taro flour in composite bread systems. However, the techno-functional properties of taro flour presented in Chapter 4 of this thesis showed that combining taro flour with egg white protein can produce a dough with improved structural integrity, suggesting potential for broader application in bakery products.

This study aims to evaluate the potential of partially substituting wheat flour with taro flour in three common bakery products: crackers, shortbread biscuits, and bread. Specifically, it seeks to identify optimal substitution levels that maintain acceptable product quality. This research will assess the nutritional composition, physical characteristics, and textural properties of the resulting baked goods to determine the functional stability of taro flour as a local substitute in Tonga's bakery sector.

Through this analysis, the study will advance local food system development by evaluating taro flour as a functional gluten-free alternative to wheat in bakery products. The findings provide practical evidence to support Tonga's import substitution efforts and promote the use of local crops in value-added food production.

5.2 Materials and Methods

5.2.1 Materials

5.2.1.1. Ingredients and formulation of crackers

Formulation of crackers from Mihiranie et al. (2014) with slight modification. A standard wheat flour was used for making the control sample and the substituted wheat-taro crackers. The standard wheat flour (Gilmour bakers' flour) contains 10.3 g protein, 1.4 g total fat, 0.2 g carbohydrates, 3.5 g dietary fibre and 3mg of sodium. The control crackers were made from 100.0 g of standard wheat flour, 2.0 g of sugar, 10.0 g of vegetable shortening, 1 g of salt, 1 g of baking soda, 0.5 g of Lecithin, 7.0 g of coconut oil and 40 g of water. For the partially substituted wheat-taro flour crackers, 25%, 50% and 75 % of the wheat flour was substituted with taro flour samples. The same ingredients and quantities used for the control formulation were maintained across all substituted samples, except for the water content, which was increased by 10 mL at each substitution level to ensure a consistent dough consistency.

5.2.1.2. Preparations of crackers

The crackers were prepared following the steps outlined in Figure 19. All ingredients were mixed and kneaded using a food processor (Click Clack CFP001W). The dough was then removed and proofed at 5 °C for 30 minutes before being sheeted, cut and baked.

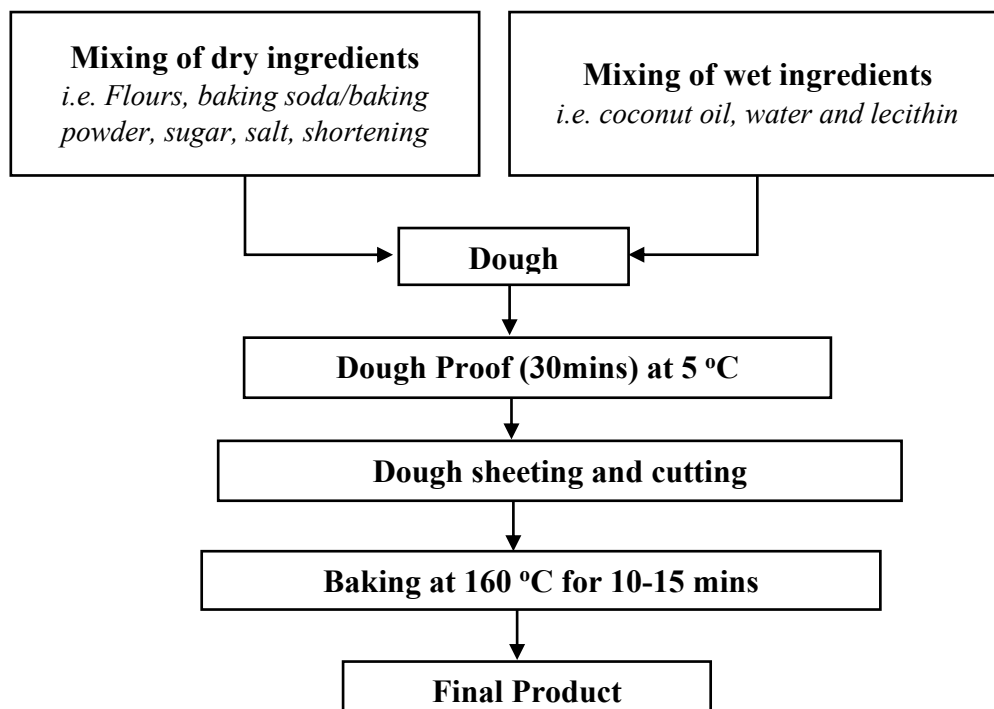


Figure 19 Preparation of wheat-taro crackers

5.2.1.3. Ingredients and formulations of shortbread cookies

Shortbread cookies were prepared using a formulation adapted from Sanchez et al. (1995) with modifications. The ingredients and formulations of the control shortbread cookies were prepared as follows: 100 g of standard wheat flour (Gilmour bakers' flours), 66.7 g of unsalted butter, 26 g of powdered sugar, 0.6 g of salt, 2.3 g of vanilla extract, and 0.5 g of lecithin. For the substitute formulation, wheat flour was partially substituted with taro flour at 25 %, 50 %, 75 %, and 100 % w/w. In the 100% taro shortbread formulation, 2.4 g of xanthan gum and 17.7 g of tapioca starch were added to compensate for the absence of gluten. Additionally, the unsalted butter content was increased to 87.0 g to maintain a consistent dough texture.

5.2.1.4. Preparation of shortbread cookies

The shortbread cookies were made following Figure 20, where the ingredients were mixed and kneaded in a food processor (Click clack CFP001W) for 3 minutes before removing the dough and proofing for 30 minutes at 5 °C, followed by sheeting, cutting and baking.

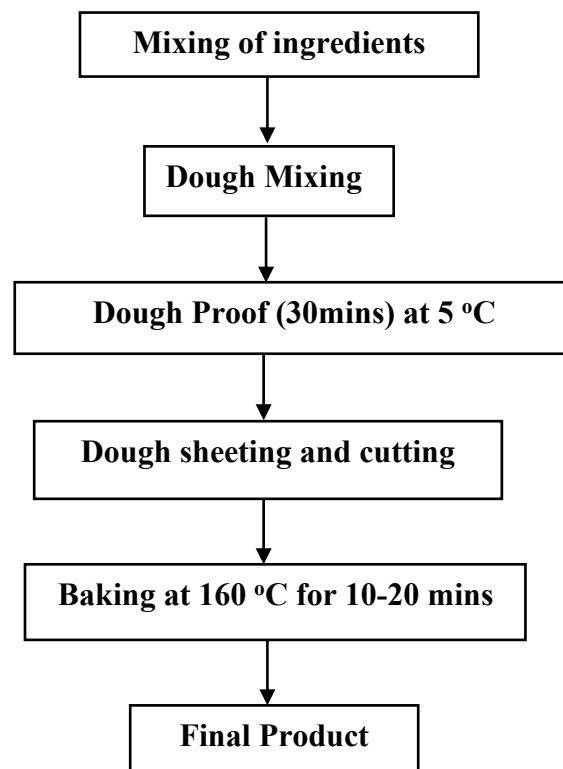


Figure 20 Preparation of shortbread cookies

5.2.1.5. Ingredients and formulations of bread

Bread formulation was adapted from Schmiele et al. (2012) with slight modifications to incorporate albumin and egg white for texture improvement. The ingredients and formulations of the control sample are as follows: 300 g of wheat flour (Gilmour baker's flour), 9.6 g of egg white, 12.80 g of yeast, 5.69 g of salt, 28.35 g of unsalted butter, 5.69 g of apple cider and 220 g of water. There were two controls used in this study, the first was with egg white and the other was without egg white. For the other versions of bread, the wheat flour was partially substituted with 25%, 50% and 75% w/w of taro flour samples. Xanthan gum (1.43 g) was added to the substituted breads with 10 g of water increased as the portion of taro increases, i.e. 230 g, 240 g, and 250 g of water were added to 25, 50 and 75% substitutions.

5.2.1.6. Preparation of composite bread

The ingredients were added to a bread maker machine (Sunbeam Smartbake® Custom Programmable Bread Maker, MB7850) and set it on Menu 4 (Wheat bread setting). This menu was selected due to the portion of gluten still present in the system from the standard wheat flour, and it provides enough time for kneading and proofing to accommodate the development of the gluten network. After mixing, kneading and proofing, the dough was removed from the bread maker for a final gentle knead to release air and then placed onto a baking silicone tray. It was then proofed again at room temperature for 60 minutes before baking at 170 °C for 30 minutes. After baking, the bread was placed on a wire rack to cool at room temperature before further analysis.

5.2.2 Methods

5.2.1.1. Nutrition Composition of the bakery products

The nutritional composition of the formulated products was theoretically calculated using the Food Standards Australia New Zealand (FSANZ) Nutritional Panel Calculator (NPC). This tool provides an estimate of the nutrient profile of food products based on the ingredient list, quantities used and preparation details.

Each product formulation was entered into the NPC using the exact quantities (in grams) of raw ingredients used per 100 grams of the final product. The NPC uses a comprehensive database of food composition data to estimate the nutrient values per 100g and serving of the

final product. Macronutrients and components were generated, including the Energy (kJ), Protein (g), Total fat (g), Saturated fat (g), Carbohydrates (g), Sugars (g), Dietary fibre (g), Sodium (mg).

5.2.1.2. Measuring the puffiness (%) of crackers

The thicknesses of the crackers before and after baking were measured using a vernier calliper in six replicates. Puffiness (%) was calculated based on the change in thickness during baking, using Equation 9 as described by Nammakuna et al. (2016).

Equation 9

$$\text{puffiness (\%)} = \left(\frac{\text{thickness of baked cracker} - \text{thickness of cracker dough}}{\text{thickness of cracker dough}} \right) * 100$$

5.2.1.3. Measuring the volume of shortbread cookies

The volume of shortbread cookies was measured following the method described by Mihiranie et al. (2014). The diameter was determined by aligning six round cookies edge to edge in a straight line, measuring the total length using a vernier calliper, and calculating the average diameter per cookie. Thickness was assessed by stacking six crackers vertically, measuring the total height and dividing the number of cookies to obtain the mean thickness (mm).

5.2.1.4. Measuring the loaf weight, height and width

The weight of bread samples was determined after sufficient cooling using a digital balance of 0.01g accuracy. The loaf height and width were determined by measuring the height and width of three slices taken from the middle section of the loaves.

5.2.1.5. Colour analysis of crackers and breadcrumbs

The CIE L*, a*, b* colour values of crackers and breadcrumbs were measured using a colourimeter (Minolta Chroma meter CR-400, Minolta Ltd). The instrument was calibrated against a standard white reference tile (L* = 94.72, a* = -0.40 and b* = 3.61). The colour of the cracker samples was measured on the surface in triplicate. The colour of the crumb and crest was measured by taking readings at 4 points on the surface of the bread samples and the surface of the slices. Triplicate readings were taken from different positions, and mean values were recorded. The average of the triplicates was recorded.

5.2.1.6. Texture analysis of bakery products

The textural profile of the products was analyzed following Giannoutsos et al. (2023). The three-point bend test were carried out using a texture analyzer (TA. XT, plus 100C, Stable Micro Systems, Surrey, England). A three-point bending rig (HDP/3PB) with a 40 mm span between the supports. Pre-test speed (1.0 mms-1), test speed (2.0 mms-1), post-test speed (10.0 mms-1) and distance (6.0mm). The load cell was 5 kg, and the data acquisition rate was set at 500pps. The measured parameters were hardness, distance at break, and fracturability. All tests were performed in triplicate.

The TPA of shortbreads were analyzed using a cylindrical probe (P/35) according to the following procedures: Pretest speed (1.0 mms-1), test speed (2.0 mm-1), post-test speed (10 mms-1), distance (3.0 mm) and interval time (5 seconds). The load cell was 50 kg, and the data acquisition rate was set at 500 pps. The parameters obtained from the force-time diagram are the hardness, springiness, cohesiveness, and chewiness. All tests were performed in triplicate, and the results were the average of samples taken from the middle of the trays located at the centre and sides of the ovens.

The TPA of loaves were analyzed for its hardness, cohesiveness, springiness, chewiness, resilience and gumminess. A sample of 30 x 30 mm was taken from the middle of the bread and placed under a cylinder probe (P/35) to make a flat surface. The compression test was done by using a loading cell of 5 kg, 1.6 mms-1 test speed, compression strain of 25%, and a force of 0.05 N and the waiting time between the first and second compression is 5 seconds.

5.2.1.7. Statistical Analysis

Statistical analysis was performed using Origin Pro software from Origin Lab Corporation, Northampton, Massachusetts, USA. Analysis of Variance (ANOVA) was performed on the set of data from two cultivars, and a difference is considered significant only at a confidence level of more than 95% ($p \leq 0.05$).

5.3. Results and Discussions

5.3.1. Crackers

5.3.1.1. Effects of partially substituting wheat flour with taro flour on the nutritional composition of composite crackers

The incorporation of taro flours, derived from Holoitounga (HT) and Lau'ila (LT) cultivars, led to progressive alterations in the nutritional profile of wheat-taro crackers. Table 20 presents a clear trend where the increasing levels of taro flour substitution significantly reduced energy and protein contents while elevating carbohydrates and sugar levels. The control cracker, composed solely of wheat flour, had the highest energy and protein content. At 100% substitution, the energy values dropped by 52% and 55% for Holoitounga and Lau'ila, respectively, while protein levels declined to 76% and 74% g, respectively. These reductions are attributed to the low protein content of taro flours compared to wheat.

In contrast, the carbohydrate content increased proportionally with substitution, reaching 73.1 and 68.0 g/100g in 100% Holoitounga and Lau'ila flour, compared to 62 g in the control. Sugar levels followed a similar trend. Interestingly, total and saturated fat content, as well as sodium levels, remained relatively stable across all substitution levels, indicating that these parameters were primarily influenced by added formulation components rather than the flour source.

Table 20 Nutritional composition of wheat-taro crackers per 100 g

Sample IDs	Energy (kCal)	Protein (g)	Fat, total (g)	Saturated (g)	Carbohydrates (g)	Sugars (g)	Sodium (mg)
Control	1800	9	15.3	9.3	62	1.7	414
HT25%	1560	7.3	15.4	9.3	64.8	1.9	415
HT50%	1330	5.6	15.5	9.2	67.2	2.1	416
HT75%	1100	3.9	15.6	9.2	70.4	2.4	417
HT100%	867	2.2	15.7	9.2	73.1	2.6	419
LT25%	1560	7.4	15.3	9.3	64.4	1.9	416
LT50%	1330	6	15.3	9.2	67.7	2.1	417
LT75%	1100	4.5	15.3	9.2	69.6	2.3	418
LT100%	813	2.8	14.4	8.6	68	2.4	395

To better understand the multivariate relationship among these nutritional variables, Principal Component Analysis (PCA) was performed (Figure 21). The first two principal components

accounted for 85.85 % of the total variance, with PC1 explaining 56.17% and PC2 explaining 29.68%. The PCA biplot differentiates samples based on flour type and substitution level.

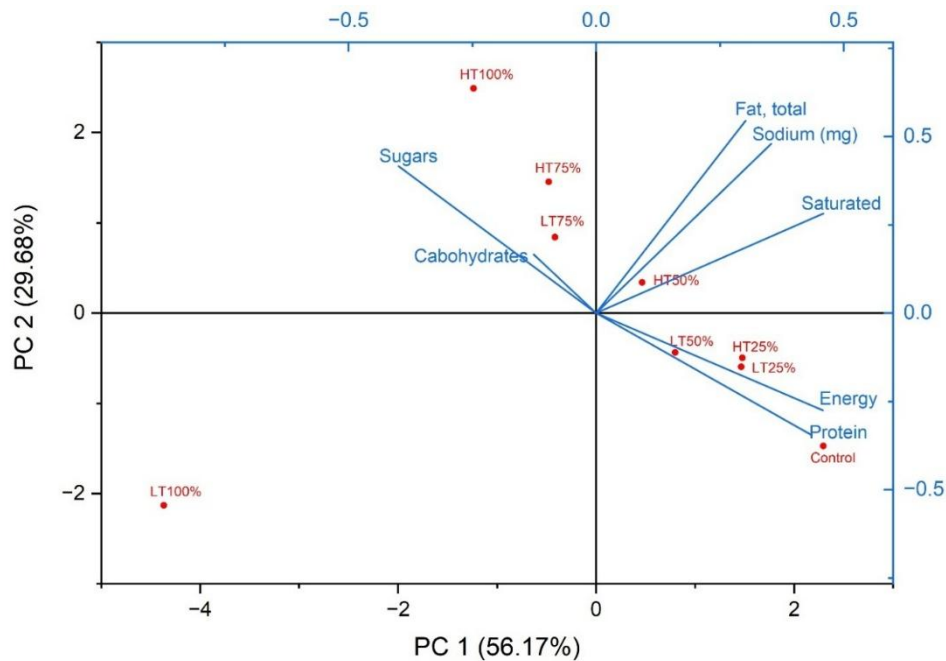


Figure 21 PCA of the nutritional composition of wheat flour crackers

Samples positioned on the right side of the biplot, including the Control, HT25%, and LTF 25-50% are associated with higher energy and protein contents. These samples cluster closely, suggesting that low substitution levels (25%) maintain a nutritional composition similar to the wheat control. Conversely, samples with high taro substitution, particularly 75-100% substitution, are projected in the left quadrants, show a strong association with the sugar and carbohydrates, reflecting their enriched starch content and reduced protein density. Notably, 100% Lau'ila is isolated in the lower left quadrant, indicating it is the most compositionally distinct sample, characterised by low protein, energy, and moderate sugars and carbohydrates.

From a nutritional standpoint, moderate substitution of wheat flour with taro flour (25-50%) offers potential health benefits, such as reduced energy density and gluten content, as well as increased dietary starch content, which may be favourable for individuals requiring controlled caloric intake or gluten avoidance. However, at high substitution levels, the pronounced reduction in protein may necessitate complementary protein enrichment to meet nutritional adequacy, especially in snacks intended for vulnerable populations.

5.3.1.2. Effects of substituting wheat flour with taro flour on the physical properties of composite crackers

The physical quality of crackers, particularly puffiness and surface colour, was markedly influenced by the level of taro flour substitution. Puffiness, an important indicator of product aeration and expansion during baking, was highest in the control wheat cracker, and declined progressively with increasing substitution of Holoitounga and Lau'ila taro flours (Table 21). These findings are consistent with those of Alflen et al. (2016), who reported that cookie thickness and puffiness decreased as the proportion of taro flour increased. This reduction was directly linked to the decline in gluten content, which plays a critical role in gas retention and dough development.

Crackers substituted with Holoitounga flour maintained moderate puffiness across substitution levels and consistently exhibited higher puffiness than their Lau'ila counterparts. This may be attributed to the higher amylose content of the Holoitounga cultivar, which likely contributed to a more rigid dough structure capable of resisting collapse during baking (Ranok et al., 2021). In contrast, the pronounced reduction in puffiness observed in Lau'ila crackers may be due to its waxy nature, which is associated with weaker structural integrity, reduced gas retention, and the formation of a denser cracker matrix (Emide et al., 2023).

Table 21 Puffiness and colour characteristics of wheat-taro crackers

Sample ID	Puffiness (%)	L*	a*	b*	Browning index	Baking time (min)
Control	121.99 ^a	74.12 ^a	3.39 ^c	31.28 ^{bc}	56.66 ^{ef}	10
HT25%	92.61 ^b	70.23 ^c	2.21 ^c	29.63 ^d	55.51 ^{cd}	10
HT50%	73.04 ^c	67.79 ^c	2.65 ^c	30.33 ^{cd}	60.34 ^{de}	10
HT75%	65.34 ^d	66.41 ^b	2.97 ^c	29.87 ^d	61.2 ^f	10
LT25%	51.88 ^e	69.84 ^d	5.73 ^a	30.37 ^a	65.02 ^a	10
LT50%	32.97 ^f	66.09 ^c	6.56 ^b	31.77 ^{cd}	67.17 ^b	15
LT75%	0.98 ^g	51.82 ^b	11.18 ^b	34.1 ^b	115.78 ^{bc}	20

Values are a means of triplicate measurements. Means in the same column with different superscripts are significantly different ($p \leq 0.05$).

Colour metrics also changed significantly. The control cracker showed the highest L^* , indicating a pale, lightly baked surface. Increasing substitution with Holoitounga and Lau'ila taro flours caused only minor declines in L^* , with a gradual increase in a^* , indicating a more reddish colour. Lau'ila exhibited the highest a^* , especially at 75% substitution, and that is due to the high baking time. Lau'ila crackers remained soft after 10 minutes of baking, indicating the need for a longer baking time to allow sufficient moisture evaporation and hardening. As a result, the extended baking led to an increase in surface browning as seen in Figure 23. This behaviour is attributed to its higher amylopectin content and greater swelling power, which delays moisture loss and crisping (Oladunmoye et al., 2014). Despite these changes, the b^* values were comparable to those of the control, suggesting that taro flour substitution did not significantly affect the yellow hue of the crackers.

These trends were further elucidated in the PCA biplot (Figure 22). The first two principal components (PC1 and PC2) explained 92.08% of the total variation. The control sample, located in the upper left quadrant, is closely associated with puffiness and high L^* values, indicating its superior expansion and light colouration. In contrast, Holoitounga substituted crackers cluster toward the lower left quadrant, suggesting moderate decreases in puffiness and lightness, but still relatively close to the control, particularly at lower substitution levels.

On the other hand, Lau'ila substituted samples, particularly LT50% and LT75%, appear distinctly separated on the far right of PC1, showing strong alignment with a^* , b^* and browning index. This positioning confirms that high substitution with Lau'ila flour results in significantly darker, redder, and more intensely browned crackers, consistent with its longer baking time due to delayed crispiness. These findings highlight the divergent impact of taro cultivar and substitution level on cracker quality, with Holoitounga flour maintaining functional properties more comparable to wheat, while Lau'ila leads to greater structural collapse and colour intensification, especially at high substitution levels.

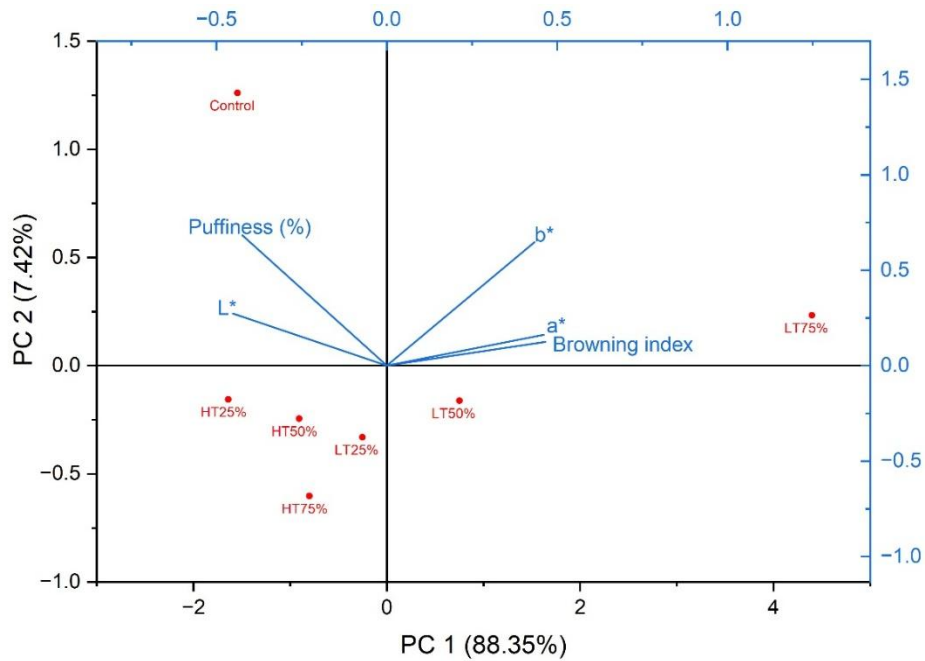


Figure 22 PCA of the puffiness and colour characteristics of wheat-taro crackers

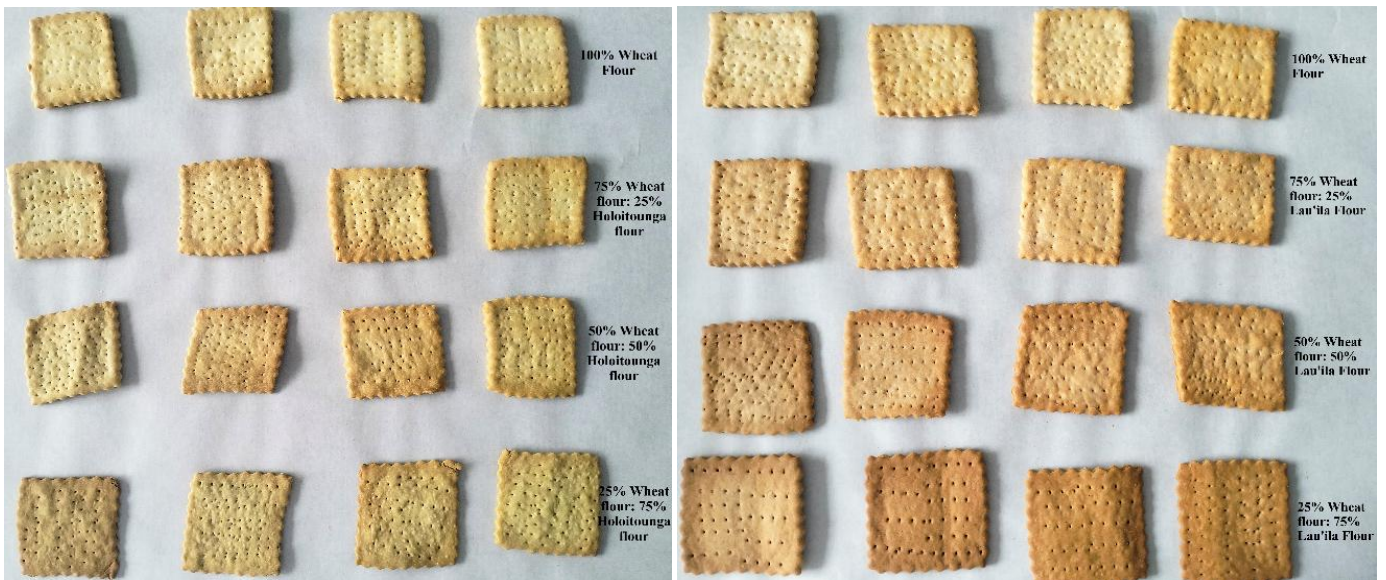


Figure 23 Photographs of wheat-taro crackers after baking at different times

5.3.1.3. Effect of substituting wheat flour with taro flour on the textural properties of composite crackers

The textural analysis, particularly the crispiness, is one of the most desired sensory attributes in crackers, and it is important to be considered, especially when the usual ingredients are being substituted. Figure 24 illustrates the effects of Holoitounga and Lauila taro flour substitution on the textural properties of crackers, especially hardness and fracturability. In terms of hardness, the control sample (100% wheat) showed a moderate firmness, while substitution

with Holoitounga led to a significant decrease in hardness, especially at higher substitution levels, with HT75% exhibiting the lowest value. Interestingly, Lau'ila substituted crackers showed more variability, with LT25% displaying the highest hardness significantly higher than all other samples, while hardness declined again at higher substitution levels. The high hardness value of LT25% may be attributed to the presence of gluten network from wheat flour and high amylopectin content. Also, the decrease in hardness when the substitution level increases for both cultivars may be due to an increase in starch content, particularly amylopectin, which has a high water binding capacity that traps water, leading to a softer texture (Oladunmoye et al., 2014).

Fracturability, representing the force required to initiate cracking (linked to crispiness), followed a somewhat different trend. The highest fracturability was observed in HT25% and LT25%, indicating that low taro flour substitution enhances cracker crispiness, possibly due to the presence of the gluten network and less taro starch content. However, fracturability declined significantly at 75% substitution for both cultivars, particularly LT75%, which showed the lowest value. This suggests that high substitution levels may produce denser, less crisp structures, likely due to the softer texture from the high water-holding capacity of the taro starch content. Overall, these results suggest that Holoitounga and Lau'ila can substitute up to 50% of wheat flour in crackers, but excessive substitution compromises both hardness and crispness.

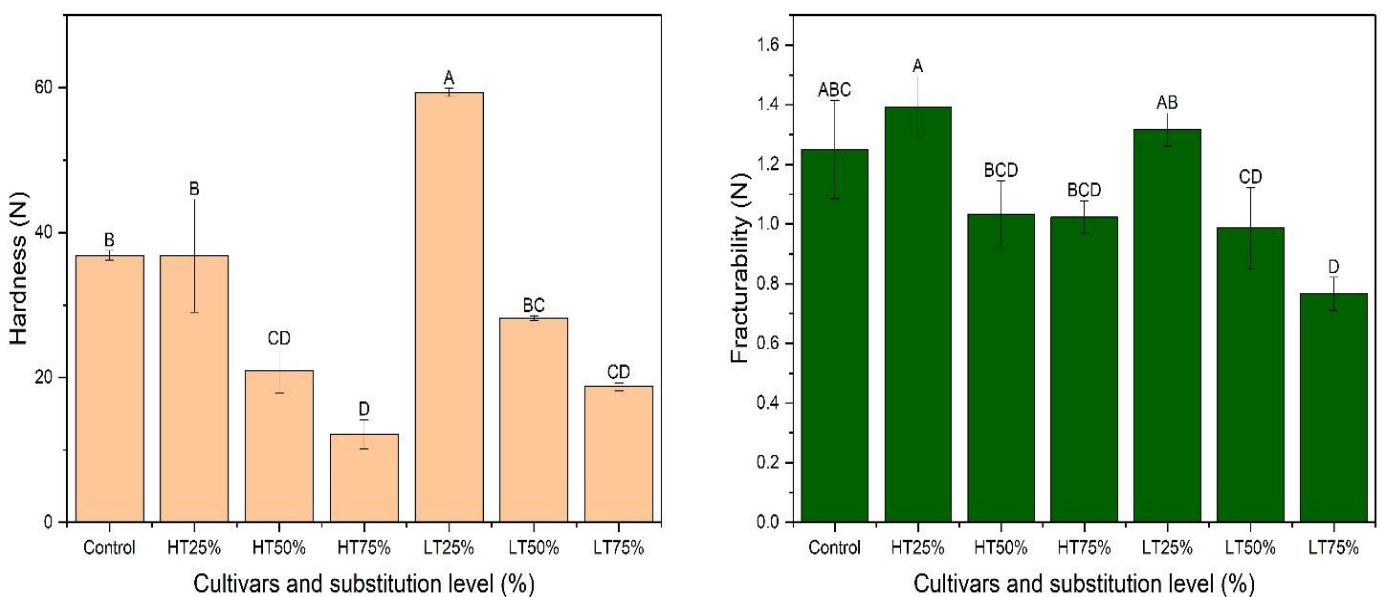


Figure 24 Hardness and fracturability of wheat-taro crackers

5.3.2. Shortbread Cookies

5.3.2.1. Effects of substituting wheat flour with taro flour on the nutritional composition of shortbread cookies

Shortbreads are a traditional bakery product typically made as a snack or treat, characterised by their high fat and sugar. It has low moisture content and has a long shelf life, which holds a strong market appeal and offers opportunities for innovation using taro flour.

The substitution of wheat flour with taro flours derived from Holoitounga and Lau'ila cultivars resulted in distinct nutritional modifications in the shortbread formulations. As shown in Table 22 and visualised in the PCA biplot (Figure 25), increasing levels of taro flour substitution led to a progressive decrease in energy protein, while increase in carbohydrates while most changes were observed in total fat, saturated fat, sugars and sodium.

The wheat shortbread sample (control) exhibited the highest energy, protein and carbohydrate contents. In contrast, full substitution with taro flours significantly reduced energy, carbohydrates and protein content. This nutritional trend indicates that taro flour possesses lower protein and carbohydrate densities compared to wheat flour, aligning with previous studies that reported taro's high starch but low protein profile(Kaur et al., 2013). While the total fat and saturated fat contents remained relatively stable across substitution levels, a slight increase was observed at 100% substitution, likely attributable to the increased butter content added to maintain dough consistency across all samples.

Table 22 Nutritional compositions of wheat-taro shortbreads

Samples	Energy (kJ)	Protein (g)	Total fat (g)	Saturated Fat (g)	Carbohydrates (g)	Sugars (g)	Sodium (mg)
Control	2410	6.9	33.6	21.7	59.6	15.8	143
HT25%	2200	5.4	33.5	21.7	61.7	15.9	143
HT50%	2000	4	33.4	21.6	63.7	15.9	143
HT75%	1790	2.5	33.3	21.6	65.8	16	143
HT100%	1750	1	35.8	23.3	67.8	16.5	128
LT25%	2200	5.5	33.5	21.7	61.5	15.9	143
LT50%	2000	4.1	33.4	21.6	63.4	15.9	143
LT75%	1790	2.6	33.3	21.6	65.3	16	143
LT100%	1750	1.1	35.8	23.3	67.2	16.5	128

PCA further elucidated the overall nutritional variation among the samples. The control sample, strongly associated with higher levels of energy and protein, as indicated by its placement in the upper left quadrant. Both HT25% and LT25% samples cluster near the control, suggesting that low levels of substitution retain a nutritional profile comparable to traditional wheat-based shortbread. As the substitution level increases to 50%, samples begin to diverge from the control, showing reductions in protein and a slight rise in carbohydrate association. This shift reflects the lower protein content and higher starch concentration of taro flour compared to wheat.

At higher substitution levels (75% and 100%), both HT and LT samples shift markedly toward the right of PC1, where they are associated with greater levels of total fat, saturated fat, sugars and carbohydrates. The LT100% and HT100% samples were particularly distinct, indicating a substantial alteration in macronutrient composition. This trend highlights a trade-off in nutritional functionality. While full taro substitution eliminates gluten and reduces energy and protein content, it increases the product’s fat and sugar concentrations, likely due to increased fat content (butter) added for dough consistency. Overall, the PCA suggests that moderate substitution levels may offer a nutritional compromise, preserve key attributes of wheat shortbreads while incorporate functional properties of taro flour.

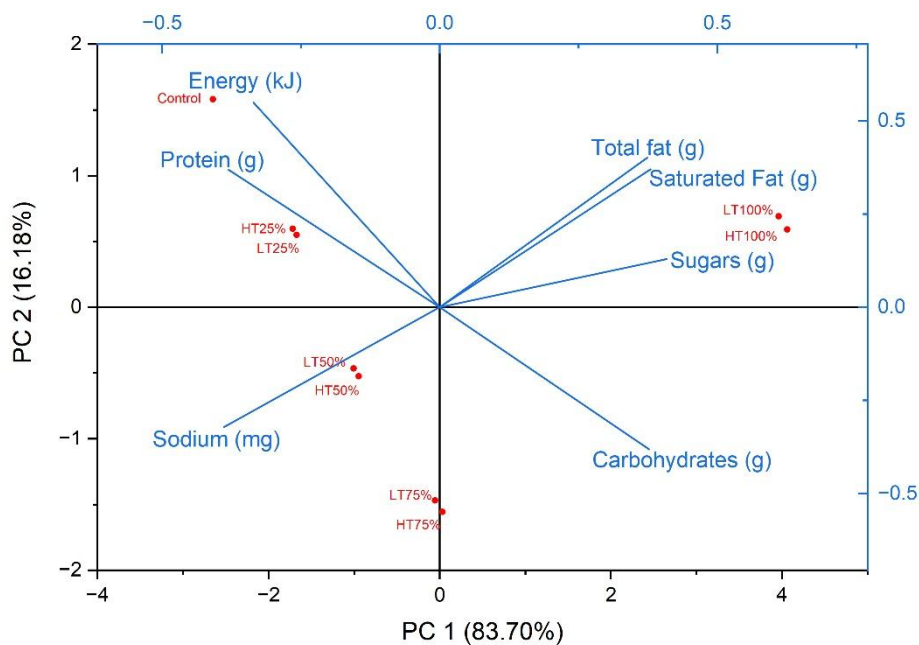


Figure 25 PCA biplot of the nutritional composition of wheat-taro shortbreads

5.3.2.2. Effects of substituting wheat flour with taro flour on the physical properties of composite shortbread cookies

Figure 27 illustrates the volume of the baked shortbreads, revealing that partial substitution of wheat flour up to 75% with both Holoitounga and Lau'ila flour had no statistically significant effect on product volume ($p > 0.05$). However, full substitution with Lau'ila flour (LT100%) resulted in a significant decrease in volume, suggesting reduced gas retention or expansion capability during baking. This may be attributed to the absence of gluten network formation in the absence of wheat flour and weaker structural integrity of the formulation, which likely contributed to collapse during baking. The HT100% sample showed a significantly higher volume than the LT100%, suggesting cultivar-dependent differences in starch-water interactions and batter matrix stability.

Visual comparison (Figure 26) supports these findings. Control and lower substitution samples retained a uniform, golden brown colour typical of well-baked shortbread, while LT 75% and especially LT100% showed a darker browning colour. The darker hue observed in LT50%, LT75% and LT100% shortbreads is associated with their longer baking times, as all other samples were fully baked within 10 minutes, whereas higher substitution of Lau'ila required an additional 5-10 minutes, respectively, to reach the desired hardness. This is attributable to the higher swelling power of Lau'ila due to its higher amylopectin content.

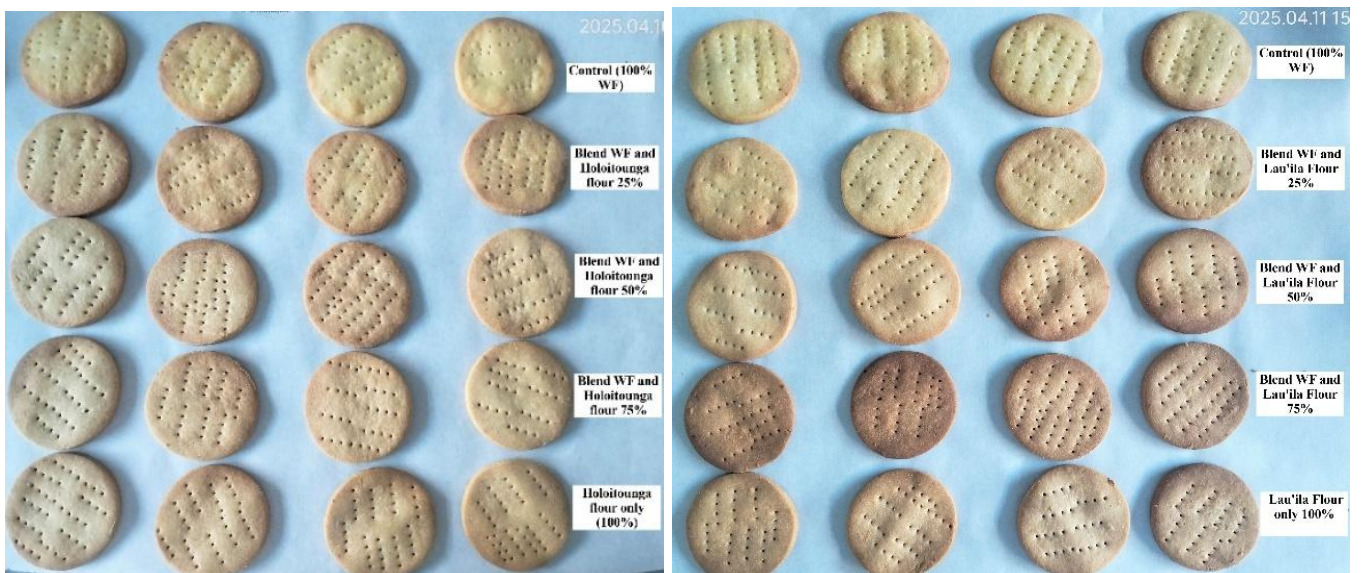


Figure 26 Visual comparison of Holoitounga and Lau'ila shortbreads

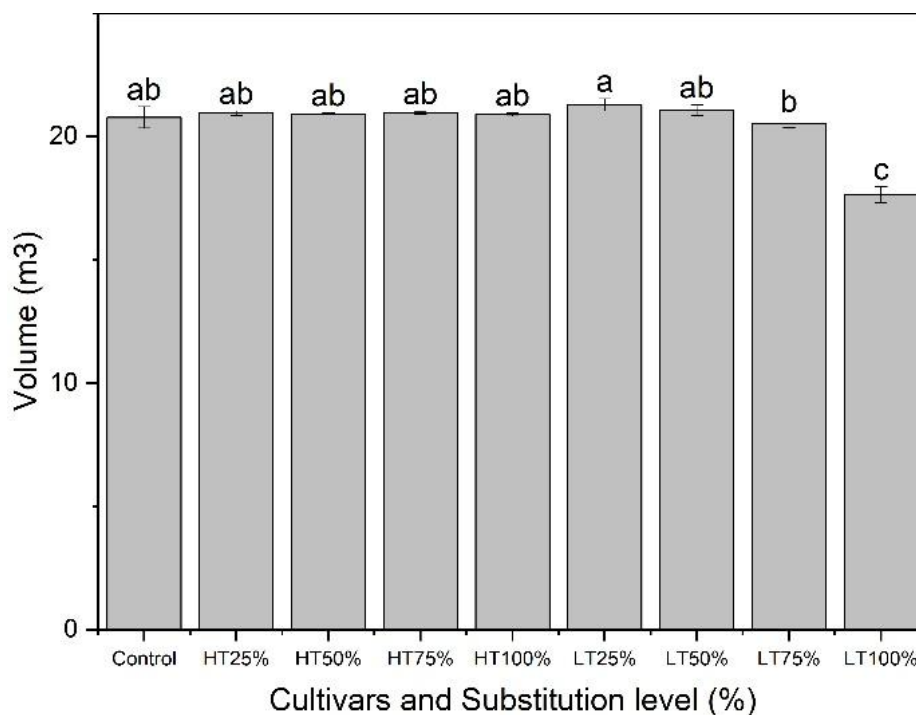


Figure 27 Volume of shortbread on different substitution levels

5.3.2.3. Effect of substituting wheat flour with taro flour on the textural properties of composite shortbread cookies

The texture profile is also an important component that needs to be considered when substituting the usual ingredients, as it directly influences consumer acceptability, mouthfeel, and overall sensory perception of the final product. Figure 28 revealed changes in textural attributes with increasing substitution of wheat flour using Holoitounga and Lau'ila taro flours in shortbread making.

In the case of Holoitounga substituted shortbread, the control sample exhibited high hardness, cohesiveness, chewiness, springiness and adhesiveness, which are desirable traits contributing to a dense, cohesive and resilient structure with some resistance to crumbling. As the level of Holoitounga taro flour substitution increased, these values gradually declined, particularly at 75% and 100%, suggesting a disruption of the gluten network and reduced structural integrity. Interestingly, the HT100% shortbread showed a sharp increase in fracturability and springiness, indicating a firmer and more brittle texture. This brittleness may stem from the dense starch matrix formed in the absence of gluten, resulting in a product that is less elastic and more prone to cracking upon force. The springiness may have been associated with the addition of other ingredients during formulations, such as xanthan gum and tapioca starch.

Similarly, the Lau'ila substituted shortbreads demonstrated marked changes in textural parameters compared to the control. With increasing substitution, the hardness, chewiness, and springiness values decreased, indicating a softer, brittle, and less elastic texture, which may reflect a weaker internal structure, resulting in less cohesive and less elastic cookies. However, at 100% substitution, it was seen with higher fracturability and springiness values, and that is probably due to the lack of gluten network and effects of other ingredients similar to HT100%.

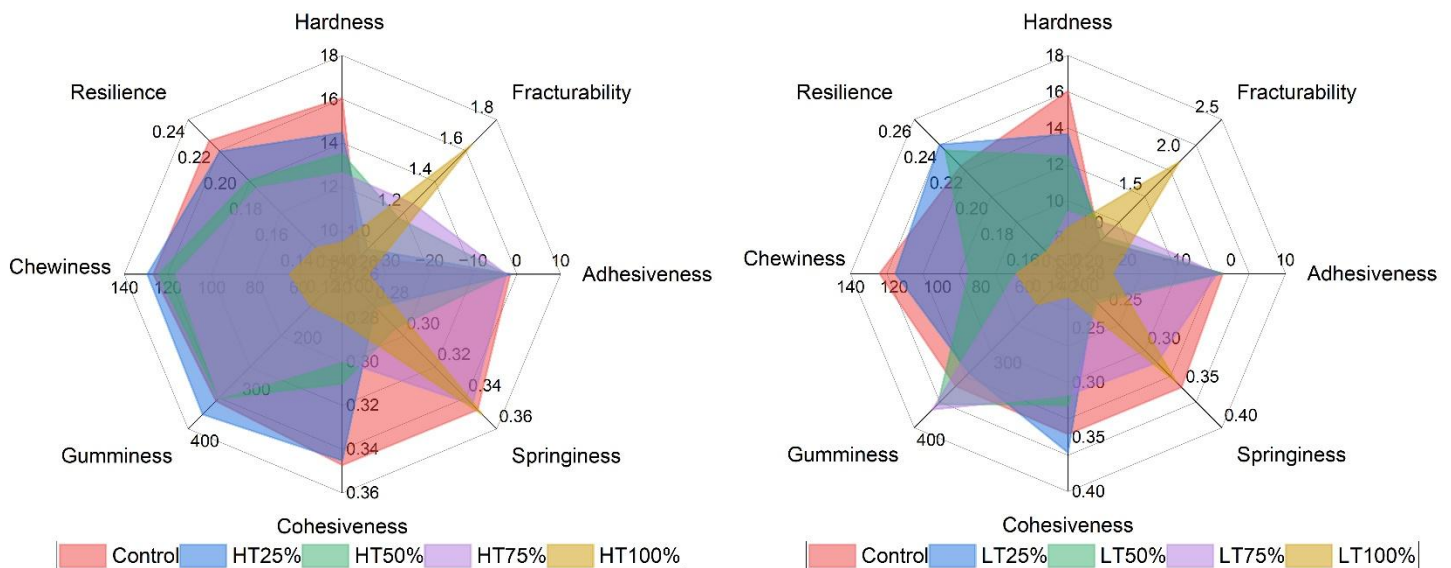


Figure 28 Texture profile analysis of wheat-taro composite shortbread cookies

The TPA results indicate that substitution of wheat flour, up to 75% with Holoitounga and up to 50% with Lau'ila, can produce shortbreads with textural properties that are relatively comparable to the control. However, full substitution significantly alters the mechanical properties of the shortbreads, resulting in higher brittleness, lower cohesiveness and reduced chewiness, which may not be desirable in standard shortbread formulations.

5.3.3. Breads

5.3.3.1. Effect of substituting wheat flour with taro flour on the nutritional composition of composite bread

The substitution of wheat flour with Holoitounga and Lau'ila taro flours in bread formulations significantly influenced the nutritional profile of the resulting breads, particularly concerning energy content, protein, and carbohydrate (Table 23). These changes provide insights into the potential health benefits and trade-offs associated with incorporating taro flours into bakery products.

Energy content showed a consistent decline with increasing levels of taro substitution for both cultivars. A notable reduction of approximately 55% in energy was observed in breads containing 75% taro flour compared to wheat control. This is attributed to the inherently lower energy density of taro flour due to its lower protein and fat content relative to wheat (Banti et al., 2025), which highlights its potential in formulation calorie-reduced bread products suitable for developing lower-calorie bread formulations targeting weight management and combating non-communicable diseases in the Pacific.

Table 23 Nutritional Composition of wheat-taro breads

Sample ID	Energy (kJ)	Protein (g)	Fat (tot) (g)	Saturated Fat (g)	Carbohydrate (g)	Sugars (g)	Sodium (mg)
Control	1140	7.8	5.6	3.3	45.4	0.1	453
Control + P	1150	9.2	5.5	3.2	44.8	0.2	470
HT25%	976	8	5.6	3.2	46.9	0.4	471
HT50%	805	6.8	5.7	3.2	48.9	0.6	471
HT75%	635	5.5	5.8	3.1	51	0.7	472
LT25%	975	8.1	5.5	3.2	46.7	0.4	471
LT50%	804	7.1	5.6	3.2	48.6	0.6	471
LT75%	633	6	5.6	3.1	50.6	0.7	472

The trends are further supported by the PCA biplot Figure 29, which shows that PC1, accounting for 76.96% of the variation, distinctly separates samples based on their macronutrient composition. Samples with high taro substitution levels, particularly HT75% and LT75%, are positioned on the far right quadrant of the biplot and closely associated with higher carbohydrate and sugar contents, confirming the starch-rich profile of taro flour (Hegazy, 2019). Conversely, the control samples (with and without protein fortification) are located on the left side of the plot and show strong associations with higher protein, energy, and saturated fat contents, indicating the nutritional density conferred by wheat flour and egg-white protein. Notably, the Control with fortified albumin protein (control +P) sample is positioned furthest along the protein vector, emphasising the impact of egg-white addition. Meanwhile, samples like HT25% and LT25% are positioned closer to the centre, indicating moderate nutritional alteration and potential as balanced composite formulations. The relatively uniform fat and sodium content across samples in both the PCA and Table 23 further supports the assertion that these components are more influenced by consistent ingredient additions (e.g. butter and salt)

rather than the flour type. Overall, the PCA strengthens the interpretation that increasing taro substitution shifts the nutritional composition toward higher carbohydrates and lower protein and energy, with implications for both dietary planning and functional bread development.

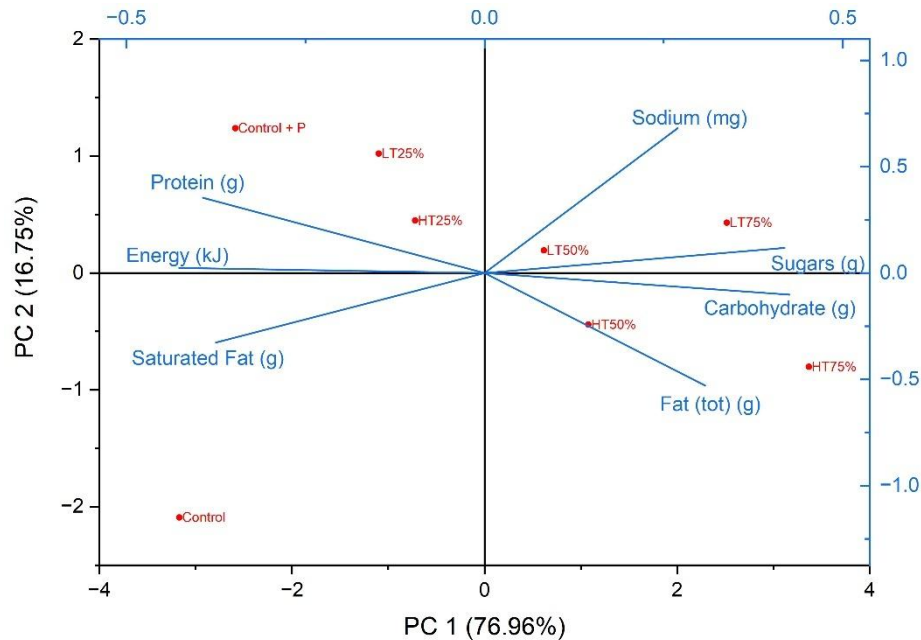


Figure 29 PCA biplot of the nutritional composition of bread

5.3.3.2. 5.3.3.2. Effect of substituting wheat flour with taro flour on the physical properties of composite bread

Figure 30 presents the physical characteristics such as loaf height, width and weight of bread samples formulated with different levels (25%, 50%, 75%) of Holoitounga and Lau’ila taro flours, compared to wheat control breads (with and without added protein).

Loaf height and width significantly decreased with increasing taro flour substitution. The HT25% formulation yielded the highest loaf height among taro substitutions indicating a better ability of the Holoitounga flour at low substitution to retain gas and support dough rise. Lau’ila substituted breads were significantly shorter in height than the Holoitounga samples.

The control sample with fortified albumin protein exhibited the broadest dimensions, followed by the HT25%, unfortified control and LT25%. This suggests that a 25% substitution level maintains dough extensibility and structural integrity reasonably well due to the amount of gluten from the wheat flour and the enhancement effects of egg white protein(Han et al., 2018). However, substitutions beyond 50% caused significant reductions in both loaf dimensions,

reflecting weakened gluten networks that are known to form an elastic network capable of holding gas and, in turn, result in higher loaf volume and dimensions (Banti et al., 2024).

Interestingly, loaf weight increased with higher taro flour substitution, regardless of cultivar. LT75% and LT50% yielded the heaviest loaves, followed by the HT75%. In contrast, the lowest loaf weights were recorded in the control samples. This increase in mass may be attributed to the higher water absorption capacity and moisture retention of taro flours, especially at higher inclusion rates, as well as their dense starch matrix (Gidmwork Abera et al., 2017). This study is consistent with previous studies, in which they reported an increased trend in loaf weight as the amount of taro flour in the composite bread increased (Gidmwork Abera et al., 2017; Banti et al., 2024). While higher weights can be beneficial for yield and shelf-life extension, the significant shrinkage in loaf volume at higher substitution levels compromises overall bread quality. This presents a trade-off between nutritional functionality, such as higher moisture retention, and structural quality.

Moreover, Figure 31 provides a visual comparison of the physical appearance of the bread loaves made with varying levels of Holoitounga and Lau'ila taro flour substitution. Loaves incorporating Holoitounga flour displayed relatively good loaf development, particularly at the 25% substitution level, which was comparable in height, shape and appearance to the wheat flour controls. Although a noticeable reduction in loaf height was observed at 50% Holoitounga substitution, the resulting bread still maintained acceptable characteristics for gluten-reduced formulations. In contrast, loaves with Lau'ila flour showed a more pronounced decline in volume and structural quality with increasing substitution levels. However, the 25% Lau'ila substitution yielded a loaf with a shape and puffing quality similar to that of the 50% Holoitounga blend, suggesting its potential viability at lower inclusion rates.

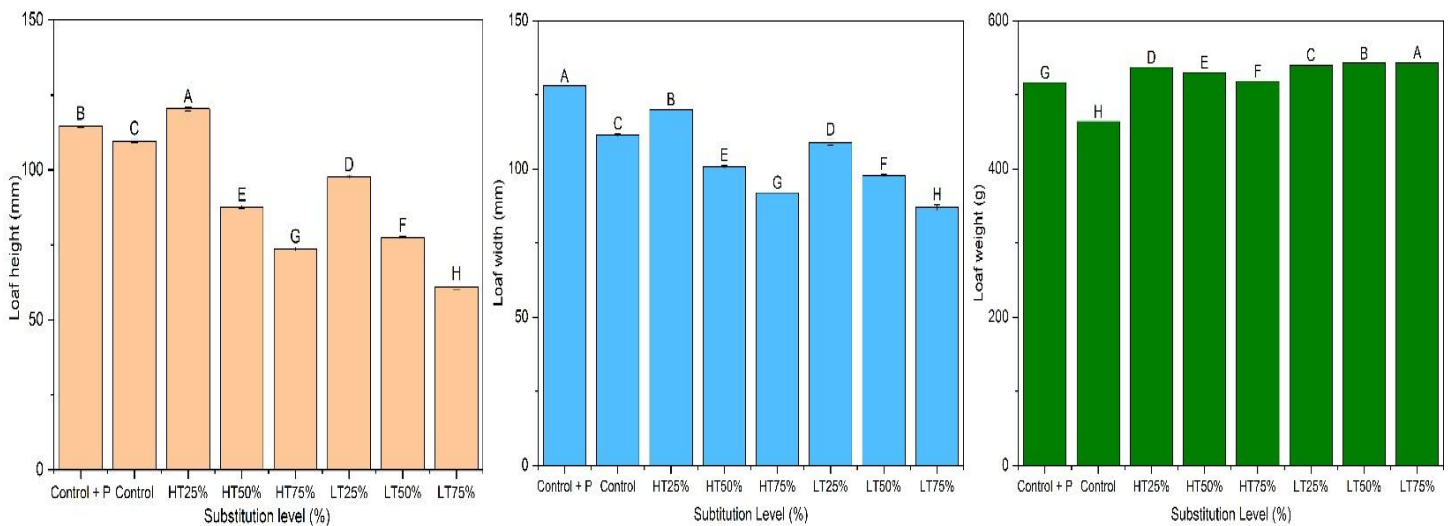


Figure 30 Physical properties of wheat-taro composite breads

Among all formulations, HT25% demonstrated the most similar physical profile to both control breads, especially in terms of loaf dimensions. It did not significantly differ from the controls in either dimension, while offering a modest increase in loaf weight. This suggests that substituting wheat flour with 25% Holoitounga flour offers the best balance between maintaining bread structure and incorporating functional taro flour. Lau'ila can also be substituted for 25% of wheat flour, given its potential to provide comparable characteristics to the control samples.

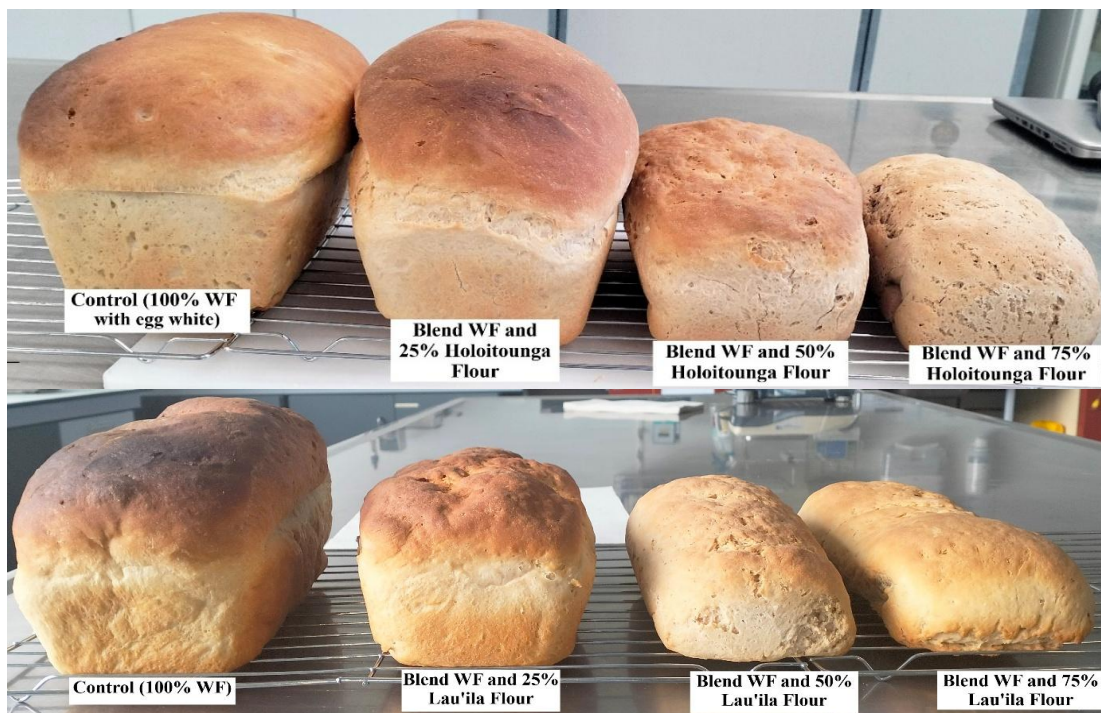


Figure 31 Physical appearance of wheat-taro composite breads

5.3.3.3. Effect of substituting wheat flour with taro flour on the crumb characteristics of composite bread

The characteristic of breadcrumbs helps reveal how flour substitution affects the internal structure and texture of bread. This is important because gluten-free flours like taro are lacking in gluten, which provides the structure and textural properties of bread desired by consumers (Scanlon & Zghal, 2001). Understanding the crumb of composite bread provides insight into whether the substituted flour maintains desirable textural properties.

The PCA biplot (Figure 32) provides a multivariate interpretation of the crumb colour data of wheat-taro composite breads, explaining a cumulative 94.66% of the total variation through the first two principal components. This high percentage explained a variance demonstrating that the three colour parameters, L* (lightness), a* (red-green), and b* (yellow-blue), are sufficient to effectively differentiate between the bread samples. PC1 is strongly and positively associated with L* and b* values, indicating that samples located toward the positive end of PC1 exhibit lighter and more yellow crumb, typical of traditional wheat breads. As seen in the plot, the control breads (with and without fortified protein) clustered closely together along this axis, confirming their high lightness and yellow tones. Along with the controls, are the Lau'ila substituted breads in which they are all clustered on the PC1 vector, indicating a lighter and yellow tone crumb with LT75% located closely to the PC2, indicating a slightly darker colour than the low Lau'ila substitution samples and the controls. The positioning of Lau'ila substitution level near the control samples along PC1 suggests that crumb colour remains closest to wheat-only bread, preserving the consumer's expected appearance.

PC2 is primarily influenced by a* parameter (redness). Samples such as HT25% show high positive PC2 scores, indicating stronger reddish tones in the crumb. This may be due to a combination of anthocyanins and the way starch gelatinizes can lead to the absorption of more light and a reduced reflection of white light, resulting in a greyish or reddish hue (Jr et al., 2006). On the other hand, samples like HT75% and HT50% scored lower on PC2, suggesting reduced red hues, possibly due to a darker, more uniformly brown crumb appearance overwhelming red tones.

The bread crumb texture and porosity in Figure 33 exhibited that control breads had a well-developed, open crumb with uniform air cell distribution, indicative of strong gluten networks that effectively trapped gas during fermentation. In contrast, as substitution levels increased, there was a noticeable reduction in crumb openness and an increase in density, especially in

the 75% substitution levels for both cultivars. This is consistent with Hegazy (2019), who reported a significant reduction in the crumb values of bread when the percentage of taro substitution increases to 20%.

HT25% and LT25% loaves maintained moderately open crumb structures, still showing some alignments with the wheat flour. HT50% and LT50% loaves were visibly denser, with smaller and fewer air pockets, indicating compromised gluten matrix and reduced gas retention. HT75% and LT75% exhibited the most compact and dense crumbs, with minimal porosity, suggesting severely limited leavening capability. This could be attributed to the dilution or replacement of gluten-forming proteins and the higher water absorption and swelling of taro starch, which disrupts the dough structure.

The image confirms that low-level substitution of wheat flour with taro flour maintains crumb colour and texture relatively close to control samples. However, the higher substitution levels result in significantly darker, denser, and less aerated crumbs, reflecting the weakening of the gluten network and poor gas retention capacity.

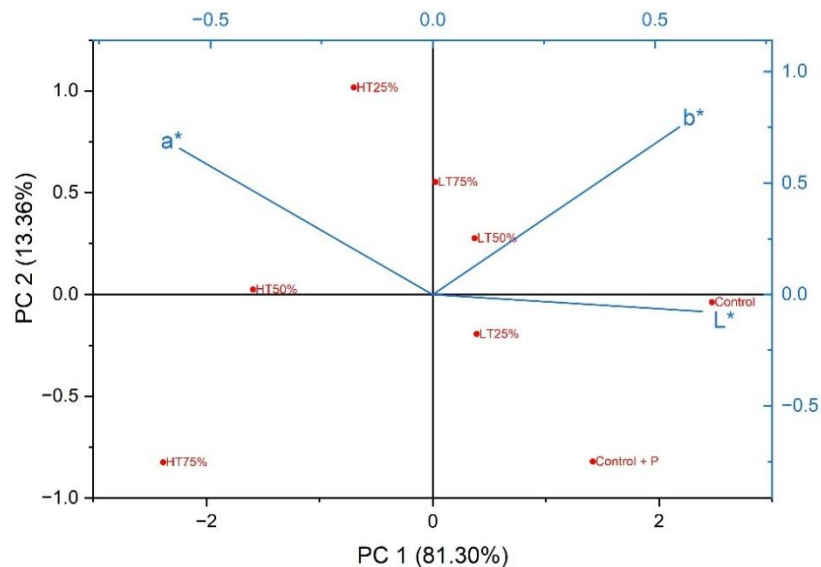


Figure 32 PCA of wheat-taro composite bread crumb colour

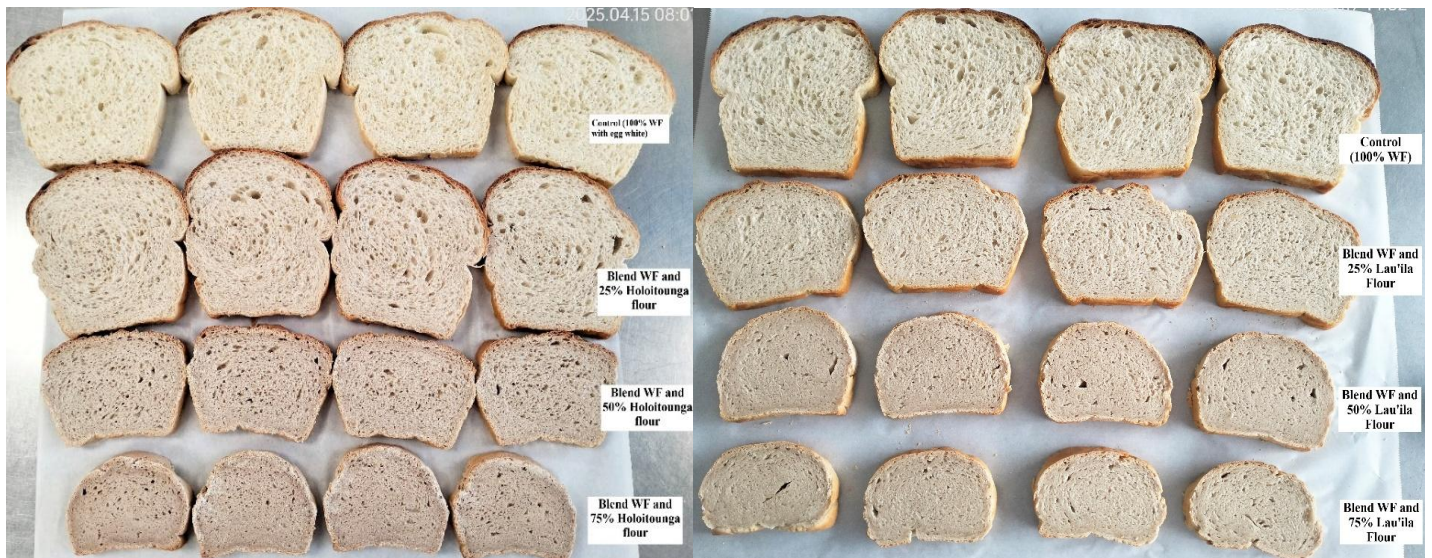


Figure 33 Wheat-taro flour bread crumb

5.3.3.4. Effect of substituting wheat flour with taro flour on the textural properties of composite bread crumb

The textural profile of breads formulated with varying levels of Holoitounga and Lau'ila taro flours is shown in Figure 34. The results reveal that increasing taro flour substitution had a pronounced effect on the mechanical attributes of the bread crumb, particularly in hardness, chewiness and elasticity-related parameters. Notably, both Holoitounga and Lau'ila breads showed a substantial increase in hardness as the substitution level increased. The HT75% and LT75% formulations exhibited the highest hardness values, indicating firmer and denser crumb textures compared to the control breads. Chewiness followed a similar trend, with HT75% and LT75% registering the highest value, suggesting that these breads required greater effort to masticate due to their compact crumb structure. These changes are consistent with the dilution of gluten proteins and the dominant presence of starch, particularly from taro flour, which alters the aeration and softness of the bread.

Elastic properties such as springiness and cohesiveness were also affected by taro flour substitution. The highest springiness values were recorded in the fortified control sample, which reflects the intact and elastic gluten matrix, likely from the cohesive network of the albumin egg white that binds the texture together, preventing it from collapsing or crumbling (A. Han et al., 2019). As the substitution level increased, a decline in springiness was observed, particularly at 75% substitution. Similarly, cohesiveness decreased with higher levels of taro flour, reflecting a weaker internal bonding structure within the bread crumb. However, both HT25% and LT25% maintained springiness and cohesiveness values relatively

close to the control, indicating that the gluten network remained partially functional at this substitution level, as well as the binding effects of the albumin protein.

Further differences were noted in gumminess and resilience, which increased and decreased, respectively, with rising substitution. HT75% and LT75% had the highest gumminess scores, likely due to the dense and crumbly matrix that resulted from their high water-binding capacity of taro starch (Hegazy, 2019). Conversely, resilience, which measures the crumbs' ability to recover from deformation, was highest in substituted samples, particularly the 75% while the control had the lowest value. This suggests chewier breads in the taro-substituted samples, likely due to the higher starch content of taro flour, especially from the Lau'ila cultivar.

These findings suggest that high levels of taro flour substitution adversely affect the bread's textural qualities by reducing its elasticity and increasing its density. In contrast, low substitution levels, particularly at 25%, preserved most of the desirable textural attributes. Both HT25% and LT25% produced bread with acceptable hardness, chewiness and elastic properties that closely resembled those of the wheat control. These results support the potential of using Holoitounga and Lau'ila taro flours at low levels as partial substitutes for wheat flour in breadmaking without compromising textural quality.

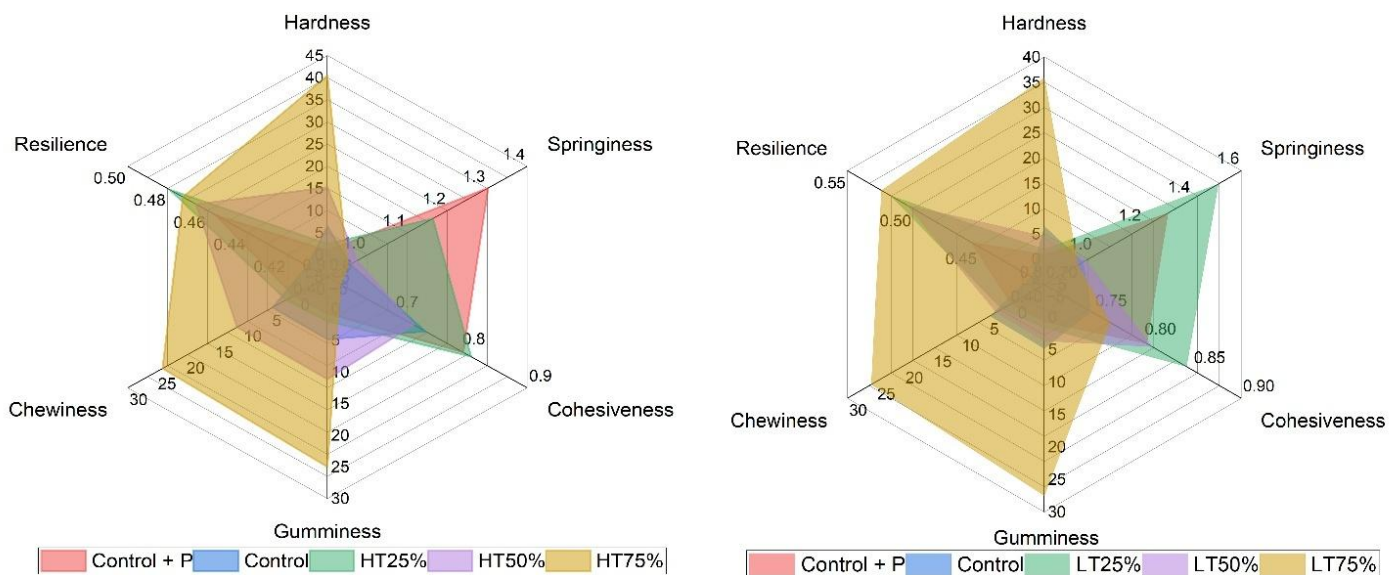


Figure 34 Textural profile analysis of wheat-taro composite breads

5.4. Conclusion

The substitution of wheat flour with Holoitounga and Lau'ila taro flours produced notable differences in the physical, textural, and nutritional properties of crackers, shortbread biscuits, and bread. Low to moderate substitution levels (25-50 %) generally maintained acceptable quality across all products, with Holoitounga consistently outperforming Lau'ila in preserving puffiness, colour and texture. These attributes are likely due to its higher amylose content, which enhances dough structure and stability. Shortbreads and crackers tolerated higher substitution levels more effectively than bread, where gluten's structural role made quality more sensitive to replacement. Nutritionally, substitution lowered energy and protein contents while increasing carbohydrates and sugars, indicating the need for protein fortification in high substitution applications. Incorporation of egg white protein into bread formulations improved elasticity and structural integrity in gluten-reduced systems, enabling partial substitution without substantial quality loss. Overall, 25% substitution with either cultivar offered the best balance of structure, texture and nutritional profile, although Holoitounga-based formulations could sustain up to 50% replacement with acceptable bread quality.

Chapter 6: General Discussions and Conclusions

6.1 Introduction

This thesis investigated whether the flour from the locally grown *Colocasia esculenta* var. *esculenta* (taro) could be used as a partial substitute for wheat flour in food applications. The underlying aim was to gain a deeper understanding of the characteristics of taro corms, how these influence the properties of ungelatinized taro flours, and the implications for their potential use in bakery products. Generating such knowledge can provide valuable insights for the development of value-added products that would benefit the food security and economic development of Tonga. This chapter presents a synthesis of the most important findings, followed by concluding remarks and recommendations.

6.2 Main findings and discussions

A review of literature on the characteristics of taro corms has been explored; however, reported characteristics, particularly regarding the physicochemical properties of taro cultivars from different regions, vary depending on cultivar type, geographical location, stage of maturation, and other factors. Within *Colocasia esculenta* var. *esculenta* corms, starch is not uniformly distributed as the central parenchyma region contains higher starch concentrations, whereas the basal, apical, and outer regions have comparatively lower levels. This heterogeneity presents a potential challenge for food product development. Converting taro corms into flour is considered a practical option, as unequal starch distribution within the tuber becomes less problematic. However, compositional differences among cultivars may still influence flour quality. Variations in starch content, amylose-to-amylopectin ratio, and nutritional composition play a critical role in determining the functionality of derived taro flours. Alongside these, the microstructural properties of taro corms are also important determinants of processing behaviour for each cultivar. These considerations provided the rationale for the detailed characterization of taro corms presented in Chapter 3.

The taro corms of *C. esculenta* var. *esculenta* Holoitounga and *C. esculenta* var. *esculenta* Lau'ila exhibited distinct chemical composition and microstructural properties. Holoitounga contained higher dry matter (38.43%), and amylose content (12.75%). Microstructural analysis revealed a loosely packed cell arrangement with larger cells and individually distributed starch

granules, features that may explain its lower cooking time, higher water absorption, and greater total solid loss during boiling. These characteristics also contribute to the soft, crumbly texture and high fracture toughness observed in Holoitounga. In contrast, Lau'ila had slightly lower dry matter (37.23 %) but slightly higher starch content (68.40 %) and amylopectin levels (90.55%). Its microstructure was characterized by tightly packed cells and agglomerated starch granules, resulting in longer cooking times. Correspondingly, Lau'ila demonstrated a firmer texture with greater adhesiveness, springiness, cohesiveness, gumminess, and chewiness. These textural attributes may be associated with its higher swelling power, attributable to the predominance of amylopectin. Further, the two cultivars displayed colour differences. Holoitounga presented a darker yellow hue with reddish fibres, whereas Lau'ila exhibited a lighter yellow parenchyma. Such variations suggest that their processing characteristics are cultivar-dependent, and their conversion into primary products such as taro flour is likely to yield distinct functional properties.

These compositional and structural differences became even more evident during flour processing. Differences in hardness were observed in the dried chips: Holoitounga, with its slightly higher amylose content, was easier to mill and break, whereas Lau'ila, with more waxy characteristics, was tougher to process, confirming the corm properties reported in Chapter 3. As a result, Holoitounga produced significantly finer flour particles (55.67 μm) compared to Lau'ila (84.98 μm), a factor that strongly influenced their physicochemical and functional properties. Holoitounga exhibited higher bulk density (0.59g/mL), tapped density (0.47 g/mL), and water absorption index (4.70 g/mL), and water absorption index (4.70 g/g), the latter likely due to its smaller particle size providing greater surface area for water interaction via hydrogen bonding (Pang et al., 2021). Both flours retained the lightly yellow hue of the native corms, with Holoitounga showing a reddish tint and Lau'ila a greenish hue. Thermal properties also differed: Holoitounga had a slightly higher gelatinization temperature (78.92 °C) compared to Lau'ila (76.86 °C), which may be related to its higher amylose content, forming more ordered crystalline structures that require more energy to disrupt (Aprianita et al., 2014). A similar phenomenon explained the high pasting temperature of Holoitounga (82.28 °C). Holoitounga also exhibited the highest peak viscosity attributed to its high amylopectin content, although it was significantly lower than Lau'ila. This high pasting viscosity may be influenced by other factors, including the chain length distribution of amylopectin, starch granule size, crystalline structure, and fiber content. The ordered crystalline structure of Holoitounga, reflected by its higher setback viscosity, reflects its more stable pasting. Gelation properties further

distinguished the cultivars, with Lau'ila forming weaker gels at 4% m/v, while Holoitounga required a higher concentration (6% m/v) to gel, consistent with the differences in their amylopectin composition.

Nutritionally, both flours exhibited similar amounts of carbohydrates (85.71 – 86.72 g/100g) and ash content of 1.95-1.97g/100g, but differed significantly in other constituents. Holoitounga had the highest crude fat content (1.72 g/100g), whereas the Lau'ila had the highest moisture content (7.40%) and crude protein (3.59%). The high crude protein of Lau'ila may have contributed to its high foaming capacity; however, the Holoitounga demonstrated superior foaming stability, likely reflecting differences in the surface-active properties of the native proteins in the two flours. A similar trend was observed for emulsion properties, with Holoitounga exhibiting higher emulsion capacity and stability. These functional differences highlight the importance of cultivar-specific protein interactions when evaluating flour performance.

Beyond physicochemical properties, rheological assessments further confirmed that Holoitounga flour, particularly when fortified with egg white and milk protein (casein isolates), closely approximated the viscoelastic characteristics of wheat flour, by exhibiting enhanced elasticity and structural integrity. In terms of thermal stability, dough supplemented with egg white protein demonstrated greater stability compared to those containing casein. By contrast, Lau'ila-based systems remained structurally limited despite modest improvements with protein supplementation. Collectively, these findings underscore the potential of high amylose taro flour, especially in combination with functional proteins such as egg white and casein, as a viable gluten-free alternative in bakery applications, offering both improved technological functionality and enhanced nutritional value.

The implications of these functional differences were further evaluated in bakery applications, where taro flour was partially substituted for wheat flour in crackers, shortbreads, and bread. The substitution of wheat flour with Holoitounga and Lau'ila taro flour resulted in a notable variation in the physical and textural characteristics of the crackers, shortbread biscuits and bread. The results revealed that low to moderate levels of substitution (up to 50%) maintained acceptable physical, textural and nutritional attributes across all product categories. Specifically, Holoitounga flour consistently showed superior performance over Lau'ila in maintaining puffiness, colour and texture, likely due to its high amylose content, which supports better dough structure and stability. Shortbreads and crackers tolerated higher

substitution levels more successfully than bread, which was significantly affected due to the structural role of gluten. Nutritionally, substitution reduced energy and protein content while increasing carbohydrates and sugars, highlighting a need for protein fortification in high-substitution applications.

The integration of egg white protein into bread formulations demonstrated potential in improving the structure and elasticity of gluten-reduced dough, enabling partial substitution without significantly compromising product quality. Among all formulations, 25% substitution using either cultivar emerged as the most promising strategy, balancing structural integrity, consumer-relevant texture, and nutritional modification. However, a floury cultivar like Holoitounga may permit substitution levels up to 50%, owing to its superior ability to support acceptable bread structure. These findings provide valuable insights for advancing import substitution strategies in Tonga by incorporating locally available taro flours into commonly consumed bakery products. Future research should explore long-term storage stability, consumer sensory evaluation, and further protein enrichment to expand the applicability of taro flour in gluten-reduced and gluten-free bakery systems.

6.3 Concluding remarks

Collectively, these findings address the central aim of this study by demonstrating how the characterization of Holoitounga and Lau'ila corms and their derived flours informs their technological and nutritional functionality in bakery applications. The cultivar-specific differences in composition, microstructure, functional properties, and rheological behaviour directly influenced product performance, highlighting the superior suitability of the high-amylose Holoitounga flour, particularly when fortified with protein, as a viable partial substitute for wheat flour. Beyond advancing scientific understanding, this work provides baseline knowledge that supports the diversification of food products, reduces dependence on imported wheat, and contributes to strategies for strengthening Tonga's agricultural resilience and food security.

6.4 Future recommendations and Way forward

Future research should focus on

- Consumer acceptance through structured sensory evaluations, alongside the optimization of substitution levels and protein fortification strategies to balance nutrition, structure, and quality in bakery applications.
- Large-scale processing trials are necessary to test scalability and cost-effectiveness, while studies on storage stability will ensure product safety and shelf life.
- Expanding this work to other underutilized root crops such as yams, cassava, and sweet potatoes could further support import substitution and food diversification.
- Assessing the economic impact, value chain benefits, and policy frameworks will be essential for integrating local flours into Tonga's food system and strengthening national food security.

References

- AACC 46-12.01 Crude Protein—Kjeldahl Method, Boric Acid Modification. (2011). In: ACC International St Paul, MN, USA.
- AACC, I. (1999). Method 44-15.02: moisture–air-oven methods. In: AACC International St. Paul, MN.
- Aalbersberg, B. (1990). Food composition. *Food and Nutrition in Fiji: Food production, composition, and intake*, 1, 108.
- Abera, G., Solomon, W. K., & Bultosa, G. (2017). Effect of drying methods and blending ratios on dough rheological properties, physical and sensory properties of wheat-taro flour composite bread. *Food Sci Nutr*, 5(3), 653-661. <https://doi.org/10.1002/fsn3.444>
- Abera, G., Solomon, W. K., & Bultosa, G. (2017). Effect of drying methods and blending ratios on dough rheological properties, physical and sensory properties of wheat–taro flour composite bread. *Food Science & Nutrition*, 5(3), 653-661. <https://doi.org/https://doi.org/10.1002/fsn3.444>
- Aboubakar, Njintang, N. Y., Scher, J., & Mbofung, C. M. F. (2009). Texture, microstructure and physicochemical characteristics of taro (*Colocasia esculenta*) as influenced by cooking conditions. *Journal of Food Engineering*, 91(3), 373-379. <https://doi.org/https://doi.org/10.1016/j.jfoodeng.2008.09.030>
- Aboubakar, Njintang, Y. N., Scher, J., & Mbofung, C. M. F. (2008). Physicochemical, thermal properties and microstructure of six varieties of taro (*Colocasia esculenta* L. Schott) flours and starches. *Journal of Food Engineering*, 86(2), 294-305. <https://doi.org/https://doi.org/10.1016/j.jfoodeng.2007.10.006>
- Adane, T., Shimelis, A., Negussie, R., Tilahun, B., & Haki, G. (2013). Effect of processing method on the Proximate composition, mineral content and antinutritional factors of Taro (*Colocasia esculenta*, L.) growth in Ethiopia. *African Journal of Food, Agriculture, Nutrition and Development*, 13(2).
- Adebowale, K., & Lawal, O. (2004). Comparative study of the functional properties of bambarra groundnut (*Voandzeia subterranean*), jack bean (*Canavalia ensiformis*) and mucuna bean (*Mucuna pruriens*) flours. *Food Research International*, 37(4), 355-365.
- Agama-Acevedo, E., Garcia-Suarez, F. J., Gutierrez-Meraz, F., Sanchez-Rivera, M. M., San Martin, E., & Bello-Pérez, L. A. (2011). Isolation and partial characterization of Mexican taro (*Colocasia esculenta* L.) starch. *Starch - Stärke*, 63(3), 139-146. <https://doi.org/https://doi.org/10.1002/star.201000113>
- Aguilera, J. M., & Stanley, D. W. (1999). *Microstructural principles of food processing and engineering*. Springer Science & Business Media.
- Ahmed, A., & Khan, F. (2013). Extraction of Starch from Taro (*Colocasia esculenta*) and Evaluating it and further using Taro Starch as Disintegrating Agent in Tablet Formulation with Over All Evaluation. *Inventi Rapid: Novel Excipients*, 2.
- Aidoo, R., Oduro, I. N., Agbenorhevi, J. K., Ellis, W. O., & Pepra-Ameyaw, N. B. (2022). Physicochemical and pasting properties of flour and starch from two new cassava accessions. *International Journal of Food Properties*, 25(1), 561-569. <https://doi.org/10.1080/10942912.2022.2052087>
- Akpata, M., & Akubor, P. (1999). Chemical composition and selected functional properties of sweet orange (*Citrus sinensis*) seed flour. *Plant foods for human nutrition*, 54, 353-362.
- Akubor, P. I. (2007). Chemical, functional and cookie baking properties of soybean/maize flour blends.
- Alcantara, R. M., Hurtada, W. A., & Dizon, E. I. (2013). The nutritional value and phytochemical components of taro [*Colocasia esculenta* (L.) Schott] powder and its selected processed foods. *J. Nutr. Food Sci*, 3(3), 207.

- Alflen, T., Quast, E., Bertan, L., & Bainy, E. (2016). Partial substitution of wheat flour with taro (*Colocasia esculenta*) flour on cookie quality. *Revista Ciencias Exatas e Naturais*, 18. <https://doi.org/10.5935/RECEN.2016.02.01>
- Ammar, M. S. A., Hegazy, A. E., & Bedeir, S. H. (2009). Using of taro flour as partial substitute of wheat flour in bread making. *World Journal of Dairy & Food Sciences*, 4, 94-99.
- Amon, A., Soro, Y., Koffi, P., Dué, E., & Patrice, K. (2011). Biochemical Characteristics of Flours from Ivorian Taro (*Colocasia Esculenta*, Cv Yatan) Corm as Affected by Boiling Time. *Advance Journal of Food Science and Technology*, 3, 424-435.
- Andersson, A., Gekas, V., Lind, I., Oliveira, F., Öste, R., & Aguilfra, J. M. (1994). Effect of preheating on potato texture. *Critical Reviews in Food Science & Nutrition*, 34(3), 229-251.
- Anuntagool, J., Asavasaksakul, S., & Pradipasena, P. (2006). Chemical and Physical Properties of Flour Extracted from Taro *Colocasia esculenta* (L.) Schott Grown in Different Regions of Thailand. *ScienceAsia*, 32. <https://doi.org/10.2306/scienceasia1513-1874.2006.32.279>
- Aprianita, A., Purwandari, U., Watson, B., & Vasiljevic, T. (2009). Physico-chemical properties of flours and starches from selected commercial tubers available in Australia. *International Food Research Journal*, 16(4), 507-520.
- Aprianita, A., Vasiljevic, T., Bannikova, A., & Kasapis, S. (2014). Physicochemical properties of flours and starches derived from traditional Indonesian tubers and roots. *J Food Sci Technol*, 51(12), 3669-3679. <https://doi.org/10.1007/s13197-012-0915-5>
- Aprodu, I., Badiu, E., & Banu, I. (2016). Influence of Protein and Water Addition on Gluten-Free Dough Properties and Bread Quality. *International Journal of Food Engineering*, 12. <https://doi.org/10.1515/ijfe-2015-0308>
- Arici, M., Metin, R., Özülkü, G., Kahraman, B., & Toker, O. (2016). Physicochemical and nutritional properties of taro (*Colocasia esculenta* L. Schott) flour as affected by drying temperature and air velocity. *LWT - Food Science and Technology*, 74. <https://doi.org/10.1016/j.lwt.2016.08.006>
- Arici, M., Özülkü, G., Kahraman, B., Metin, R., & Toker, O. (2020). Taro flour usage in wheat flour bread and gluten-free bread: Evaluation of rheological, technological and some nutritional properties. *Journal of Food Process Engineering*, 43. <https://doi.org/10.1111/jfpe.13454>
- Arici, M., Özülkü, G., Kahraman, B., Metin Yıldırım, R., & Toker, Ö. S. (2021). The effect of taro-wheat flour and taro-gluten free flour on cake batters and quality. *Journal of Food Measurement and Characterization*, 15(1), 531-540. <https://doi.org/10.1007/s11694-020-00656-1>
- Arici, M., Özülkü, G., Kahraman, B., Yıldırım, R. M., & Toker, Ö. S. (2020). Taro flour usage in wheat flour bread and gluten-free bread: Evaluation of rheological, technological and some nutritional properties. *Journal of Food Process Engineering*, 43(9), e13454. <https://doi.org/https://doi.org/10.1111/jfpe.13454>
- Arici, M., Yıldırım, R. M., Özülkü, G., Yaşar, B., & Toker, O. S. (2016). Physicochemical and nutritional properties of taro (*Colocasia esculenta* L. Schott) flour as affected by drying temperature and air velocity. *LWT*, 74, 434-440. <https://doi.org/https://doi.org/10.1016/j.lwt.2016.08.006>
- Augustin, M. A., Clarke, P. T., & Craven, H. (2003). Powdered Milk | Characteristics of Milk Powders. In B. Caballero (Ed.), *Encyclopedia of Food Sciences and Nutrition (Second Edition)* (pp. 4703-4711). Academic Press. <https://doi.org/https://doi.org/10.1016/B0-12-227055-X/00956-1>
- Awuchi, C., Victory, I., & Echeta, C. (2019). The Functional Properties of Foods and Flours. 5, 139-160.
- Badia-Olmos, C., Laguna, L., Haros, C. M., & Tárrega, A. (2023). Techno-Functional and Rheological Properties of Alternative Plant-Based Flours. *Foods*, 12(7), 1411.
- Balet, S., Guelpa, A., Fox, G., & Manley, M. (2019). Rapid Visco Analyser (RVA) as a Tool for Measuring Starch-Related Physicochemical Properties in Cereals: a Review. *Food Analytical Methods*, 12(10), 2344-2360. <https://doi.org/10.1007/s12161-019-01581-w>
- Bandana, Sharma, V., Kaushik, S. K., Singh, B., & Raigond, P. (2016). Variation in biochemical parameters in different parts of potato tubers for processing purposes. *J Food Sci Technol*, 53(4), 2040-2046. <https://doi.org/10.1007/s13197-016-2173-4>

- Bangladesh, J., Bot, Subrin, S., Satter, M., Rahman, J., Zannat, M., Chowdhury, F., & Hossain, A. (2022). Physico-Functional and Nutritional Properties of Pigmented and Non-pigmented Maize Available In Bangladesh. *Bangladesh Journal of Botany*, 51, 2022. <https://doi.org/10.3329/bjb.v51i3.62006>
- Banti, M., Atlaw, T., Urugo, M. M., Agza, B., Hailu, D., & Teka, T. A. (2025). Characterization of taro (*Colocasia esculenta*) genotypes for nutrients, anti-nutrients, phytochemicals composition, and antioxidant potentials in Southwest Ethiopia. *Journal of Agriculture and Food Research*, 19, 101591. <https://doi.org/https://doi.org/10.1016/j.jafr.2024.101591>
- Banti, M., Teka, T. A., Agza, B., & Hailu, D. (2024). Proximate, Physical, and Sensory Properties of Bread From Taro–Wheat Composite Flour. *Journal of Food Processing and Preservation*, 2024(1), 3575144. <https://doi.org/https://doi.org/10.1155/jfpp/3575144>
- Basiev, S. S., Kozaev, P. Z., Doeva, A. T., & Kozaeva, D. P. (2021). The availability of new potato cross-breeds for industrial processing. E3S Web of Conferences,
- Batey, I. (2007). Interpretation of RVA curves.
- Bathgate, G., Clapperton, J., & Palmer, G. (1973). The significance of small starch granules. Proc. Congr. Eur. Brew. Conv,
- Berk, Z. (2013). Chapter 15 - Extrusion. In Z. Berk (Ed.), *Food Process Engineering and Technology (Second Edition)* (pp. 373-393). Academic Press. <https://doi.org/https://doi.org/10.1016/B978-0-12-415923-5.00015-0>
- Bethke, P. C., & Jansky, S. H. (2008). The effects of boiling and leaching on the content of potassium and other minerals in potatoes. *J Food Sci*, 73(5), H80-85. <https://doi.org/10.1111/j.1750-3841.2008.00782.x>
- Blazek, J., & Copeland, L. (2008). Pasting and swelling properties of wheat flour and starch in relation to amylose content. *Carbohydrate polymers*, 71(3), 380-387. <https://doi.org/https://doi.org/10.1016/j.carbpol.2007.06.010>
- Boahemaa, L. V., Dzandu, B., Amisah, J. G. N., Akonor, P. T., & Saalia, F. K. (2024). Physico-chemical and functional characterization of flour and starch of taro (*Colocasia esculenta*) for food applications. *Food and Humanity*, 2, 100245. <https://doi.org/https://doi.org/10.1016/j.foohum.2024.100245>
- Bordoloi, A., Kaur, L., & Singh, J. (2012). Parenchyma cell microstructure and textural characteristics of raw and cooked potatoes. *Food Chemistry*, 133(4), 1092-1100. <https://doi.org/https://doi.org/10.1016/j.foodchem.2011.11.044>
- Bringhurst, T. A., Harrison, B. M., & Brosnan, J. (2022). Chapter 10 - Scotch whisky: Raw material selection and processing. In I. Russell, G. G. Stewart, & J. Kellersohn (Eds.), *Whisky and Other Spirits (Third Edition)* (pp. 137-203). Academic Press. <https://doi.org/https://doi.org/10.1016/B978-0-12-822076-4.00018-8>
- Bussell, W., & Goldsmith, Z. (1999). Possibilities for production of South Pacific taro in New Zealand. Proceedings of the Agronomy Society of New Zealand,
- Buzera, A., Nkirote, E., Abass, A., Orina, I., & Sila, D. (2023). Chemical and Pasting Properties of Potato Flour (*Solanum tuberosum* L.) in relation to Different Processing Techniques. *Journal of Food Processing and Preservation*, 2023(1), 3414760. <https://doi.org/https://doi.org/10.1155/2023/3414760>
- Cai, C., Zhao, L., Huang, J., Chen, Y., & Wei, C. (2014). Morphology, structure and gelatinization properties of heterogeneous starch granules from high-amylose maize. *Carbohydrate polymers*, 102, 606-614. <https://doi.org/https://doi.org/10.1016/j.carbpol.2013.12.010>
- Calix-Rivera, C. S., Mendoza-Perez, R. J., Rivera-Flores, O., & Felicidad, R. (2023). Physicochemical, hydration and steady shear rheological properties of flours derived from different crop residues from the Honduran Agro-food industry. *Revis Bionatura*, 8(3), 34.
- Calle, J., Benavent-Gil, Y., & Rosell, C. M. (2020). Development of gluten free breads from *Colocasia esculenta* flour blended with hydrocolloids and enzymes. *Food Hydrocolloids*, 98, 105243. <https://doi.org/https://doi.org/10.1016/j.foodhyd.2019.105243>

- Chandra, S., Singh, S., & Kumari, D. (2015). Evaluation of functional properties of composite flours and sensorial attributes of composite flour biscuits. *J Food Sci Technol*, 52(6), 3681-3688. <https://doi.org/10.1007/s13197-014-1427-2>
- Chandrasekara, A. (2018). Roots and tubers as functional foods. *Bioactive Molecules in Food. Reference Series in Phytochemistry*. Springer, Cham. DOI, 10, 978-973.
- Chang, Q., Zheng, B., Zhang, Y., & Zeng, H. (2021). A comprehensive review of the factors influencing the formation of retrograded starch. *International Journal of Biological Macromolecules*, 186, 163-173. <https://doi.org/https://doi.org/10.1016/j.ijbiomac.2021.07.050>
- Chanphai, P., Bekale, L., & Tajmir-Riahi, H. A. (2015). Effect of hydrophobicity on protein–protein interactions. *European Polymer Journal*, 67, 224-231. <https://doi.org/https://doi.org/10.1016/j.eurpolymj.2015.03.069>
- Chávez-Murillo, C. E., Veyna-Torres, J. I., Cavazos-Tamez, L. M., de la Rosa-Millán, J., & Serna-Saldívar, S. O. (2018). Physicochemical characteristics, ATR-FTIR molecular interactions and in vitro starch and protein digestion of thermally-treated whole pulse flours. *Food Research International*, 105, 371-383.
- Chen, Y.-F. N. (2020). *Starch retrogradation in tuber: mechanisms and its implications on microstructure and glycaemic features of potatoes: a thesis presented in partial fulfilment of the requirements for the degree of Doctor of Philosophy in School of Food and Advanced Technology at Massey University, Palmerston North, Manawatū, New Zealand Massey University*].
- Choi, I., Han, O.-K., Chun, J., Kang, C.-S., Kim, K.-H., Kim, Y.-K., Cheong, Y.-K., Park, T.-I., Choi, J.-S., & Kim, K.-J. (2012). Hydration and Pasting Properties of Oat (*Avena sativa*) Flour. *Preventive nutrition and food science*, 17, 87-91. <https://doi.org/10.3746/pnf.2012.17.1.087>
- Coffman, C. W., & Garciaj, V. V. (1977). Functional properties and amino acid content of a protein isolate from mung bean flour*. *International Journal of Food Science and Technology*, 12(5), 473-484. <https://doi.org/10.1111/j.1365-2621.1977.tb00132.x>
- Cornejo-Ramírez, Y. I., Martínez-Cruz, O., Del Toro-Sánchez, C. L., Wong-Corral, F. J., Borboa-Flores, J., & Cinco-Moroyoqui, F. J. (2018). The structural characteristics of starches and their functional properties. *CyTA - Journal of Food*, 16(1), 1003-1017. <https://doi.org/10.1080/19476337.2018.1518343>
- Coronell-Tovar, D. C., Chavez-Jauregui, R. N., Bosques-Vega, A., & Lopez-Moreno, M. L. (2018). Characterization of cocoyam (*Xanthosoma* spp.) corm flour from the Nazareno cultivar. *Food Science and Technology*, 39(02), 349-357.
- Dayakar Rao, B., Anis, M., Kalpana, K., Sunooj, K. V., Patil, J. V., & Ganesh, T. (2016). Influence of milling methods and particle size on hydration properties of sorghum flour and quality of sorghum biscuits. *LWT - Food Science and Technology*, 67, 8-13. <https://doi.org/https://doi.org/10.1016/j.lwt.2015.11.033>
- Deguchi, M., Ito, S., Motohashi, R., & Arai, E. (2021). Effects of taro *Colocasia esculenta* L. Schott drying on the properties of taro flour and taro flour products. *Food Science and Technology Research*, 27(3), 369-379. <https://doi.org/10.3136/fstr.27.369>
- Deka, D., & Sit, N. (2016). Dual modification of taro starch by microwave and other heat moisture treatments. *International Journal of Biological Macromolecules*, 92, 416-422.
- Del Gaudio, P., Ventura, G., & Taddeucci, J. (2013). The effect of particle size on the rheology of liquid-solid mixtures with application to lava flows: Results from analogue experiments. *Geochemistry, Geophysics, Geosystems*, 14(8), 2661-2669. <https://doi.org/https://doi.org/10.1002/ggge.20172>
- Del Rosarlo, M., Vinas, A., & Lorenz, K. (1999). Pasta products containing Taro (*Colocasia esculenta* L. Schott) and Chaya (*Cnidioscolus Chavamansa* L. Mcvaugh). *Journal of Food Processing and Preservation*, 23(1), 1-20. <https://doi.org/https://doi.org/10.1111/j.1745-4549.1999.tb00366.x>

- Deo, P., Tyagi, A., Taylor, M., Becker, D., & Harding, R. (2009). Improving taro (*Colocasia esculenta* var. *esculenta*) production using biotechnological approaches. *South Pac. J. Nat. Sci.*, 27. <https://doi.org/10.1071/SPO9002>
- Dilek, N., Meziyet., & Bilgiçli, N. (2021). Effect of taro [*Colocasia esculenta* (L.) Schott] flour and different shortening ratio on physical and chemical properties of gluten-free cookie. *Journal of Food Processing and Preservation*, 45(11), e15894. <https://doi.org/https://doi.org/10.1111/jfpp.15894>
- Djeukeu, W. A., Assiene, J. A. A., Dongho, F. F. D., Boudjeka, V. G., Demasse, A. M., Nyangono, F. C. B., Fongzossie, E. F., & Gouado, I. (2024). Improving gluten-free bread volume using additives: A review. *Food Chemistry Advances*, 5, 100738. <https://doi.org/https://doi.org/10.1016/j.focha.2024.100738>
- Do, D. T., Singh, J., Oey, I., & Singh, H. (2020). Isolated potato parenchyma cells: Physico-chemical characteristics and gastro-small intestinal digestion in vitro. *Food Hydrocolloids*, 108, 105972. <https://doi.org/https://doi.org/10.1016/j.foodhyd.2020.105972>
- Du, S.-k., Jiang, H., Yu, X., & Jane, J.-I. (2014). Physicochemical and functional properties of whole legume flour. *LWT-Food Science and Technology*, 55(1), 308-313.
- Duarte-Correa, Y., Vega-Castro, O., López-Barón, N., & Singh, J. (2021). Fortifying compounds reduce starch hydrolysis of potato chips during gastro-small intestinal digestion in vitro. *Starch-Stärke*, 73(9-10), 2000196.
- Durrani, C. M., & Donald, A. M. (1995). Physical characterisation of amylopectin gels. *Polymer Gels and Networks*, 3(1), 1-27. [https://doi.org/https://doi.org/10.1016/0966-7822\(94\)00005-R](https://doi.org/https://doi.org/10.1016/0966-7822(94)00005-R)
- Elgeti, D., Jekle, M., & Becker, T. (2015). Strategies for the aeration of gluten-free bread – A review. *Trends in Food Science & Technology*, 46(1), 75-84. <https://doi.org/https://doi.org/10.1016/j.tifs.2015.07.010>
- Elmi Sharlina, M. S., Yaacob, W. A., Lazim, A. M., Fazry, S., Lim, S. J., Abdullah, S., Noordin, A., & Kumaran, M. (2017). Physicochemical Properties of Starch from *Dioscorea pyrifolia* tubers. *Food Chemistry*, 220, 225-232. <https://doi.org/https://doi.org/10.1016/j.foodchem.2016.09.196>
- Emide, D., Magni, C., Saitta, F., Cardone, G., Botticella, E., Fessas, D., Iametti, S., Lafiandra, D., Sestili, F., Marti, A., & Barbiroli, A. (2023). Molecular insights into the role of amylose/amylopectin ratio on gluten protein organization. *Food Chem*, 404(Pt B), 134675. <https://doi.org/10.1016/j.foodchem.2022.134675>
- Emmanuel, C., Osuchukwu, N., & Oshiele, L. (2010). Functional and sensory properties of wheat (*Aestium triticum*) and taro flour (*Colocasia esculenta*) composite bread. *African Journal of Food Science*, 4(5), 248-253.
- Falade, K. O., & Okafor, C. A. (2015). Physical, functional, and pasting properties of flours from corms of two Cocoyam (*Colocasia esculenta* and *Xanthosoma sagittifolium*) cultivars. *J Food Sci Technol*, 52(6), 3440-3448. <https://doi.org/10.1007/s13197-014-1368-9>
- Fatima, S. (2024). Physico-chemical, functional and anti-nutritional properties of taro (*Colocasia esculenta*) flour as affected by cooking and drying methods. *African Journal of Food Science*, 17, 241-255. <https://doi.org/10.5897/AJFS2015.1370>
- Faubion, J. M., & Hosney, R. C. (1990). The Viscoelastic Properties of Wheat Flour Doughs. In H. Faridi & J. M. Faubion (Eds.), *Dough Rheology and Baked Product Texture* (pp. 29-66). Springer US. https://doi.org/10.1007/978-1-4613-0861-4_2
- Ferdaus, M. J., Chukwu-Munsen, E., Foguel, A., & da Silva, R. C. (2023). Taro Roots: An Underexploited Root Crop. *Nutrients*, 15(15). <https://doi.org/10.3390/nu15153337>
- Fredriksson, H., Silverio, J., Andersson, R., Eliasson, A.-C., & Åman, P. (1998). The influence of amylose and amylopectin characteristics on gelatinization and retrogradation properties of different starches. *Carbohydrate polymers*, 35(3-4), 119-134.

- Friero, I., Martínez-Subirà, M., Romero, M.-P., & Moralejo, M. (2024). Improving functional and nutritional profiles of barley flours with diverse starch types through pearling. *Food Chemistry*, 460, 140611. <https://doi.org/https://doi.org/10.1016/j.foodchem.2024.140611>
- Fufa, T. W., Oselebe, H. O., Abteu, W. G., & Amadi, C. O. (2023). Physicochemical Analysis of Taro (*Colocasia esculenta* (L.) Schott) Accessions. *Asian Journal of Research in Agriculture and Forestry*, 9(4), 29-41. <https://doi.org/10.9734/ajraf/2023/v9i4232>
- Ganongo-Po, F., Matos, L., Kimbonguila, A., Ndangui, C., Nzikou, J., & Scher, J. (2018). Sieving Effect on the Physicochemical and Functional Properties of Taro (*Colocasia esculenta*.) Flour. *Advance Journal of Food Science and Technology*, 14(2), 42-49.
- Gaosong, J., Ramsden, L., & Corke, H. (1997). Effect of Water-soluble Non-Starch Polysaccharides from Taro on Pasting Properties of Starch. *Starch - Stärke*, 49(7-8), 259-261. <https://doi.org/https://doi.org/10.1002/star.19970490702>
- Gavgani, H. N., Fawaz, R., Ehyaei, N., Walls, D., Pawlowski, K., Fulgos, R., Park, S., Assar, Z., Ghanbarpour, A., & Geiger, J. H. (2022). A structural explanation for the mechanism and specificity of plant branching enzymes I and IIb. *Journal of Biological Chemistry*, 298(1), 101395. <https://doi.org/https://doi.org/10.1016/j.jbc.2021.101395>
- Genet, R. (1992). Potatoes-the quest for processing quality. Proceedings Agronomy Society of New Zealand,
- Giannoutsos, K., Zalidis, A. P., Koukoumaki, D. I., Menexes, G., Mourtzinis, I., Sarris, D., & Gkatzionis, K. (2023). Production of functional crackers based on non-conventional flours. Study of the physicochemical and sensory properties. *Food Chemistry Advances*, 2, 100194. <https://doi.org/https://doi.org/10.1016/j.focha.2023.100194>
- Giri, N. A., Sakhale, B. K., & Krishnakumar, T. (2022). Nutrient composition, bioactive components, functional, thermal and pasting properties of sweet potato flour-incorporated protein-enriched and low glycemic composite flour. *Journal of Food Processing and Preservation*, 46(2), e16244.
- Gong, Y., Xiao, S., Yao, Z., Deng, H., Chen, X., & Yang, T. (2024). Factors and modification techniques enhancing starch gel structure and their applications in foods:A review. *Food Chemistry: X*, 24, 102045. <https://doi.org/https://doi.org/10.1016/j.fochx.2024.102045>
- Gong, Y., Xiao, S., Yao, Z., Deng, H., Chen, X., & Yang, T. (2024). Factors and modification techniques enhancing starch gel structure and their applications in foods:A review. *Food Chem X*, 24, 102045. <https://doi.org/10.1016/j.fochx.2024.102045>
- Goñi, I., Garcia-Alonso, A., & Saura-Calixto, F. (1997). A starch hydrolysis procedure to estimate glycemic index. *Nutrition research*, 17(3), 427-437.
- González, M. P., López-Laiz, P., Achón, M., de la Iglesia, R., Fajardo, V., García-González, Á., Úbeda, N., & Alonso-Aperte, E. (2025). Determination and Comparison of Fat and Fibre Contents in Gluten-Free and Gluten-Containing Flours and Breads: Nutritional Implications. *Foods*, 14(5), 894.
- Gross Domestic Product*. (2023). Tonga Statistic Department. Retrieved 31st July from <https://tongastats.gov.to/statistics/economics/national-accounts/>
- Gupta, R. K., Guha, P., & Srivastav, P. P. (2024). Exploring the potential of taro (*Colocasia esculenta*) starch: Recent developments in modification, health benefits, and food industry applications. *Food Bioengineering*, 3(3), 365-379. <https://doi.org/https://doi.org/10.1002/fbe2.12103>
- Ha'unga, P., & Taufatofua, P. (2021). *Tonga Root Crops (Cassava and Yams) Case Study*.
- Han, A., Motta Romero, H., Nishijima, N., Ichimura, T., Handa, A., Xu, C., & Zhang, Y. (2018). Effect of egg white solids on the rheological properties and bread making performance of gluten-free batter. *Food Hydrocolloids*, 87. <https://doi.org/10.1016/j.foodhyd.2018.08.022>
- Han, A., Romero, H. M., Nishijima, N., Ichimura, T., Handa, A., Xu, C., & Zhang, Y. (2019). Effect of egg white solids on the rheological properties and bread making performance of gluten-free

- batter. *Food Hydrocolloids*, 87, 287-296.
<https://doi.org/https://doi.org/10.1016/j.foodhyd.2018.08.022>
- Han, H., Hou, J., Yang, N., Zhang, Y., Chen, H., Zhang, Z., Shen, Y., Huang, S., & Guo, S. (2019). Insight on the changes of cassava and potato starch granules during gelatinization. *International Journal of Biological Macromolecules*, 126, 37-43.
<https://doi.org/https://doi.org/10.1016/j.ijbiomac.2018.12.201>
- Hasjim, J., Li, E., & Dhital, S. (2013). Milling of rice grains: Effects of starch/flour structures on gelatinization and pasting properties. *Carbohydrate polymers*, 92(1), 682-690.
- Hasmadi, M., Merlynda, M., Mansoor, A., Salwa, I., Zainol, M., & Jahurul, M. (2021). Comparative studies of the physicochemical and functional properties of sweet potato (*Ipomoea batatas* L.) flour. *Food Res*, 5, 145-152.
- Havea, P. (1993). *A study on the functional properties of taro starches from Tonga: a thesis presented in partial fulfilment of the requirements for the degree of Master of Technology in Food Technology at Massey University Massey University*].
- He, F., Dong, W., Wei, S., Qiu, Z., Huang, J., Jiang, H., Huang, S., & Liu, L. (2021). Transcriptome analysis of purple pigment formation in *Colocasia esculenta*. *Biocell*, 45(3), 785-796.
<https://doi.org/https://doi.org/10.32604/biocell.2021.014418>
- Hegazy, A. (2019). Using of taro (*Colocasia Escuenta*) flour as a partial substitute of wheat flour in biscuit making 235-246.
- Himeda, M., Njintang, N., Nguimbou, R., Gaiani, C., Scher, J., Facho, J., & Mbofung, C. (2012). Physicochemical, rheological and thermal properties of taro (*Colocasia esculenta*) starch harvested at different maturity stages. *International Journal of Biosciences*, 2, 14-27.
- Himeda, M., Njintang Yanou, N., Fombang, E., Facho, B., Kitissou, P., Mbofung, C. M., & Scher, J. (2014). Chemical composition, functional and sensory characteristics of wheat-taro composite flours and biscuits. *J Food Sci Technol*, 51(9), 1893-1901.
<https://doi.org/10.1007/s13197-012-0723-y>
- Himeda, M., Njintang, Y. N., Gaiani, C., Nguimbou, R. M., Scher, J., Facho, B., & Mbofung, C. M. (2014). Physicochemical and thermal properties of taro (*Colocasia esculenta* sp) powders as affected by state of maturity and drying method. *J Food Sci Technol*, 51(9), 1857-1865.
<https://doi.org/10.1007/s13197-012-0697-9>
- Holloway, W. D., Argall, M. E., Jealous, W. T., Lee, J. A., & Bradbury, J. H. (1989). Organic acids and calcium oxalate in tropical root crops. *Journal of Agricultural and Food Chemistry*, 37(2), 337-341.
- Hollyer, J., Paull, R., & Huang, A. (2000). Processing taro chips.
- Hong, G., & Nip, W. (1990). Functional properties of precooked taro flour in sorbets. *Food Chemistry*, 36(4), 261-270.
- Hossain, B. (2016). Effect of taro flour addition on the functional and physiochemical properties of wheat flour and dough for the processing of bread. *Nutrition & Food Science International Journal*, 1(2), 1-4.
- Hoyos-Leyva, J., Bello-Pérez, L. A., Agama-Acevedo, E., & Alvarez-Ramirez, J. (2018). Potential of taro starch spherical aggregates as wall material for spray drying microencapsulation: Functional, physical and thermal properties. *International Journal of Biological Macromolecules*, 120, 237-244.
- Hoyos-Leyva, J. D., Bello-Pérez, L. A., Alvarez-Ramirez, J., & Agama-Acevedo, E. (2017). Structural characterization of aroid starches by means of chromatographic techniques. *Food Hydrocolloids*, 69, 97-102.
- Huang, A. S., Titchenal, C. A., & Meilleur, B. A. (2000). Nutrient Composition of Taro Corms and Breadfruit. *Journal of Food Composition and Analysis*, 13(5), 859-864.
<https://doi.org/https://doi.org/10.1006/jfca.2000.0936>

- Ide, P., Oluka, S., & Eze, P. (2019). Determination of the pasting properties of horse-eye bean flour (*Mucuna sloanei*) varieties relevant to its processing. *Journal of Agriculture and Food Sciences*, 17(2), 14-20.
- International Merchandise Trade Statistics*. (2024). T. S. Department.
- Ishigaki, M., Kato, Y., Chatani, E., & Ozaki, Y. (2023). Variations in the Protein Hydration and Hydrogen-Bond Network of Water Molecules Induced by the Changes in the Secondary Structures of Proteins Studied through Near-Infrared Spectroscopy. *J Phys Chem B*, 127(32), 7111-7122. <https://doi.org/10.1021/acs.jpcc.3c01803>
- Ivancic, A., Garcia, J. Q., & Lebot, V. (2003). Development of visual tools for selecting qualitative corm characteristics of taro (*Colocasia esculenta* (L.) Schott). *Australian Journal of Agricultural Research*, 54(6), 581-587. <https://doi.org/10.1071/AR02182>
- Jane, J.-I. (2007). Structure of Starch Granules. *Journal of Applied Glycoscience*, 54(1), 31-36. <https://doi.org/10.5458/jag.54.31>
- Jane, J., Shen, L., Chen, J., Lim, S., Kasemsuwan, T., & Nip, W. (1992). Physical and chemical studies of taro starches and flours. *Cereal Chem*, 69(5), 528-535.
- Jojo, L., Goswami, D., Babu, S., Singh, A., Krishnan, V., & Thomas, B. (2023). Starch: Hierarchy, Types, General Features, and Applications. In S. Thomas, M. Hosur, D. Pasquini, & C. Jose Chirayil (Eds.), *Handbook of Biomass* (pp. 1-46). Springer Nature Singapore. https://doi.org/10.1007/978-981-19-6772-6_32-1
- Jr, H., Kao-Jao, T., & Nakayama, T. O. M. (2006). Anthocyanin composition of taro. *Journal of Food Science*, 42, 19-21. <https://doi.org/10.1111/j.1365-2621.1977.tb01208.x>
- Kapoor, L., Simkin, A. J., George Priya Doss, C., & Siva, R. (2022). Fruit ripening: dynamics and integrated analysis of carotenoids and anthocyanins. *BMC Plant Biology*, 22(1), 27. <https://doi.org/10.1186/s12870-021-03411-w>
- Kaur, L. (2004). Physico-chemical properties of potatoes in relation to thermal and functional properties of their starches. *Guru Nanak Dev University, Amritsar, India*.
- Kaur, L., Singh, J., McCarthy, O. J., & Singh, H. (2007). Physico-chemical, rheological and structural properties of fractionated potato starches. *Journal of Food Engineering*, 82(3), 383-394.
- Kaur, L., Singh, J., Singh, N., & Ezekiel, R. (2006). Textural and pasting properties of potatoes (*Solanum tuberosum* L.) as affected by storage temperature. *Journal of the Science of Food and Agriculture*, 87(3), 520-526. <https://doi.org/10.1002/jsfa.2750>
- Kaur, L., Singh, N., Sodhi, N., & Gujral, H. (2002). Some properties of potatoes and their starches I. Cooking, textural and rheological properties of potatoes. *Food Chemistry*, 79, 177-181. [https://doi.org/10.1016/S0308-8146\(02\)00129-2](https://doi.org/10.1016/S0308-8146(02)00129-2)
- Kaur, M., Kaushal, P., & Sandhu, K. S. (2013). Studies on physicochemical and pasting properties of Taro (*Colocasia esculenta* L.) flour in comparison with a cereal, tuber and legume flour. *J Food Sci Technol*, 50(1), 94-100. <https://doi.org/10.1007/s13197-010-0227-6>
- Kaushal, P., Kumar, V., & Sharma, H. (2015). Utilization of taro (*Colocasia esculenta*): a review. *Journal of Food Science and Technology*, 52(1), 27-40.
- Kaushal, P., Kumar, V., & Sharma, H. K. (2012). Comparative study of physicochemical, functional, antinutritional and pasting properties of taro (*Colocasia esculenta*), rice (*Oryza sativa*) flour, pigeonpea (*Cajanus cajan*) flour and their blends. *LWT - Food Science and Technology*, 48(1), 59-68. <https://doi.org/10.1016/j.lwt.2012.02.028>
- Khatkar, B. S., & Schofield, J. D. (2002). Dynamic rheology of wheat flour dough. I. Non-linear viscoelastic behaviour. *Journal of the Science of Food and Agriculture*, 82(8), 827-829.
- Koffi, K. P., Robet, E. J., Yao, A. R., Kouadio, A. P., & Amoikon, K. E. (2020). Comparative study of the nutritional potential of some starchy food (potato, yam, cassava, sweet potato, and taro) in rats. *International Journal of Development Research*, 10(05), 36108-36112. <https://doi.org/10.37118/ijdr.18839.05.2020>

- Korus, J., Chmielewska, A., Witczak, M., Ziobro, R., & Juszcak, L. (2021). Rapeseed protein as a novel ingredient of gluten-free bread. *European Food Research and Technology*, 247(8), 2015-2025.
- Kristl, J., Sem, V., Mergeduš, A., Zavišek, M., Ivančič, A., & Lebot, V. (2021). Variation in oxalate content among corm parts, harvest time, and cultivars of taro (*Colocasia esculenta* (L.) Schott). *Journal of Food Composition and Analysis*, 102, 104001. <https://doi.org/https://doi.org/10.1016/j.jfca.2021.104001>
- Kumar, L., Brennan, M., Brennan, C., & Zheng, H. (2022). Thermal, pasting and structural studies of oat starch-caseinate interactions. *Food Chemistry*, 373, 131433. <https://doi.org/https://doi.org/10.1016/j.foodchem.2021.131433>
- Kumar, R., & Khatkar, B. S. (2017). Thermal, pasting and morphological properties of starch granules of wheat (*Triticum aestivum* L.) varieties. *J Food Sci Technol*, 54(8), 2403-2410. <https://doi.org/10.1007/s13197-017-2681-x>
- Kumar, S. R., Sadiq, M. B., & Anal, A. K. (2022). Comparative study of physicochemical and functional properties of soaked, germinated and pressure cooked Faba bean. *J Food Sci Technol*, 59(1), 257-267. <https://doi.org/10.1007/s13197-021-05010-x>
- Kumar, V., Sharma, H., & Singh, K. (2023). Physico-chemical, functional and anti-nutritional properties of taro (*Colocasia esculenta*) flour as affected by cooking and drying methods.
- Lako, J., Trenerry, V., & Rochfort, S. (2008). Routine Analytical Methods for Use in South Pacific Regional Laboratories for Determining Naturally Occurring Antioxidants in Food. *International Food Research Journal*, 15.
- Laxminarayana, K. (2020). Bio-chemical constituents, value addition and alternative uses of *Colocasia esculenta* (L.). *Compar Psychol Monograph*, 4, 01-11.
- Leach, H. (1965). Gelatinization of starch. In "Starch: Chemistry and Technology," Vol. 1, (Ed.) Whistler, RJ and Paschall. In: EF Academic Press, New York.
- Lebot, V., Champagne, A., Malapa, R., & Shiley, D. (2009). NIR determination of major constituents in tropical root and tuber crop flours. *Journal of Agricultural and Food Chemistry*, 57(22), 10539-10547.
- Lebot, V., & Legendre, L. (2015). HPTLC screening of taro hybrids (*Colocasia esculenta* (L.) Schott) with high flavonoids and antioxidants contents. *Plant Breeding*, 134(1), 129-134. <https://doi.org/https://doi.org/10.1111/pbr.12225>
- Lebot, V., Prana, M. S., Kreike, N., van Heck, H., Pardales, J., Okpul, T., Gendua, T., Thongjiem, M., Hue, H., & Viet, N. (2004). Characterisation of taro (*Colocasia esculenta* (L.) Schott) genetic resources in Southeast Asia and Oceania. *Genetic Resources and Crop Evolution*, 51, 381-392.
- Lewu, M. N., Adebola, P. O., & Afolayan, A. J. (2010). Effect of cooking on the mineral contents and anti-nutritional factors in seven accessions of *Colocasia esculenta* (L.) Schott growing in South Africa. *Journal of Food Composition and Analysis*, 23(5), 389-393. <https://doi.org/https://doi.org/10.1016/j.jfca.2010.02.006>
- Li, H.-T., Kerr, E. D., Schulz, B. L., Gidley, M. J., & Dhital, S. (2022). Pasting properties of high-amylose wheat in conventional and high-temperature Rapid Visco Analyzer: Molecular contribution of starch and gluten proteins. *Food Hydrocolloids*, 131, 107840. <https://doi.org/https://doi.org/10.1016/j.foodhyd.2022.107840>
- Liang, C., Han, Y., Xu, H., Liu, D., Jiang, C., Li, Q., Hu, Y., & Xiang, X. (2025). The high molecular weight and large particle size and high crystallinity of starch increase gelatinization temperature and retrogradation in glutinous rice. *Carbohydrate polymers*, 348, 122756. <https://doi.org/https://doi.org/10.1016/j.carbpol.2024.122756>
- Lin, M. J.-Y., Humbert, E., & Sosulski, F. (1974). Certain functional properties of sunflower meal products. *Journal of Food Science*, 39(2), 368-370.
- Liu, Z., Cheng, G., Gu, Z., Zhou, Q., Yang, Y., Zhang, Z., Zhao, R., Li, C., Tian, J., Feng, J., & Jiang, H. (2024). Dynamic rheological behavior of high-amylose wheat dough during various heating stages: Insight from its starch characteristics. *International Journal of Biological*

- Macromolecules*, 271, 132111.
<https://doi.org/https://doi.org/10.1016/j.ijbiomac.2024.132111>
- Lu, T.-J., Lin, J.-H., Chen, J.-C., & Chang, Y.-H. (2008). Characteristics of Taro (*Colocasia esculenta*) Starches Planted in Different Seasons and Their Relations to the Molecular Structure of Starch. *Journal of Agricultural and Food Chemistry*, 56(6), 2208-2215.
<https://doi.org/10.1021/jf0727894>
- Lucy, M., Reed, E., & Glick, B. R. (2004). Applications of free living plant growth-promoting rhizobacteria. *Antonie van leeuwenhoek*, 86, 1-25.
- Lynch, J. M., Barbano, D. M., Healy, P. A., & Richard Fleming, J. (2020). Performance Evaluation of the Babcock and Ether Extraction Methods: 1989 through 1992. *Journal of AOAC INTERNATIONAL*, 77(4), 976-981. <https://doi.org/10.1093/jaoac/77.4.976>
- Marin, G. (1988). Oscillatory rheometry. In *Rheological measurement* (pp. 297-343). Springer.
- Mauro, R. R., Vela, A. J., & Ronda, F. (2023). Impact of Starch Concentration on the Pasting and Rheological Properties of Gluten-Free Gels. Effects of Amylose Content and Thermal and Hydration Properties. *Foods*, 12(12), 2281.
- Mergedus, A., Kristl, J., Ivancic, A., Sober, A., Sustar, V., Krizan, T., & Lebot, V. (2015). Variation of mineral composition in different parts of taro (*Colocasia esculenta*) corms. *Food Chemistry*, 170, 37-46. <https://doi.org/https://doi.org/10.1016/j.foodchem.2014.08.025>
- Mihiranie, S., Jayasundera, M., Pathiraja, D., & Perera, N. (2014). *Formulation of value added crackers using defatted coconut flour*.
- Minaker, S., Mason, R., & Chow, D. (2021). Optimizing Color Performance of the Ngenuity® 3D Visualization System. *Ophthalmology Science*, 1, 100054.
<https://doi.org/10.1016/j.xops.2021.100054>
- Mine, Y. (1995). Recent advances in the understanding of egg white protein functionality. *Trends in Food Science & Technology*, 6(7), 225-232. [https://doi.org/https://doi.org/10.1016/S0924-2244\(00\)89083-4](https://doi.org/https://doi.org/10.1016/S0924-2244(00)89083-4)
- Ministry of Agriculture, Food and Forests Annual Report* (2024).
- Mir, S. A., Shah, M. A., Naik, H. R., & Zargar, I. A. (2016). Influence of hydrocolloids on dough handling and technological properties of gluten-free breads. *Trends in Food Science & Technology*, 51, 49-57.
- Moorthy, S. N. (2004). 11 - Tropical sources of starch. In A.-C. Eliasson (Ed.), *Starch in Food* (pp. 321-359). Woodhead Publishing. <https://doi.org/https://doi.org/10.1533/9781855739093.2.321>
- Moscetti, R., Sturm, B., Crichton, S. O., Amjad, W., & Massantini, R. (2018). Postharvest monitoring of organic potato (cv. Anuschka) during hot-air drying using visible–NIR hyperspectral imaging. *Journal of the Science of Food and Agriculture*, 98(7), 2507-2517.
- Mua, J. P., & Jackson, D. S. (1997). Relationships between Functional Attributes and Molecular Structures of Amylose and Amylopectin Fractions from Corn Starch. *Journal of Agricultural and Food Chemistry*, 45(10), 3848-3854. <https://doi.org/10.1021/jf9608783>
- Mweta, D. E., Labuschagne, M. T., Bonnet, S., Swarts, J., & Saka, J. D. (2010). Isolation and physicochemical characterisation of starch from cocoyam (*Colocasia esculenta*) grown in Malawi. *Journal of the Science of Food and Agriculture*, 90(11), 1886-1896.
- Nagar, C. K., Dash, S. K., Rayaguru, K., Pal, U. S., & Nedunchezhiyan, M. (2021). Isolation, characterization, modification and uses of taro starch: A review. *International Journal of Biological Macromolecules*, 192, 574-589.
<https://doi.org/https://doi.org/10.1016/j.ijbiomac.2021.10.041>
- Nammakuna, N., Barringer, S. A., & Ratanatriwong, P. (2016). The effects of protein isolates and hydrocolloids complexes on dough rheology, physicochemical properties and qualities of gluten-free crackers. *Food Science & Nutrition*, 4(2), 143-155.
- Nawaz, H., Aslam, M., Rehman, T., & Mehmood, R. (2021). Modification of emulsifying properties of cereal flours by blending with legume flours. *Asian Journal of Dairy and Food Research*, 40(3), 315-320.

- Netam, U., Thakur, P., & Kar, B. S. S. (2022). Morphological characterization of Taro [*Colocasia esculenta* var. *antiquorum* (L.) Schott.] Genotypes. In
- Nguimbou, R. (2012). *Potentiel nutritionnel et propriétés physico-chimiques des poudres de tubercules de *Cyrtosperma merkusii* (H. Schott), taro bicolore non-conventionnel* Thèse de Doctorat/Ph. D, Université de Ngaoundéré, Cameroun et université de ...].
- Nigam, S., & Tomar, S. (2022). Development and Quality Evaluation of Bread Fortified With Partial Substituent Raw Taro Flour” Impact of Raw Taro Flour on Bread. *Quality. International Journal of Advances in Engineering and Management (IJAEM)*, 4(5), 809-818.
- Nip, W.-K. (2023). Taro. In *Processing Vegetables* (pp. 355-388). Routledge.
- Nip, W., K., Whitaker, C., S., & Vargo, D. (1994). Application of taro flour in cookie formulations. *International Journal of Food Science and Technology*, 29(4), 463-468.
<https://doi.org/10.1111/j.1365-2621.1994.tb02088.x>
- Njintang, N., Mbofung, C., Balaam, F., Kitissou, P., & Scher, J. (2008). Effect of taro (*Colocasia esculenta*) flour addition on the functional and alveographic properties of wheat flour and dough. *Journal of the Science of Food and Agriculture*, 88(2), 273-279.
<https://doi.org/https://doi.org/10.1002/jsfa.3085>
- Njintang, N., Parker, M., Moates, G., Faulds, C., Smith, A., Waldron, K., Mbofung, C., & Scher, J. (2008). Microstructure and creep-recovery characteristics of achu (a taro based paste) made from freeze dried taro chips as affected by moisture content and variety. *Journal of Food Engineering*, 87(2), 172-180. <https://doi.org/https://doi.org/10.1016/j.jfoodeng.2007.11.033>
- Njintang, N. Y., Mbofung, C., Moates, G. K., Parker, M. L., Craig, F., Smith, A. C., & Waldron, W. (2007). Functional properties of five varieties of taro flour, and relationship to creep recovery and sensory characteristics of achu (taro based paste). *Journal of Food Engineering*, 82(2), 114-120.
- Nkurikiye, E., Pulivarthi, M. K., Bhatt, A., Siliveru, K., & Li, Y. (2023). Bulk and flow characteristics of pulse flours: A comparative study of yellow pea, lentil, and chickpea flours of varying particle sizes. *Journal of Food Engineering*, 357, 111647.
<https://doi.org/https://doi.org/10.1016/j.jfoodeng.2023.111647>
- Nurilmala, F., Jannah, A., Palupi, E., Sonani, N., Mala, R., Nurdin, N. M., Zahidah, F. U., Bila, N. S., Sharannie, & Dewi, S. A. (2024). High-fiber and low-glycemic index egg-roll cookies made from non-itchy taro (*Colocasia esculenta* var. *Febi521*). *Journal of Agriculture and Food Research*, 18, 101308. <https://doi.org/https://doi.org/10.1016/j.jafr.2024.101308>
- Official methods of analysis of the Association of Official Analytical Chemists*. (1980).
- Okonkwo, C. A. C. (1993). 48 - Taro: *Colocasia* spp. In G. Kalloo & B. O. Bergh (Eds.), *Genetic Improvement of Vegetable Crops* (pp. 709-715). Pergamon.
<https://doi.org/https://doi.org/10.1016/B978-0-08-040826-2.50052-7>
- Oladunmoye, O. O., Aworh, O. C., Maziya-Dixon, B., Erukainure, O. L., & Elemo, G. N. (2014). Chemical and functional properties of cassava starch, durum wheat semolina flour, and their blends. *Food Sci Nutr*, 2(2), 132-138. <https://doi.org/10.1002/fsn3.83>
- Olakanmi, S. J., Jayas, D. S., Paliwal, J., & Aluko, R. E. (2024). Impact of Particle Size on the Physicochemical, Functional, and In Vitro Digestibility Properties of Fava Bean Flour and Bread. *Foods*, 13(18). <https://doi.org/10.3390/foods13182862>
- Onwueme, I. (1999). Taro cultivation in Asia and the Pacific. *RAP publication*, 16, 1-9.
- Onwuka, G. I. (2005). *Food analysis and instrumentation: theory and practice*. Naphthali prints.
- Ooms, N., & Delcour, J. A. (2019). How to impact gluten protein network formation during wheat flour dough making. *Current Opinion in Food Science*, 25, 88-97.
<https://doi.org/https://doi.org/10.1016/j.cofs.2019.04.001>
- Ouédraogo, N., Sombié, D., Eric, P. A., Traoré, R. E., Sama, H., Bationo Kando, P., Sawadogo, M., & Lebot, V. (2023). Nutritional and phytochemical characterization of taro (*Colocasia esculenta*) germplasm from Burkina Faso.

- Ozgolet, M., Karasu, S., & Kasapoglu, M. Z. (2025). Development of Gluten-Free Cakes Using Protein Concentrate Obtained from Cold-Pressed Terebinth (*Pistacia terebinthus* L.) Oil By-Products. *Foods*, 14(6), 1049.
- Pang, J., Guan, E., Yang, Y., Li, M., & Bian, K. (2021). Effects of wheat flour particle size on flour physicochemical properties and steamed bread quality. *Food Sci Nutr*, 9(9), 4691-4700. <https://doi.org/10.1002/fsn3.2008>
- Panyoo, E. A., Njintang, N. Y., Hussain, R., Gaiani, C., Scher, J., & Mbofung, C. M. F. (2014). Physicochemical and Rheological Properties of Taro (*Colocasia esculenta*) Flour Affected by Cormels Weight and Method of Peeling. *Food and Bioprocess Technology*, 7(5), 1354-1363. <https://doi.org/10.1007/s11947-013-1175-8>
- Paschoalin, V., Pereira, P., Mattos, É., & Corrêa, A. (2021). *Taro Corms*.
- Pérez, E., Schultz, F. S., & de Delahaye, E. P. (2005). Characterization of some properties of starches isolated from *Xanthosoma sagittifolium* (tannia) and *Colocassia esculenta* (taro). *Carbohydrate polymers*, 60(2), 139-145. <https://doi.org/https://doi.org/10.1016/j.carbpol.2004.11.033>
- Pico, J., Reguilon, M. P., Bernal, J., & Gómez, M. (2019). Effect of rice, pea, egg white and whey proteins on crust quality of rice flour-corn starch based gluten-free breads. *Journal of Cereal Science*, 86, 92-101.
- Piluk, P., Khemthong, C., Chupeerach, C., Suttisansanee, U., Chamchan, R., Thangsiri, S., & On-nom, N. (2025). Development and characterization of high protein and fiber gluten free bread formulations from egg white powder and resistant starch. *LWT*, 227, 117984. <https://doi.org/https://doi.org/10.1016/j.lwt.2025.117984>
- Pramodrao, K. S., & Riar, C. S. (2014). Comparative study of effect of modification with ionic gums and dry heating on the physicochemical characteristic of potato, sweet potato and taro starches. *Food Hydrocolloids*, 35, 613-619. <https://doi.org/https://doi.org/10.1016/j.foodhyd.2013.08.006>
- Prescott, N., Finau, P., Kami, V., Ngaluafe, P., Kilisimasi, K., Hoponoa, T., Palaki, A., Matoto, L., & Samani, T. (2004). National Biodiversity Strategy & Action Plan. In: Department of Environment.
- Ranok, A., Dissamal, P., Kupradit, C., Khongla, C., Musika, S., & Mangkalan, S. (2021). Physicochemical properties and antioxidant activity of gluten-free riceberry-cheese cracker under simulated gastrointestinal transit. *J Food Sci Technol*, 58(7), 2825-2833. <https://doi.org/10.1007/s13197-021-04978-w>
- Renzetti, S., & Rosell, C. M. (2016). Role of enzymes in improving the functionality of proteins in non-wheat dough systems. *Journal of Cereal Science*, 67, 35-45.
- Rickard, J. (1991). Study on the factors affecting storage of edible aroids. *Annals of Applied Biology*, 119.
- Rodriguez Furlán, L. T., Pérez Padilla, A., & Campderrós, M. E. (2015). Improvement of gluten-free bread properties by the incorporation of bovine plasma proteins and different saccharides into the matrix. *Food Chemistry*, 170, 257-264. <https://doi.org/https://doi.org/10.1016/j.foodchem.2014.08.033>
- Rogers, S., Rosecrance, R., Chand, K., & Iosefa, T. (1992). Effects of shade and mulch on the growth and dry matter accumulation of taro (*Colocasia esculenta* L. Schott). *Journal of South Pacific agriculture* 1 (3), 1-4.
- Saha, D., & Bhattacharya, S. (2010). Hydrocolloids as thickening and gelling agents in food: a critical review. *Journal of Food Science and Technology*, 47(6), 587-597.
- Sahagún, M., Bravo-Núñez, Á., Bascónes, G., & Gómez, M. (2018). Influence of protein source on the characteristics of gluten-free layer cakes. *LWT*, 94, 50-56. <https://doi.org/https://doi.org/10.1016/j.lwt.2018.04.014>

- Saklani, A., Kaushik, R., Chawla, P., Kumar, N., & Kumar, M. (2021). Effect of taro (*Colocasia esculenta*) enrichment on physicochemical and textural properties of cake. *International Journal of Food Studies*, 10.
- Salazar-Montoya, O., Idárraga-Arcila, V., Torres-Martínez, P., & Duarte-Correa, Y. (2024). Evaluation of Different Anti-Browning Treatments on the Quality of Four Colombian Potato Varieties. *Horticulturae*, 10(12), 1265.
- Salvador, A., Sanz, T., & Fiszman, S. M. (2006). Dynamic rheological characteristics of wheat flour–water doughs. Effect of adding NaCl, sucrose and yeast. *Food Hydrocolloids*, 20(6), 780-786. <https://doi.org/https://doi.org/10.1016/j.foodhyd.2005.07.009>
- Sanchez, C., Klopfenstein, C., & Walker, C. (1995). Use of carbohydrate-based fat substitutes and emulsifying agents in reduced-fat shortbread cookies. *Cereal chemistry*, 72(1), 25-29.
- Sanful, R., Elsie. (2011). Organoleptic and nutritional analysis of taro and wheat flour composite bread. *World Journal of Dairy and Food Sciences*, 6(2), 175-179.
- Saxby, S. M. (2020). *The potential of Taro (Colocasia esculenta) as a dietary prebiotic source for the prevention of colorectal cancer* University of Hawai'i at Manoa].
- Saxby, S. M., Dong, L., Ho, K., Lee, C. N., Wall, M., & Li, Y. (2024). Nutritional, physicochemical, and functional properties of Hawaiian taro (*Colocasia esculenta*) flours: A comparative study. *J Food Sci*, 89(5), 2629-2644. <https://doi.org/10.1111/1750-3841.17053>
- Scanlon, M. G., & Zghal, M. C. (2001). Bread properties and crumb structure. *Food Research International*, 34(10), 841-864. [https://doi.org/https://doi.org/10.1016/S0963-9969\(01\)00109-0](https://doi.org/https://doi.org/10.1016/S0963-9969(01)00109-0)
- Schmiele, M., Jaekel, L. Z., Patricio, S. M. C., Steel, C. J., & Chang, Y. K. (2012). Rheological properties of wheat flour and quality characteristics of pan bread as modified by partial additions of wheat bran or whole grain wheat flour. *International Journal of Food Science and Technology*, 47(10), 2141-2150. <https://doi.org/10.1111/j.1365-2621.2012.03081.x>
- Scott, G., & Awika, J. (2023). Effect of protein–starch interactions on starch retrogradation and implications for food product quality. *Comprehensive Reviews in Food Science and Food Safety*, 22. <https://doi.org/10.1111/1541-4337.13141>
- Shubhangi, N., Sanjana, T., & Shivani, G. (2023). Bread with flour obtained from raw taro flour as partial substitute for wheat flour: functional, physical, chemical characteristics and acceptance. *International Journal of Emerging Technologies and Innovative Research*, 10(9).
- Simsek, S., & El, S. N. (2012). Production of resistant starch from taro (*Colocasia esculenta* L. Schott) corm and determination of its effects on health by in vitro methods. *Carbohydrate polymers*, 90(3), 1204-1209. <https://doi.org/https://doi.org/10.1016/j.carbpol.2012.06.039>
- Simsek, S., & El, S. N. (2015). In vitro starch digestibility, estimated glycemic index and antioxidant potential of taro (*Colocasia esculenta* L. Schott) corm. *Food Chemistry*, 168, 257-261. <https://doi.org/https://doi.org/10.1016/j.foodchem.2014.07.052>
- Singh, N., Kaur, L., Ezekiel, R., & Singh Guraya, H. (2005). Microstructural, cooking and textural characteristics of potato (*Solanum tuberosum* L) tubers in relation to physicochemical and functional properties of their flours. *Journal of the Science of Food and Agriculture*, 85(8), 1275-1284. <https://doi.org/https://doi.org/10.1002/jsfa.2108>
- Singh, N., Singh, J., Kaur, L., Singh Sodhi, N., & Singh Gill, B. (2003). Morphological, thermal and rheological properties of starches from different botanical sources. *Food Chemistry*, 81(2), 219-231. [https://doi.org/https://doi.org/10.1016/S0308-8146\(02\)00416-8](https://doi.org/https://doi.org/10.1016/S0308-8146(02)00416-8)
- Sit, N., Misra, S., & Deka, S. C. (2014). Characterization of Physicochemical, Functional, Textural and Color Properties of Starches from Two Different Varieties of Taro and Their Comparison to Potato and Rice Starches. *Food Science and Technology Research*, 20(2), 357-365. <https://doi.org/10.3136/fstr.20.357>
- Storck, C. R., da Rosa Zavareze, E., Gularte, M. A., Elias, M. C., Rosell, C. M., & Guerra Dias, A. R. (2013). Protein enrichment and its effects on gluten-free bread characteristics. *LWT - Food*

- Science and Technology*, 53(1), 346-354.
<https://doi.org/https://doi.org/10.1016/j.lwt.2013.02.005>
- Szymonska, J., Targosz-Korecka, M., & Krok, F. (2009). Characterization of starch nanoparticles. *J. Phys.: Conf. Ser.*, 146, No pp. given. <https://doi.org/10.1088/1742-6596/146/1/012027>
- Tabilo-Munizaga, G., & Barbosa-Cánovas, G. V. (2005). Rheology for the food industry. *Journal of Food Engineering*, 67(1-2), 147-156.
- Tagodoe, A., & Nip, W. K. (1994). Functional properties of raw and precooked taro (*Colocasia esculenta*) flours. *International journal of food science & technology*, 29(4), 457-462.
- Tari, T. A., & Singhal, R. S. (2002). Starch-based spherical aggregates: stability of a model flavouring compound, vanillin entrapped therein. *Carbohydrate polymers*, 50(4), 417-421.
- Tattiyakul, J., Pradipasena, P., & Asavasaksakul, S. (2007). Taro *Colocasia esculenta* (L.) Schott Amylopectin Structure and Its Effect on Starch Functional Properties. *Starch - Stärke*, 59(7), 342-347. <https://doi.org/https://doi.org/10.1002/star.200700620>
- Taufatofua, P., & Mana'ia, H. (1995). *TONGA: Country report to the FAO International Conference on plant genetic resources*.
- Temesgen, M., & Retta, N. (2015a). Nutritional potential, Health and Food Security Benefits of Taro *Colocasia esculenta* (L.): A Review. *The Open Food Science Journal*.
- Temesgen, M., & Retta, N. (2015b). Nutritional potential, health and food security benefits of taro *Colocasia esculenta* (L.): A review. *Food Science and Quality Management*, 36(0), 23-30.
- Tester, R. F., & Karkalas, J. (1996). Swelling and gelatinization of oat starches. *Cereal chemistry*, 73(2), 271-277.
- Tester, R. F., & Morrison, W. R. (1990). Swelling and gelatinization of cereal starches. I. Effects of amylopectin, amylose, and lipids. *Cereal Chem*, 67(6), 551-557.
- Thiex, N., Novotny, L., & Crawford, A. (2019). Determination of Ash in Animal Feed: AOAC Official Method 942.05 Revisited. *Journal of AOAC INTERNATIONAL*, 95(5), 1392-1397.
<https://doi.org/10.5740/jaoacint.12-129>
- Tian, J., Chen, S., Chen, J., Liu, D., & Ye, X. (2018). Cooking methods altered the microstructure and digestibility of the potato. *Starch-Stärke*, 70(5-6), 1700241.
- Tian, J., Qin, L., Zeng, X., Ge, P., Fan, J., & Zhu, Y. (2023). The Role of Amylose in Gel Forming of Rice Flour. *Foods*, 12(6), 1210.
- Toozandehjani, M., Matori, K. A., Ostovan, F., Abdul Aziz, S., & Mamat, M. S. (2017). Effect of Milling Time on the Microstructure, Physical and Mechanical Properties of Al-Al₂O₃ Nanocomposite Synthesized by Ball Milling and Powder Metallurgy. *Materials*, 10(11), 1232.
- Tran, T., Zhang, X., Ceballos, H., Moreno, J. L., Luna, J., Escobar, A., Morante, N., Belalcazar, J., Becerra, L. A., & Dufour, D. (2020). Correlation of cooking time with water absorption and changes in relative density during boiling of cassava roots. *International Journal of Food Science and Technology*, 56(3), 1193-1205. <https://doi.org/10.1111/ijfs.14769>
- Tsegay, N., Admassu, H., Zegale, B., & Gosu, A. (2024). Nutritional and functional potentials of wheat, cowpea, and yam composite flours on bread formulations: Effect of blending ratio and baking parameters. *Journal of Agriculture and Food Research*, 18, 101294.
<https://doi.org/https://doi.org/10.1016/j.jafr.2024.101294>
- Tu, L., Nisar, T., Lv, C.-Q., Yang, Z.-F., Fang, Z., Wang, Z.-C., & Lin, Y. (2023). Physicochemical and digestive properties of Lipu taro (*Colocasia esculenta* (L.) Schott) flour and starch. *International journal of food science & technology*, 58(3), 1444-1453.
<https://doi.org/https://doi.org/10.1111/ijfs.16307>
- Vamadevan, V., & Bertoft, E. (2020). Observations on the impact of amylopectin and amylose structure on the swelling of starch granules. *Food Hydrocolloids*, 103, 105663.
<https://doi.org/https://doi.org/10.1016/j.foodhyd.2020.105663>
- van Riemsdijk, L. E., van der Goot, A. J., & Hamer, R. J. (2011). The use of whey protein particles in gluten-free bread production, the effect of particle stability. *Food Hydrocolloids*, 25(7), 1744-1750. <https://doi.org/https://doi.org/10.1016/j.foodhyd.2011.03.017>

- Vasanthan, T. (1996). Physicochemical properties of small-and large-granule starches of waxy, regular, and high-amylose barleys. *Cereal Chem.*, *73*, 199-207.
- Wang, H., Yang, Q., Gao, L., Gong, X., Qu, Y., & Feng, B. (2020). Functional and physicochemical properties of flours and starches from different tuber crops. *International Journal of Biological Macromolecules*, *148*, 324-332.
<https://doi.org/https://doi.org/10.1016/j.ijbiomac.2020.01.146>
- Wang, J.-K., & Higa, S. (1983). Taro, a review of *Colocasia esculenta* and its potentials.
- Wang, S., Li, C., Copeland, L., Niu, Q., & Wang, S. (2015). Starch retrogradation: A comprehensive review. *Comprehensive Reviews in Food Science and Food Safety*, *14*(5), 568-585.
- Wang, X., Reddy, C. K., & Xu, B. (2018). A systematic comparative study on morphological, crystallinity, pasting, thermal and functional characteristics of starches resources utilized in China. *Food Chemistry*, *259*, 81-88.
- Wang, Y., Ou, X., Al-Maqtari, Q. A., He, H. J., & Othman, N. (2024). Evaluation of amylose content: Structural and functional properties, analytical techniques, and future prospects. *Food Chem X*, *24*, 101830. <https://doi.org/10.1016/j.fochx.2024.101830>
- Wibisono, Y., Ubaidillah, U., & Hawa, L. (2019). Microstructure changes of taro (*Colocasia esculenta* L. Schott) chips and grains during drying. IOP Conference Series: Earth and Environmental Science,
- Williams, P. (1970). A rapid colorimetric procedure for estimating the amylose content of starches and flours. *Cereal Chem.*, *47*, 411-420.
- Wills, R., Lim, J., Greenfield, H., & Bayliss-Smith, T. (1983). Nutrient composition of taro (*Colocasia esculenta*) cultivars from the Papua New Guinea Highlands. *Journal of the Science of Food and Agriculture*, *34*, 1137-1142. <https://doi.org/10.1002/jsfa.2740341015>
- Young, D., & Wiseman, B. (2016). *Kingdom of Tonga: Infrastructure Requirements for Processing and Packaging Horticultural Products for Export*. P. H. a. A. M. A. (PHAMA).
- Yu, X., Zhang, Y., Ran, L., Lu, W., Zhang, E., & Xiong, F. (2022). Accumulation and physicochemical properties of starch in relation to eating quality in different parts of taro (*Colocasia esculenta*) corm. *International Journal of Biological Macromolecules*, *194*, 924-932.
<https://doi.org/https://doi.org/10.1016/j.ijbiomac.2021.11.147>
- Yuan, T. Z., Liu, S., Reimer, M., Isaak, C., & Ai, Y. (2021). Evaluation of pasting and gelling properties of commercial flours under high heating temperatures using Rapid Visco Analyzer 4800. *Food Chemistry*, *344*, 128616.
<https://doi.org/https://doi.org/10.1016/j.foodchem.2020.128616>
- Zainol, M. (2020). Physicochemical and functional properties of cassava flour grown in different locations in Sabah, Malaysia. *Food Research*, *4*(4), 991-999.
- Zeng, F.-K., Liu, H., & Liu, G. (2014). Physicochemical properties of starch extracted from *Colocasia esculenta* (L.) Schott (Bun-long taro) grown in Hunan, China. *Starch - Stärke*, *66*(1-2), 142-148. <https://doi.org/https://doi.org/10.1002/star.201300039>
- Zhang, G., & Hamaker, B. R. (2005). Sorghum (*Sorghum bicolor* L. Moench) flour pasting properties influenced by free fatty acids and protein. *Cereal chemistry*, *82*(5), 534-540.
- Zhang, Z., Zhang, L., Chen, M., & He, Z. (2022). Effects of taro powder on the properties of wheat flour and dough. *Food Science and Technology*, *42*, e116221.
- Zhao, R., Fu, W., Li, D., Dong, C., Bao, Z., & Wang, C. (2024). Structure and functionality of whey protein, pea protein, and mixed whey and pea proteins treated by pH shift or high-intensity ultrasound. *Journal of Dairy Science*, *107*(2), 726-741.
<https://doi.org/https://doi.org/10.3168/jds.2023-23742>
- Ziobro, R., Juszczak, L., Witczak, M., & Korus, J. (2016). Non-gluten proteins as structure forming agents in gluten free bread. *Journal of Food Science and Technology*, *53*(1), 571-580.
<https://doi.org/10.1007/s13197-015-2043-5>
- Zobel, H. F. (1984). Gelatinization of starch and mechanical properties of starch pastes. In *Starch: chemistry and technology* (pp. 285-309). Elsevier.

- Zubair, M. W., Imran, A., Islam, F., Afzaal, M., Saeed, F., Zahra, S. M., Akhtar, M. N., Noman, M., Ateeq, H., Aslam, M. A., Mehta, S., Shah, M. A., & Awuchi, C. G. (2023). Functional profile and encapsulating properties of *Colocasia esculenta* (Taro). *Food Sci Nutr*, *11*(6), 2440-2449. <https://doi.org/10.1002/fsn3.3357>
- Zulfa, F., Rochmah, A., Saputri, F., Suleman, D., & Anandito, R. (2023). Macronutrient Profile of Analog Rice Based on Cornstarch, Modified Cassava Flour, and Suweg Flour. *BIO Web of Conferences*,
- Zúñiga, R., Troncoso, E., Ramírez, C., Parada, J., & Germain, J. (2009). Microstructure of potato products: Effect on physico-chemical properties and nutrient bioavailability. In (pp. 41-54).